Blend Uniformity and Powder Phenomena inside the Continuous Tumble Mixer Using Experiments and DEM Simulations

by

Miguel Ángel Florián Algarín

A dissertation submitted in partial fulfillment of the requirements for the degree of

DOCTOR OF PHILOSOPHY

in

Chemical Engineering

UNIVERSITY OF PUERTO RICO
MAYAGUEZ CAMPUS
2014

_____	_____
Rafael Méndez, Ph.D. President, Graduate Committee	Date
_____	_____
Jorge Almodóvar, Ph.D. Member, Graduate Committee	Date
_____	_____
Aldo Acevedo, Ph.D. Member, Graduate Committee	Date
_____	_____
Nelson Cardona Martínez, Ph.D. Member, Graduate Committee	Date
_____	_____
Rodolfo J. Romañach, Ph.D. Member, Graduate Committee	Date
_____	_____
Aldo Acevedo, Ph.D. Chairperson of the Department	Date

Abstract

The pharmaceutical industry is in the middle of a major transition regarding manufacturing where continuous operation is a central topic. One of these operations is powder mixing, which could arguably be the principal process in pharmaceutical drug manufacturing. Currently, this operation is performed in batch mode, with limitations such as sampling methodology, unknown process scale-up behavior, and limitations to apply control strategies.

Pharmaceutical companies have been working on the implementation of continuous processes as an alternative to batch processes using the Food and Drug Administration (FDA) Process Analytical Technology (PAT) initiative. However, existing continuous mixers apply high shear to the materials causing problems in their flow properties.

To solve this problem, at the pharmaceutical operations laboratory of University of Puerto Rico at Mayaguez a low shear continuous tumble mixer was developed. This mixer is based on the existent batch drum mixers and does not have screws or paddles that affect the materials properties.

This study focused on mixing capabilities, and the powder phenomena inside the continuous mixer as a function of inlet flow rate, mixer rotation speed, feeding angle, and material properties using experiments and Discrete Element Method (DEM) simulations.

Experimental results demonstrated that the mixer is capable of achieving good mixing levels based on the relative standard deviation of the outlet concentration. The mass hold-up and powder behavior were affected by the material properties and the operating parameters. A map of material compressibility index was developed to relate the effect of the material properties and

operating conditions to the powder behavior inside the mixer. The regimes obtained were rolling, cascading, and cataracting, with the best uniformity results.

The simulation results demonstrated that the main mixing mechanism is convection. Simulations also demonstrated that cohesion reduces the concentration variability due to higher mass hold-up, particle interactions, and mean residence time. Final blend uniformity was measured and a relationship with cohesion and collision frequency was found.

Finally, a modification of the Froude number taking into account the effect of material properties was proposed and the flow regimes of the simulations were evaluated using this number.

Resumen

La industria farmacéutica está en medio de una importante transición en relación a la manufactura, donde los procesos continuos son un tópico central. Una de estas operaciones es el mezclado de materiales particulados, que argumentalmente puede ser el proceso principal en la manufactura de drogas farmacéuticas. Actualmente, esta operación es realizada en procesos por tandas, modo que presenta algunas limitaciones, como la metodología de muestreo, procesos de escalamiento desconocidos y limitaciones para aplicar estrategias de control.

Las compañías farmacéuticas han estado trabajando en la implementación de procesos continuos como una alternativa a los procesos por tandas usando la iniciativa PAT (Process Analytical Technology) de la Administración de Drogas y Alimentos, FDA por sus siglas en inglés. Sin embargo, los mezcladores continuos existentes aplican altos esfuerzos cortantes sobre el material que pueden causar problemas en sus propiedades de flujo.

Para resolver este problema, se desarrolló en el laboratorio de operaciones farmacéuticas de la Universidad de Puerto Rico en Mayagüez un mezclador continuo tipo tómbola que aplica mínimos esfuerzos cortantes sobre el material. Este mezclador está basado en los mezcladores tipo tómbola por tandas y no tiene tornillos o aspas que afecten las propiedades del material.

Este estudio se enfocó en las capacidades de mezclado y los fenómenos de flujo que ocurren dentro del mezclador como función del flujo de material alimentado, velocidad de rotación, ángulo de alimentación y propiedades del material, usando experimentos y simulaciones por el método de elementos discretos (DEM).

Los resultados experimentales demostraron que el mezclador continuo tiene la capacidad de lograr un buen nivel de mezclado basado en la desviación estándar relativa de la concentración

a la salida del mezclador. La acumulación dentro del sistema y el comportamiento del material fueron afectados por las propiedades del material y los parámetros de operación. Un mapa del índice de compresibilidad fue desarrollado para relacionar el efecto de las propiedades del material y condiciones de operación con el comportamiento del material dentro del mezclador. Los regímenes de flujo obtenidos fueron rodamiento, cascada y catarata, con los mejores resultados de uniformidad.

Los resultados obtenidos usando simulaciones demostraron que el principal mecanismo de mezclado es convección. Las simulaciones también demostraron que la cohesión reduce la variabilidad en concentración debido a las altas acumulaciones, el incremento en la interacción de las partículas y el aumento en el tiempo de residencia promedio. La uniformidad de la mezcla a la salida del sistema fue medida y se halló una relación con la cohesión y la frecuencia de colisiones.

Finalmente, se propuso una modificación al número de Froude que toma en consideración el efecto de las propiedades del material y los regímenes de flujo de las simulaciones fueron evaluados usando este número.

To God, for everything in my life

To my parents: Miguel Angel and Maria Benita,

To my siblings: Vivi, Luz, Mary, David, and Luisito

To my nieces and nephews: Mariangel, Frang,

Jennifer, Keith Jr, and Luis David

To my love: Ari

Acknowledgments

This research was possible thanks to the financial support and resources of the ERC-SOPS project. I would like to thank the Chemical Engineering Department of the University of Puerto Rico at Mayaguez, for the opportunity to complete my Ph.D. studies.

Thanks to my advisor Dr. Rafael Mendez, who guided me through my doctoral studies, by being always available to orient me both academically and as a friend. I would also like to say thanks to Zulma Marrero.

I also want to thank the members of my graduate committee, Dr. Aldo Acevedo, Dr. Nelson Cardona Martínez, and Dr. Jorge Almodóvar for their time and collaboration when I needed them.

My gratitude to the members of CPEDaL: Dr. Carlos Velázquez, Carmen Vanessa, and Catherine Pérez who were always accessible to me since I started working in the pharmaceutical operations laboratory. Thanks for their advice, support, and friendship. I would also like to thank the undergraduate students that helped this project to be completed: Argenis, Jacky, and Shakira.

Thanks to my whole family, especially to my parents: Miguel and Maria for their unconditional love and for teaching me the values necessary to reach any goal that I propose. To my siblings who are the best examples for me to follow in my life and for being available in any moment even in the distance: Vivi, Luz, Mary, David, and Luisito. To my brothers and sisters in law: Keith, Leonel, Braulio, Melina, and Adriluz, who are now part of my family, and to my nephews and nieces: Mariangel, Frang, Jennifer, Keith Jr, and Luis David who are the motivation necessary to affront every day.

I also want to give thanks to my laboratory partners who are also my friends: David, Madeline, Vladimir, Sonia, Elvin, and Daniel for their support and friendship during my stay in the pharmaceutical operations laboratory. To Stephany, Christian, and Camilo, thanks for sharing every moment in INQU, and also traveling and exploring new places. To every one of my friends; Ana, Wilman, Zalle, Boris, Noe, Aimee, Luis Enrique, thanks for making my stay in Puerto Rico a happy one and for making easier my transition into Chemical Engineering. To everyone that I did not mention and was an important part of this project, thanks!

Finally, and not less important I want to express my eternal gratitude to my love, for coming into my life and for being now an important part of it. Thanks for always supporting and advising me, and for every moment by your side. Thanks Ari!

Table of Contents

Table of Figures

List of Tables

Chapter 1

1. Introduction

The study of flow and mixing of particulate material has increased in computational and experimental studies in the last years especially in batch systems, due to the fact that the granular material mixing is a major step in diverse industries such as: cosmetics, military, food processing, cement, chemical, petrochemical, and pharmaceutical. This essential operation is currently performed principally in batch mode, which results in several problems and limitations such as: problems in the sampling methodology, difficulty in homogeneity determination, scale-up process, and limitations to apply control strategies. To reduce these difficulties and improve the manufacturing process, the Food and Drug Administration (FDA) is promoting the change from batch to continuous processes in the Pharmaceutical Companies by the implementation of an initiative named Process Analytical Technology.[1] Continuous mixing has been applied in other industries,[2–4] such as chemical and food companies, in powder processing, with excellent results.

1.1. Process Analytical Technology (PAT)

The PAT[1] is a regulatory framework of the FDA to encourage the voluntary development and implementation of innovative pharmaceutical development, manufacturing, and quality assurance. Currently, pharmaceutical companies have been hesitant to make this change, due to some existent regulations. This hesitation has been taken into account by the FDA and another initiative (August 2002) named "Pharmaceutical CGMPs for the 21st Century: A Risk-Based Approach[5]" was launched to minimize and eliminate the hesitance to changes. The final idea of this initiative is that the pharmaceutical manufacturing and regulation accomplish a desired state in which the design of effective and efficient manufacturing processes ensures product quality, there is continuous real time quality assurance, and the use of mechanistic and scientific

understanding of how formulation and process factors affect product performance and the final product quality is applied in the selection of product and process specifications.[1] This initiative is based on process understanding, a series of principles and tools, and a strategy for implementation. The tools include multivariate analysis for design, data acquisition and analysis, process analyzers, process control, and a continuous improvement and knowledge of management tools. One of the principal steps to reach these objectives is the implementation of continuous processes, due to the possibility to obtain in-line measurements, ensuring real time quality, and implementing control systems to improve efficiency and manage variability. To reach this objective, this initiative is promoting the change from batch to continuous processes in the pharmaceutical companies to improve process quality and to reduce control instabilities obtaining a more efficient process. Some of the research work in pharmaceutical continuous processes is using the PAT initiative as a base to justify the use of this mode.

1.2. Batch Drum Mixers and Mixing Mechanisms

Currently, most of the mixers used in the pharmaceutical industry are batch type based in tumble designs. This type of mixer is also utilized in other processes such as mixing, drying, and coating. The use of the tumbles in these processes with particulate material helps to study the mechanism of the granular flow. The mixing processes for particulate materials have been widely studied by different authors in different areas, using experiments and simulations applying different methods including discrete elements method.[6–9] Drum or tumble mixers are the principal mixers described in previous works,[10–12] even if there are works using different types of mixers.[13–15] These drum mixers are characterized by the folding or avalanche behavior the particulate material exhibits inside the vessel as it rotates. These rotating drums yield six different material behaviors (Figure 1.1): slipping, slumping, rolling, cascading, cataracting, and centrifuging.[11,16,17]

Several authors have mentioned a seventh behavior, denominated surging,[18–20] which is situated between slipping and slumping. In the slipping regime, the material slides as a solid bed as the mixer rotates while in slumping behavior, the material on the top of the accumulation flows to the bottom. Rolling behavior is characterized by a flat surface. In the cascading regime, the flat surface disappears to produce a curve. Cataracting occurs at high rotational velocities when the material reaches the superior part of the mixer and falls back due to the gravitational force. Finally, in the centrifuging regime the material remains on the mixer walls due to the centrifugal force.

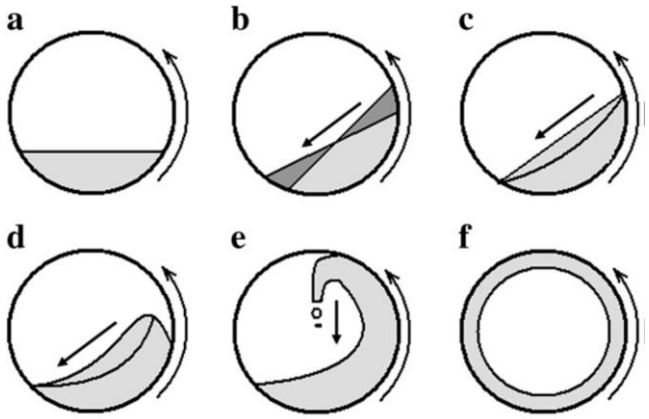

Figure 1.1. Flow regimes in a drum mixer; slipping (A), slumping (B), rolling (C), cascading (D), cataracting (E), and centrifuging (F). [17]

The rolling regime is the most extensively studied behavior because it provides the highest mixing uniformity.[10,17,21] Two principal zones can be identified[17,22–25] and these are shown in Figure 1.2: the undergoing solid-body, which is the layer near the wall of the mixer (stagnant layer) and the active layer surface, which is the top section of the material in the mixer. Mixing primarily occurs in this top section.[26]

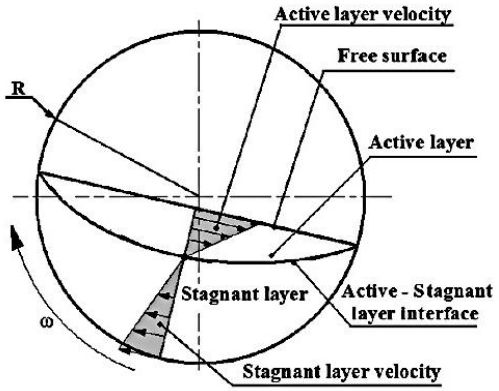

Figure 1.2. Schematic representation of the rolling regime.[17]

The effects of the density, friction coefficient, surface quality, and particle geometry on the final uniformity of granular mixtures have been previously studied demonstrating that the use of these additional parameters is essential to characterize the particle flow regimes.[26] Typically, the Froude Number (Eq. 1) is used to describe the flow regimes inside a rotary cylinder mixer, where *R* represents the radius of the drum mixer, *w* the rotational velocity, and *g* the gravitational force.[18,27,28]

$$Fr = \frac{Rw^2}{g} \qquad (1.1)$$

This number represents the ratio of the centrifugal to the gravitational forces in a drum system and does not include other factors, such as the material properties. Due to this definition, Aissa et al. concluded that this value must be complemented with the filling ratio, which is the amount of material present inside the mixer.[26] To obtain a desired flow regime it is necessary to find the optimal combination between operational parameters and the material properties.[26,29]

The mechanisms in which the mixing and de-mixing occurs were published by Donald et al., they identified two ways; radial and axial. Defining the radial mixing as the process when a particle changes from its initial path of motion to another path in the same radial plane and the

axial mixing as the phenomena occurring when a particle changes its path of motion in one radial plane to the corresponding path in an adjacent plane. Radial de-mixing is the process that takes place when a smaller particle is trapped in a void of the layer below and by the effect of the interactions with other particles flows easily between other particles with bigger size and the axial de-mixing occurs when the small particles have a propensity to move axially to the maximum velocity band.[30]

The mixing of materials with identical properties such as density, shape, size, and non-cohesive particles are considered ideal (homogeneous systems) and they do not exists in the real pharmaceutical process, but they are the basis to study and understand the real systems (non-homogeneous).

The segregation or de-mixing is a phenomenon present in mixer systems and consists in the separation of the particles due the movement during the handling of the material with different size, density, particle shape, and others. The segregation can be a desirable process in operations such as: particulate segregation and screening but in the majority of instances it is an undesirable effect.[12]

1.3. Continuous Powder Mixing

Continuous mixing processes are an alternative to batch mixing processes. Continuous processes have been used in different industries, such as the food, chemical, and petrochemical industry.[31] Continuous mixers rely on high-shear convection-blades to achieve the desired mixing. Many studies have focused on investigating the effect of the blade rotation rate,[2,4,32] blade design,[2,32] blade configuration,[31–33] mixer angle,[31,32] inlet flow rate,[2,4,33–35] and powder

properties.[2,3,31,32,35] These parameters directly affect the residence time distribution of the materials inside the mixer and the resultant mixing uniformity.[3,33,36,37]

In addition, Vanarase et al.[33] found that the blend uniformity was a contribution of the residence time and the number of blade passes; the mixing was improved at intermediate blade speeds when using an alternate blade configuration. In a separate study,[37] the authors used the residence time distribution to determine the effects of operating conditions (two feed rates) and the mixer configuration (two blade configurations and four blade speeds) on the mixing uniformity and developed a model of the output variance. The results showed that moderately low speeds improved the mixing and a change in the feed rate did not significantly influence the overall output variance. The effect of cohesion in continuous mixing has also been studied[38] using two approaches, experimental and simulated.

1.4. Discrete Elements Method (DEM) Simulations

The use of DEM to simulate and understand the behavior of granular materials has been increasing over the last years, primarily for batch systems.[6,14,39] Using computational processes it is possible to study the effect of the material properties in the final blend uniformity and previous investigations showed that the cohesion is an important parameter that affects the mixing processes.[12,14,39] The effect of the cohesion is notable for batch and continuous processes.[40]

1.4.1. Batch Drum Mixers

DEM has been used to study the particles behavior inside the mixers or similar systems to obtain a better understanding of these systems.[6,14,39] The principal disadvantage of this method is the requirement of high simulation times and computation costs to simulate particles with real shape and size in comparison to experiments. An option to decrease the simulation time is the use

of two-dimensional simulations. Xu et al.[6] used DEM to simulate a quasi 2D experimental process demonstrating that density and particle size affect the final uniformity in the system studied. They also found a relationship between the rotation ratio and the flow regime obtained. Chaudhuri et al.[14] used the DEM to study the effect of cohesion in the mixing process by comparison of the simulation results with experimental images of a similar system. The results obtained showed that mixing is influenced by material cohesion; high cohesion values produce slow mixing, and low particle cohesion produce a faster mixing. This effect is easy to visualize and has been shown in diverse studies.[12,39] The dynamics of particles in the system was studied by Alexander et al.[39] by coupling experiments and simulation results using three different cohesions: dry glass beads, wet glass beads, and "dry" cohesive powders showing that in both cases cohesion affects the avalanche phenomenon and behavior within the mixer.

1.4.2. Continuous Powder Mixing

Particulate material mixing processes, both batch and continuous, have also been studied using simulation software.[6,14,39,41] This method produces results similar to the experimental behavior of the particulate material.[42–44] A batch study of a tote blender using mono and bi-disperse particles in size was reported. The results show that the geometry of this system is sensitive to the initial loading and that the intensity and the mixing rate increase when the fill level is low.[13] When compared to the experimental part the results show an agreement between experiments and simulation of mono-disperse particles.

For continuous mixing processes of particulate material the main researches are related to the understanding of the effect of operational parameters like mixer speed, blade speed, shape of the blades, fill level, and flow rate on the final mixing uniformity. An optimal combination of these

parameters produces the most favorable uniformity for powder mixing processes.[45,46] Higher mixer speed was also demonstrated as an important factor to improve the mixing performance.[6]

DEM has been used to study the mixing process in a continuous paddle mixer. Sarkar et al.[46] simulated a periodic section of a continuous mixer to study the influence of the fill level and impeller rotation rate. The principal results showed that the combination between low fill and high impeller speeds produced higher dispersion, resulting in a better mixing homogeneity; and low fill with low impeller rotation produced a poor mixing.

Similar to the mixing process in batch mode the cohesion affects the continuous process and the effects have been studied experimentally and using simulations. Dubey et al.[7] used DEM simulations to study the powder behavior using two different strategies: first, the entire blender (Gericke GCM250) and second, a periodic slice of the entire blender in which they studied the impact of the impeller speed, fill level, and cohesion on the mixing performance and residence time distribution (RTD). Sarkar et al.[40] presented the influence of the inter-particle cohesion at various impeller speeds and different fill levels, demonstrating that the cohesion affects principally the axial mixing and the mixing performance for highly cohesive materials.

Gao et al.[47] proposed a periodic section model for continuous mixing based on the idea that this convective process is a combination of a batch-like mixing and an axial particle flow. Using DEM simulations and three different particle sizes (2, 3, and 4 mm) the authors investigated two study cases: non-segregating mixture and a case with segregation effect, finding different relationships that could be used to design and optimize continuous mixing processes. A second part of this work was performed based on the previous results. The operating conditions and their influence on axial velocity (V_x) and local mixing rate (K_b) of the mixture demonstrated that the

particles move faster and reside a shorter time inside the mixer at higher rotary speed and a lower fill level.[45]

1.5. Batch versus Continuous Mixing Processes

The continuous mode has several advantages compared to batch mixing, including lower costs, the possibility of implementing in-line analysis, the elimination of scale-up process, and the easy measure of uniformity at the outlet of the system.[34] Also, a continuous mixer can be placed before the next step of the process to reduce handling and storage of the mixtures, generally requires less space, and are useful to mix segregating materials.

The continuous mixing processes provide a possible alternative to the batch processes, solving the principal problems of the batch processes regarding the optimization of the production of homogeneous solid mixtures.[32] Despite the desirable levels in the performance of both the batch and continuous mixers, both have various drawbacks in practice. Batch mixers require large operating areas, which increase their operational costs. Currently, used continuous mixer technologies use blades and screws to promote the mixing processes.[48] These mixers represent a progress in the implementation of continuous processes but the main problem is that their attachments apply undesirable levels of shear to the blends that could cause attrition and over-lubrication especially for high shear sensitive materials.

1.6. Low Shear Continuous Tumble Mixer

Using the batch tumble mixer knowledge it is possible to extrapolate the obtained information to continuous mixers, demonstrating that the powder phenomena occurring inside a batch tumble is similar to the behavior inside a continuous tumble mixer.[49,50] Based on this statement, at the pharmaceutical operations laboratory of UPRM a low shear continuous tumble

mixer was developed for pharmaceutical blends. The continuous mixer maintains the advantages of continuous operation but, in contrast with the common screw mixers, does not have paddles or impellers, reducing the shear impact on material properties.

This thesis work demonstrates that the continuous tumble mixer can reach the same levels of performance of the current batch and continuous technologies and presents the characterization of the continuous mixer using the same parameters used to characterize the current technologies. This characterization was also performed using DEM simulations to understand the effect of operating parameters and material properties on powder phenomena inside the continuous tumble mixer, and the mixing uniformity inside and at the exit of the system.

1.7. Objectives

The overall objective of this research is to study the effect of the material properties, equipment design, operational parameters, and the powder phenomena on the final mixing uniformity, in a low shear continuous tumble mixer for pharmaceutical particulate materials; both experimentally and using DEM simulations. The following are the specific goals:

- To determine the effect of the materials properties and operational parameters on the final uniformity of the blend.
- To study the powder phenomena and the material behavior occurring inside the mixer to establish a relationship between these and the mixing uniformity.
- To study the effect of the feed angle, number of orifices, and scale-up in the homogeneity of the mixture obtained in a continuous process.
- To use the DEM simulations to study the material flow throughout the system, flow patterns and velocity profile inside the mixer, the residence time, and the behavior of the material inside the mixer.
- To design experiments to validate the simulations using materials with properties similar to the ones used in the simulations.
- To develop a methodology based on correlations between material properties, operations parameters, system's response, and final mixing uniformity, to reduce experimental trial and error.
- To modify the Froude Number to include the effect of the material properties and its effect on the flow regime inside the mixer.

1.8. References

1. FDA. *Guidance for Industry PAT — A Framework for Innovative Pharmaceutical.*; 2004.
2. Marikh K, Berthiaux H, Gatumel C, Mizonov V, Barantseva E. Influence of stirrer type on mixture homogeneity in continuous powder mixing: A model case and a pharmaceutical case. *Chem. Eng. Res. Des.* 2008;6:1027-1037. doi:10.1016/j.cherd.2008.04.001.
3. Weinekötter R. Compact and efficient continuous mixing processes for production of food and pharmaceutical powders. *Trends Food Sci. Technol.* 2009;20:S48-S50. doi:10.1016/j.tifs.2009.01.037.
4. Marikh K, Berthiaux H, Mizonov V, Barantseva E. Experimental study of the stirring conditions taking place in a pilot plant continuous mixer of particulate solids. *Powder Technol.* 2005;157:138-143. doi:10.1016/j.powtec.2005.05.020.
5. Department of health and Human Services U. F and DA. *Pharmaceutical CGMPs for the 21 Century - A Risk-Based Approach.*; 2004.
6. Xu Y, Xu C, Zhou Z, Du J, Hu D. 2D DEM simulation of particle mixing in rotating drum: A parametric study. *Particuology* 2010;8(2):141-149. doi:10.1016/j.partic.2009.10.003.
7. Dubey A, Sarkar A, Ierapetritou M, Wassgren CR, Muzzio FJ. Computational Approaches for Studying the Granular Dynamics of Continuous Blending Processes, 1 - DEM Based Methods. *Macromol. Mater. Eng.* 2011;296(3-4):290-307. doi:10.1002/mame.201000389.
8. Boukouvala F, Dubey A, Vanarase A, Ramachandran R, Muzzio FJ, Ierapetritou M. Computational Approaches for Studying the Granular Dynamics of Continuous Blending Processes, 2 - Population Balance and Data-Based Methods. *Macromol. Mater. Eng.* 2012;297(1):9-19. doi:10.1002/mame.201100054.
9. He YR, Chen HS, Ding YL, Lickiss B. Solids Motion and Segregation of Binary Mixtures in a Rotating Drum Mixer. *Chem. Eng. Res. Des.* 2007;85:963-973. doi:10.1205/cherd06216.
10. Santomaso A, Olivi M, Canu P. Mechanisms of mixing of granular materials in drum mixers under rolling regime. *Chem. Eng. Sci.* 2004;59(16):3269-3280. doi:10.1016/j.ces.2004.04.026.
11. Yang RY, Yu AB, McElroy L, Bao J. Numerical simulation of particle dynamics in different flow regimes in a rotating drum. *Powder Technol.* 2008;188(2):170-177. doi:10.1016/j.powtec.2008.04.081.
12. Abouzeid A-ZM, Fuerstenau DW. Mixing-demixing of particulate solids in rotating drums. *Int. J. Miner. Process.* 2010;95:40-46. doi:10.1016/j.minpro.2010.03.006.
13. Arratia PE, Duong N, Muzzio FJ, Godbole P, Reynolds S. A study of the mixing and segregation mechanisms in the Bohle Tote blender via DEM simulations. *Powder Technol.* 2006;164:50-57. doi:10.1016/j.powtec.2006.01.018.
14. Chaudhuri B, Mehrotra A, Muzzio FJ, Tomassone MS. Cohesive effects in powder mixing in a tumbling blender. *Powder Technol.* 2006;165:105-114. doi:10.1016/j.powtec.2006.04.001.

15. Mendez ASL, de Carli G, Garcia C V. Evaluation of powder mixing operation during batch production: Application to operational qualification procedure in the pharmaceutical industry. *Powder Technol.* 2010;198(2):310-313. doi:10.1016/j.powtec.2009.11.027.

16. Kwapinska M, Saage G, Tsotsas E. Mixing of particles in rotary drums: A comparison of discrete element simulations with experimental results and penetration models for thermal processes. *Powder Technol.* 2006;161:69-78. doi:10.1016/j.powtec.2005.08.038.

17. Aissa AA, Duchesne C, Rodrigue D. Transverse mixing of polymer powders in a rotary cylinder part I: Active layer characterization. *Powder Technol.* 2012;219:193-201. doi:10.1016/j.powtec.2011.12.040.

18. Mellmann J. The transverse motion of solids in rotating cylinders—forms of motion and transition behavior. *Powder Technol.* 2001;118(3):251-270. doi:10.1016/S0032-5910(00)00402-2.

19. Rutgers R. Longitudinal mixing of granular material flowing through a rotating cylinder-Part I. Descriptive and theorical. *Chem. Eng. Sci.* 1965;20:1079-1087.

20. Rutgers R. Longitudinal mixing of granular material flowing through a rotating cylinder-Part II. Experimental. *Chem. Eng. Sci.* 1965;20:1089-1100.

21. Ding Y, Seville J, Forster R, Parker D. Solids motion in rolling mode rotating drums operated at low to medium rotational speeds. *Chem. Eng. Sci.* 2001;56:1769-1780. Available at: http://www.sciencedirect.com/science/article/pii/S0009250900004681. Accessed October 14, 2014.

22. Ding YL, Forster R, Seville JP., Parker D. Granular motion in rotating drums: bed turnover time and slumping–rolling transition. *Powder Technol.* 2002;124:18-27. doi:10.1016/S0032-5910(01)00486-7.

23. Cheng N-S, Zhou Q, Keat Tan S, Zhao K. Application of incomplete similarity theory for estimating maximum shear layer thickness of granular flows in rotating drums. *Chem. Eng. Sci.* 2011;66:2872-2878. doi:10.1016/j.ces.2011.03.050.

24. Felix G, Falk V, Ortona UD. Segregation of dry granular material in rotating drum: experimental study of the flowing zone thickness. *Powder Technol.* 2002;128:314-319.

25. Wightman C, Muzzio FJ. Mixing of granular material in a drum mixer undergoing rotational and rocking motions II. Segregating particles. *Powder Technol.* 1998;98(2):125-134. doi:10.1016/S0032-5910(98)00011-4.

26. Aissa AA, Duchesne C, Rodrigue D. Effect of friction coefficient and density on mixing particles in the rolling regime. *Powder Technol.* 2011;212:340-347. doi:10.1016/j.powtec.2011.06.009.

27. Wightman C, Muzzio FJ. Mixing of granular material in a drum mixer undergoing rotational and rocking motions I. Uniform particles. *Powder Technol.* 1998;98:113-124.

28. Aissa A, Duchesne C, Rodrigue D. Longitudinal segregation of polymer powder in a rotating cylinder. *Powder Technol.* 2011;207:324-334. doi:10.1016/j.powtec.2010.11.014.

29. Aissa A, Duchesne C, Rodrigue D. Polymer powders mixing part I: Mixing characterization in rotating cylinders. *Chem. Eng. Sci.* 2010;65:786-795. doi:10.1016/j.ces.2009.09.031.

30. Roseman MB, Donald B. Mechanism in a horizontal drum mixer. *Br. Chem. Eng.* 1962;7:749-753.

31. Portillo PM, Ierapetritou MG, Muzzio FJ. Characterization of continuous convective powder mixing processes. *Powder Technol.* 2008;182:368 - 378. doi:10.1016/j.powtec.2007.06.024.

32. Portillo PM, Ierapetritou MG, Muzzio FJ. Effects of rotation rate ,mixing angle, and cohesion in two continuous powder mixers: A statistical approach. *Powder Technol.* 2009;194(3):217-227. doi:10.1016/j.powtec.2009.04.010.

33. Vanarase AU, Muzzio FJ. Effect of operating conditions and design parameters in a continuous powder mixer. *Powder Technol.* 2011;208(1):26-36. doi:10.1016/j.powtec.2010.11.038.

34. Berthiaux H, Marikh K, Gatumel C. Continuous mixing of powder mixtures with pharmaceutical process constraints. *Chem. Eng. Process.* 2008;47:2315-2322. doi:10.1016/j.cep.2008.01.009.

35. Portillo PM, Vanarase AU, Ingram A, Seville JK, Ierapetritou MG, Muzzio FJ. Investigation of the effect of impeller rotation rate, powder flow rate, and cohesion on powder flow behavior in a continuous blender using PEPT. *Chem. Eng. Sci.* 2010;65:5658-5668. doi:10.1016/j.ces.2010.06.036.

36. Marikh K, Berthiaux H, Mizonov V, Barantseva E, Ponomarev D. Flow analysis and Markov Chain modelling to quantify the agitation effect in a continuous powder mixer. *Chem. Eng. Res. Des.* 2006;84:1059-1074. doi:10.1205/cherd05032.

37. Gao Y, Vanarase A, Muzzio F, Ierapetritou M. Characterizing continuous powder mixing using residence time distribution. *Chem. Eng. Sci.* 2011;66:417-425. doi:10.1016/j.ces.2010.10.045.

38. Faqih AMN, Mehrotra A, Hammond S V, Muzzio FJ. Effect of moisture and magnesium stearate concentration on flow properties of cohesive granular materials. *Int. J. Pharm.* 2007;336:338-345. doi:10.1016/j.ijpharm.2006.12.024.

39. Alexander AW, Chaudhuri B, Faqih A, Muzzio FJ, Davies C, Tomassone MS. Avalanching flow of cohesive powders. *Powder Technol.* 2006;164:13-21. doi:10.1016/j.powtec.2006.01.017.

40. Sarkar A, Wassgren C. Continuous blending of cohesive granular material. *Chem. Eng. Sci.* 2010;65(21):5687-5698. doi:10.1016/j.ces.2010.04.011.

41. Marigo M, Cairns DL, Davies M, Ingram A, Stitt EH. A numerical comparison of mixing efficiencies of solids in a cylindrical vessel subject to a range of motions. *Powder Technol.* 2012;217:540-547. doi:10.1016/j.powtec.2011.11.016.

42. Bhattacharya T, McCarthy JJ. Chute flow as a means of segregation characterization. *Powder Technol.* 2014;256(2014):126-139. doi:10.1016/j.powtec.2014.01.092.

43. Komossa H, Wirtz S, Scherer V, Herz F, Specht E. Transversal bed motion in rotating drums using spherical particles: Comparison of experiments with DEM simulations. *Powder Technol.* 2014;264:96-104. doi:10.1016/j.powtec.2014.05.021.

44. Combarros M, Feise HJ, Zetzener H, Kwade a. Segregation of particulate solids: Experiments and DEM simulations. *Particuology* 2014;12(2014):25-32. doi:10.1016/j.partic.2013.04.005.

45. Gao Y, Muzzio FJ, Ierapetritou MG. Optimizing continuous powder mixing processes using periodic section modeling. *Chem. Eng. Sci.* 2012;80:70-80. doi:10.1016/j.ces.2012.05.037.

46. Sarkar A, Wassgren CR. Simulation of a continuous granular mixer: Effect of operating conditions on flow and mixing. *Chem. Eng. Sci.* 2009;64(11):2672-2682. doi:10.1016/j.ces.2009.02.011.

47. Gao Y, Ierapetritou M, Muzzio F. Periodic Section Modeling of Convective Continuous Powder Mixing Processes. *AIChE J.* 2011;58(1):69-78. doi:10.1002/aic.

48. Vanarase AU, Osorio JG, Muzzio FJ. Effects of powder flow properties and shear environment on the performance of continuous mixing of pharmaceutical powders. *Powder Technol.* 2013;246:63-72. doi:10.1016/j.powtec.2013.05.002.

49. Pernenkil L, Cooney CL. A review on the continuous blending of powders. *Chem. Eng. Sci.* 2006;61:720-742. doi:10.1016/j.ces.2005.06.016.

50. Kingston T a., Heindel TJ. Granular mixing optimization and the influence of operating conditions in a double screw mixer. *Powder Technol.* 2014;266:144-155. doi:10.1016/j.powtec.2014.06.016.

Chapter 2

2. Experimental Section

In this section a description of the experimental and the simulated system is presented. A list of materials is presented and the characterization methods used to characterize these raw materials and the final mixing uniformity are also described.

2.1. Continuous Tumble Mixer Description

2.1.1. Experimental System

A novel continuous mixer called Continuous Tumble Mixer was developed using batch drum mixers as a model. Figure 2.1 includes a diagram of the system, which has an internal diameter of 152.4 mm with multiple orifices in the radial wall. Each orifice is 4 mm in diameter and 6.35 mm in depth. The depth of the mixer cylinder is 50.5 mm. The mixer is closed at both ends with one end connected to the shaft of a variable speed motor to control the revolutions per minute (RPM). The motor specifications include: 1/4HP, 90V, 2.72A, 90 Torque and 165 RPM Max. The other end has a hole in the center to permit the entrance of the material.

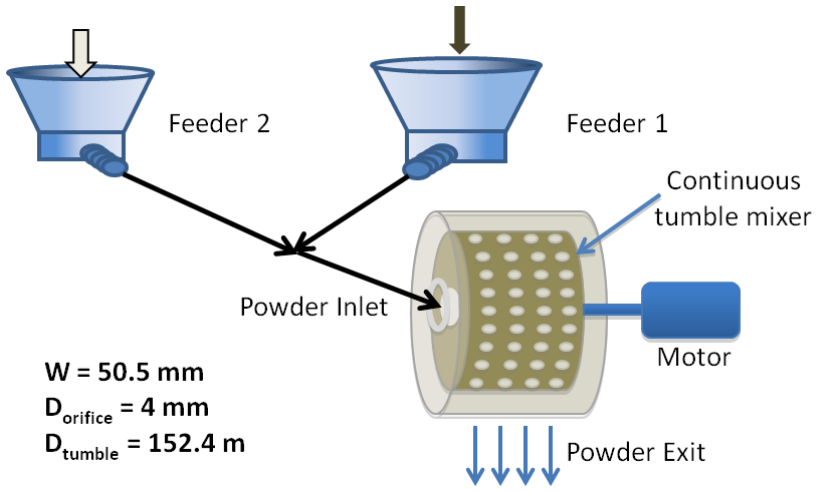

Figure 2.1. Setup of continuous tumble mixer system.

Figure 2.2 shows the schematic design of the mixer, which is comprised of two concentric cylinders that are both made of acrylic to allow the visual monitoring of the powder mixing behavior inside. The outer cylinder, which is shown in Figure 2.2, functions as a powder collector with an internal diameter of 304.8 mm and two 60° chutes to combine the powder exits in one smooth flow through a square aperture at the bottom of the cylinder. This design helps to improve the characterization of the attributes of the powder. The inner cylinder in Figure 2.2 is the continuous tumble mixer.

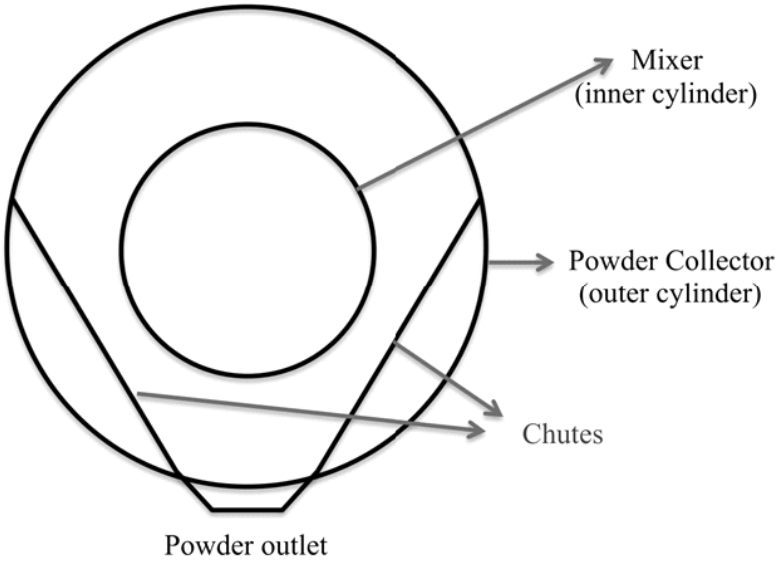

Figure 2.2. Schematic front view of mixer system.

Powders enter the mixer through a 25.4 mm internal diameter acrylic tube at an angle of 50° to the horizontal. The mixer rotates to allow the powder particles to slide or form an avalanche while simultaneously exiting through the orifices due to the centrifugal force. The mixer rotates counterclockwise, although the motor can be wired to rotate in the opposite direction.

As seen in Figure 2.1, the set up includes two feeders: one is a Schenck Accurate, model Modpharma 2007, and the other is a Gericke, model 153.

2.1.2. Discrete Element Method (DEM) and the Simulated System

A set of simulations was used to study the phenomena occurring inside the mixer and to obtain a better understanding of the mixing process using the EDEM Software®. This software is based on the Discrete Elements Model (DEM) which is a powerful tool to simulate particulate systems.[1–3] DEM software uses Newton's law[4–6] to describe the motion of each particle (Eq. 2.1 and 2.2) and the interaction between particles based on the initial particle characteristics.

$$m_i \frac{dv_i}{dt} = \sum_j \left(F_{ij}^N + F_{ij}^T\right) + m_i g \tag{2.1}$$

$$I_i \frac{dw_i}{dt} = \sum_j \left(R_i * F_{ij}^T\right) + \tau_{rij} \tag{2.2}$$

For the previous equations m_i, R_i, I_i, v_i, and w_i represent the mass, radius, moment of inertia, linear velocity, and angular velocity of particle i, respectively, and the acceleration of gravity is represented by g. Using the information provided by this method we can obtain velocity, position, and interaction forces of each particle. Simulations were performed using the No-slip Hertz-Mindlin contact model (Eq. 2.3), which is the default model included in the software program and it is used to solve the particle-particle interaction.[7–9]

$$F_n = -k_n \delta_n + C_n v_n^{rel} \tag{2.3}$$

In Equation 2.3 the terms k_n, C_n, δ_n, *and* v_n^{rel} represent spring stiffness constant, damping coefficient, the normal overlap, and the normal component of the relative velocity.

In this mixing process the incoming materials interact with the powder that is already in the system. Points A and B in Figure 2.3 represent the place where the particles are generated (factories) using a flow of 0.009 Kg/h of particles 1 and 2 which are identified with colors red and

blue, respectively. Particle generations are placed on top of the system and these positions coincide with the manner in which particles are produced in the experimental system.

The simulated system was developed using Autocad®, and has exactly the same dimensions of the real mixer (Figure 2.3). The system includes the mixer and two factories, where particles 1 and 2 are produced. These particles represent the active ingredient and the excipients used in the mixing process. Factories in the simulated system function like the feeders in the experimental part. Particles produced in these factories enter the mixer by a tube using a given flow. Particle 1, represented by the red color is considered the active pharmaceutical ingredient (API) and is generated at the left of the system, similar to the experimental part where naproxen sodium is fed at the same position.

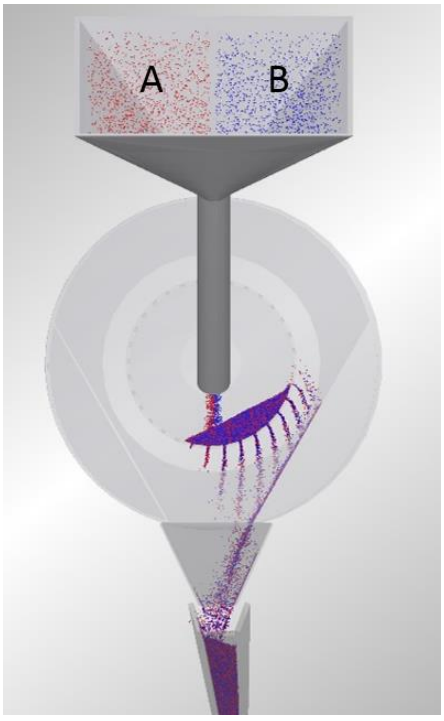

Figure 2.3. Schematic system used in the simulations.

2.2. Materials

Materials used include: (1) Naproxen Sodium (Zhejiang Tianxin Pharmaceutical Co.) with a median particle size of 28 µm as the API, (2) Tablettose 70 Agglomerated Monohydrate Lactose Ph. EUR/USP-NF/JP (Malkerei Meggle Wasserburg GmBH & Co.) with a median particle size of 125 µm, (3) GranuLac 140 with a particle size distribution (PSD) of <100 NLT 80%, (4) Blue color powder coating, (5) Ligamed MF-2-K Magnesium Stearate (Peter Greven) median particle size < 10 µm and (6) 1 mm glass beads.

2.3. Procedures and characterization techniques

2.3.1. Pre-blending step

The lactose monohydrate was pre-blended in a 22 L V-blender (Patterson-Kelly Blend Master Model B Lab Blender) with magnesium stearate (MgSt) to form a mixture of 1% w/w MgSt (to improve the flow properties of the excipients)[10]. Half of the monohydrate lactose was first added to the blender followed by the MgSt and the other half of lactose. This mixture was blended at 9 RPM for 6 minutes to avoid the over-lubrication of the powder.

2.3.2. Feeders Calibration

The pre-blend of Tablettose 70 and MgSt was placed in the Gericke feeder, while pure naproxen sodium was placed in the Modpharma 2007. The feeders were initially filled to 80% of their maximum capacity and operated in volumetric mode (the screw operated at constant speed). Vibration was added to the naproxen feeder. For the calibration, the feeder screw speed was set at a percentage of the maximum speed, and the material was collected at the feeder exit for 2 minutes, several times. Each sample was weighed, and the average flow rate was then estimated. This

procedure was repeated for several percentages (0 - 100%) to complete the flow rate calibration curve for each feeder with the specific material.

2.3.3. Validation of Simulations

To validate the simulations; mixing experiments were performed using the experimental system[11] and 1 mm spherical glass beads. Velocity profiles and flow regime were analyzed to compare these results with the simulation data obtained at similar flow rate and mixer speeds. The results show similar behavior for both, simulation and experimental system (Figure 2.4).

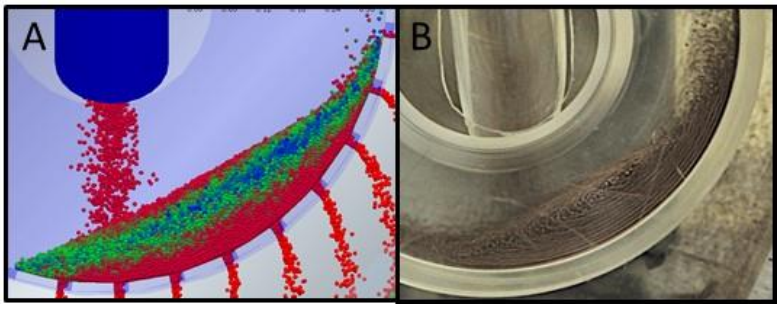

Figure 2.4. Simulation and validation using glass beads at 70 RPM.

2.3.4. Particle Size Distribution

Raw material samples (20 grams) were taken and analyzed using laser diffraction with a Malvern Insitec Analyzer (Malvern Instruments Model IDC2000) to determine the PSD. Each sample was analyzed three times and the PSD was reported as an average value. This technique has been used previously to characterize particulate material and uses laser diffraction to calculate an average distribution assuming spherical shape of the particles.[12]

2.3.5. Powder Flow Properties

The material flow properties were determined using an FT4 Powder Rheometer; which can measure the dynamic flow, shear, and bulk properties of powders and granules.[13,14] The raw material and samples collected after experimentation were analyzed for compressibility (0-15 kPa) and Shear Cell (3, 6, and 9 kPa). Each test was replicated, and an average value was calculated and reported.

2.3.6. UV-Vis Spectroscopy

Calibration curves for the concentration of naproxen (Figure 2.5) and blue powder tracer were obtained using a Genesys 10S UV-Vis Spectrophotometer at 318 nm to determine the mixing uniformity and RTD, respectively. Subsequent dilutions were prepared from a stock solution, and their absorbance value obtained. For naproxen, concentrations from 0-30% were prepared with values near 2.5, 10.5, and 20%, which are the principal targets of the experiments in this study. Validation samples were obtained to verify the calibration curve, and the maximum error percent obtained was 2.36%. For the blue powder tracer, a calibration curve from 0 to 0.3 mg/ml was prepared, and the concentration was obtained by dissolving 500 mg of each blend sample (monohydrate lactose 70, MgSt, naproxen sodium and blue powder) in 100 mL volumetric flasks filled with distilled water. Samples of this solution were analyzed in the UV spectrometer.

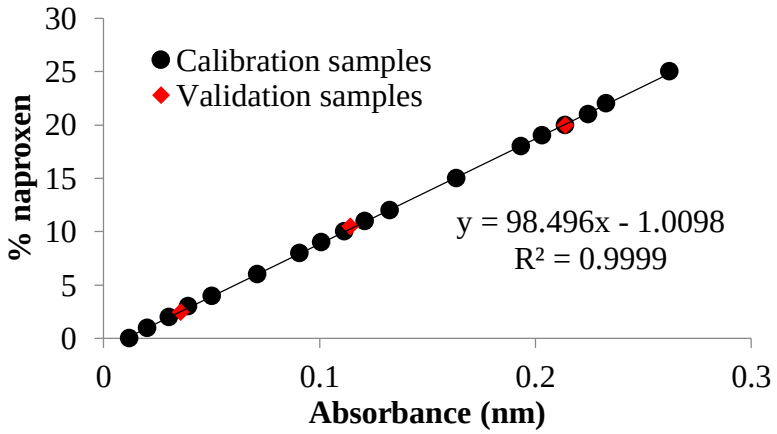

Figure 2.5. Calibration curve for naproxen.

2.3.7. Image Analysis

Pictures of the phenomena occurring inside the blender were taken using a Nikon D90 photographic camera to establish a qualitative relationship between the flow regimes and the mixing variability as a function of the API concentration, mixer parameters, and flow rate.

2.3.8. Scanning Electronic Microscopy (SEM)

Samples of lactose, magnesium stearate and naproxen sodium were analyzed in the SEM at magnifications from 500-3000X to observe the particulate morphology and the surface roughness and study the possible effects of these characteristics in the mixing process. Each sample was observed at different magnifications and for each selected magnification a minimum of three areas was observed to ensure that the characteristics are homogeneous on the surface.

2.3.9. Tap and bulk density techniques

The tap and bulk density techniques was used to compute the Carr's Compressibility Index and Hausner ratio, which are good flow indicators. These values were also related to the final homogeneity results.[15–17]

$$\boldsymbol{Carr\ Index} = \mathbf{100}\left(\mathbf{1} - \frac{\boldsymbol{\rho_{bulk}}}{\boldsymbol{\rho_{tap}}}\right) \quad (2.4)$$

$$\boldsymbol{Hausner\ Ratio} = \left(\frac{\boldsymbol{\rho_{tap}}}{\boldsymbol{\rho_{bulk}}}\right) \quad (2.5)$$

Carr Index values between 5 and 15% indicate excellent flow, and values higher than 25% indicate materials with poor flow properties. Values of the Hausner Ratio below 1.25 indicate good flow of the materials, while values over 1.25 represent materials with poor flow properties.[16]

2.4. References

1. Lu L-S, Hsiau S-S. DEM simulation of particle mixing in a sheared granular flow. *Particuology* 2008;6:445-454. doi:10.1016/j.partic.2008.07.006.
2. Xu Y, Xu C, Zhou Z, Du J, Hu D. 2D DEM simulation of particle mixing in rotating drum: A parametric study. *Particuology* 2010;8(2):141-149. doi:10.1016/j.partic.2009.10.003.
3. Arratia PE, Duong N, Muzzio FJ, Godbole P, Reynolds S. A study of the mixing and segregation mechanisms in the Bohle Tote blender via DEM simulations. *Powder Technol.* 2006;164:50-57. doi:10.1016/j.powtec.2006.01.018.
4. Remy B, Khinast J, Glasser B. Discrete element simulation of free flowing grains in a four- bladed mixer. *AIChE J.* 2009;55(8):2035-2048. doi:10.1002/aic.
5. Jayasundara CT, Yang RY, Yu AB, Curry D. Discrete particle simulation of particle flow in IsaMill—Effect of grinding medium properties. *Chem. Eng. J.* 2008;135(1-2):103-112. doi:10.1016/j.cej.2007.04.001.
6. Yang RY, Yu AB, McElroy L, Bao J. Numerical simulation of particle dynamics in different flow regimes in a rotating drum. *Powder Technol.* 2008;188(2):170-177. doi:10.1016/j.powtec.2008.04.081.
7. Barrios GKP, de Carvalho RM, Kwade A, Tavares LM. Contact parameter estimation for DEM simulation of iron ore pellet handling. *Powder Technol.* 2013;248:84-93. doi:10.1016/j.powtec.2013.01.063.
8. Weerasekara NS, Powell MS, Cleary PW, et al. The contribution of DEM to the science of comminution. *Powder Technol.* 2013;248:3-24. doi:10.1016/j.powtec.2013.05.032.
9. Mao K, Wang MY, Xu Z, Chen T. DEM simulation of particle damping. *Powder Technol.* 2004;142(2-3):154-165. doi:10.1016/j.powtec.2004.04.031.
10. Faqih AMN, Mehrotra A, Hammond S V, Muzzio FJ. Effect of moisture and magnesium stearate concentration on flow properties of cohesive granular materials. *Int. J. Pharm.* 2007;336:338-345. doi:10.1016/j.ijpharm.2006.12.024.
11. Florian M, Velázquez C, Méndez R. New continuous tumble mixer characterization. *Powder Technol.* 2014;256:188-195. doi:10.1016/j.powtec.2014.02.023.
12. Insitec dry process particle size analyzer from Malvern Instruments. Available at: http://www.malvern.com/processeng/systems/laser_diffraction/systems/insitec-dry.htm. Accessed October 21, 2012.
13. Vasilenko A, Glasser BJ, Muzzio FJ. Shear and flow behavior of pharmaceutical blends — Method comparison study. *Powder Technol.* 2011;208(3):628-636. doi:10.1016/j.powtec.2010.12.031.
14. Freeman R. Measuring the flow properties of consolidated , conditioned and aerated powders – a comparative study using a powder rheometer and a rotational shear cell. *Powder Technol.* 2007;174:25-33.

15. Kumar V, Reus-Medina M de la L, Yang D. Preparation, characterization, and tabletting properties of a new cellulose-based pharmaceutical aid. *Int. J. Pharm.* 2002;235:129-40. Available at: http://www.ncbi.nlm.nih.gov/pubmed/11879748.

16. Villanova JCO, Ayres E, Oréfice RL. Design of prolonged release tablets using new solid acrylic excipients for direct compression. *Eur. J. Pharm. Biopharm.* 2011;79(3):664-673. doi:10.1016/j.ejpb.2011.07.011.

17. Abdullah EC, Geldart D. The use of bulk density measurements as flowability indicators. *Powder Technol.* 1999;102:151-165.

Chapter 3

Published in *Journal of Powder Technology*, 2014, *Volume 256*, Pages 188-195

3. Continuous Tumble Mixer Experimental Characterization

A set of experiments was performed to characterize this continuous tumbler mixer. Based on previous work, it was determined that the parameters that affect the mixing performance are the materials properties, design parameters, and operational parameters.[1–4] The effect of different materials properties of the mixture (2.5, 10.5, and 20% of API) and operational parameters including five mixer speeds (10, 30, 50, 70, and 90) and three flow rates for each experiment were evaluated to measure their impact on the final blend uniformity. The principal responses of this combination of parameters are the powder phenomena inside the mixer, mean residence time, and relative standard deviation (RSD), which was the value used to determine the mixing uniformity at the exit of the mixer. This chapter depicts the effect of these parameters and the properties of the raw material on the final uniformity using the continuous tumble mixer.

3.1. Materials Characterization

Powder behavior depends on physical properties such as particle size and particle density, bulk powder properties, and external conditions.[5] Raw materials were characterized using the techniques explained in the experimental methods to obtain key properties: tap density, bulk density, Carr compressibility index, cohesion, and flow function. A summary of characterization results is shown in Table 3.1 and Figure 3.1.

Table 3.1. Material properties characterization

Material	Median Particle Size (µm)	Bulk Density (g/cm^3)	Tap Density (g/cm^3)	Carr Index (CI)	Flow Function (FFC)	Cohesion
Lactose 70	125	0.55	0.68	19.11	11.9	0.32
Lactose 140	63.26	0.65	1.06	38.7	3.07	1.44
Pre-blend	125	0.75	0.83	9.64	10.4	0.36
API	28.8	0.41	0.54	24.07	5.01	0.91
Blue Tracer	2.12	0.21	0.34	36.92	2.5	2.04
Glass beads	1000	1.48	1.48	0	-	-

The key result is that the pre-blend had a low cohesion or excellent flowability based on the Carr index value (< 15%) compared to the high value of the API (24.07%).[6,7] The compressibility test (Figure 3.1) was performed using the FT4 Powder Rheometer, and the results showed a higher compressibility for lactose 140, blue tracer, and naproxen sodium compared to the other materials. The compressibility of a particulate material can be related to particle size, flow properties, and cohesion.[7] Non-cohesive powders show small changes, while cohesive ones show high changes in compressibility.[8] Additionally, the flow function values are in accordance with Carr index and the cohesion material, values below 4 are considered cohesive and above 4 are classified as free-flowing.[5]

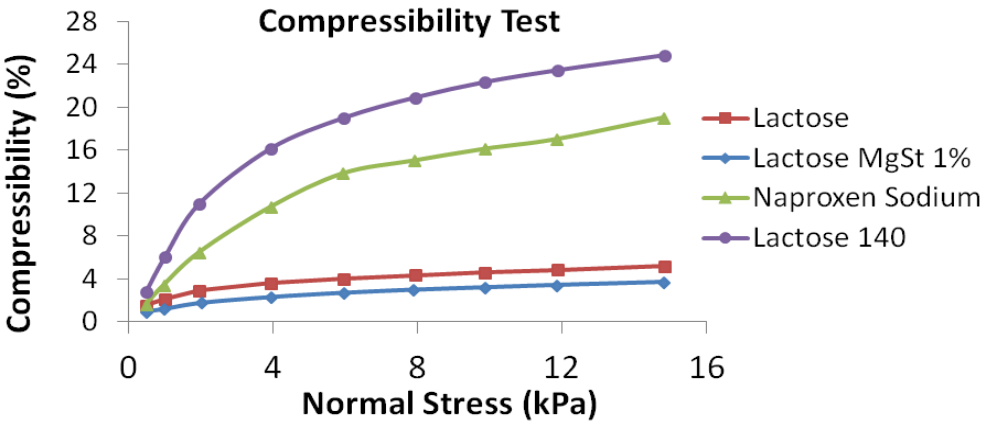

Figure 3.1. Compressibility test results.

The flow function, particle size, bulk density, tap density, and compressibility demonstrated that the excipients had better flow properties than the API. These differences presented a challenge because they are directly related to the cohesion. A high cohesion impacts the flow properties of the materials in the feeders, which directly affects the feed rate variability. Therefore, cohesion affects mixing processes and is also related to segregation.[1,9]

The particles morphology was characterized using SEM. Images of the particle surface for magnesium stearate, naproxen, and lactose, respectively are presented in Figure 3.2.

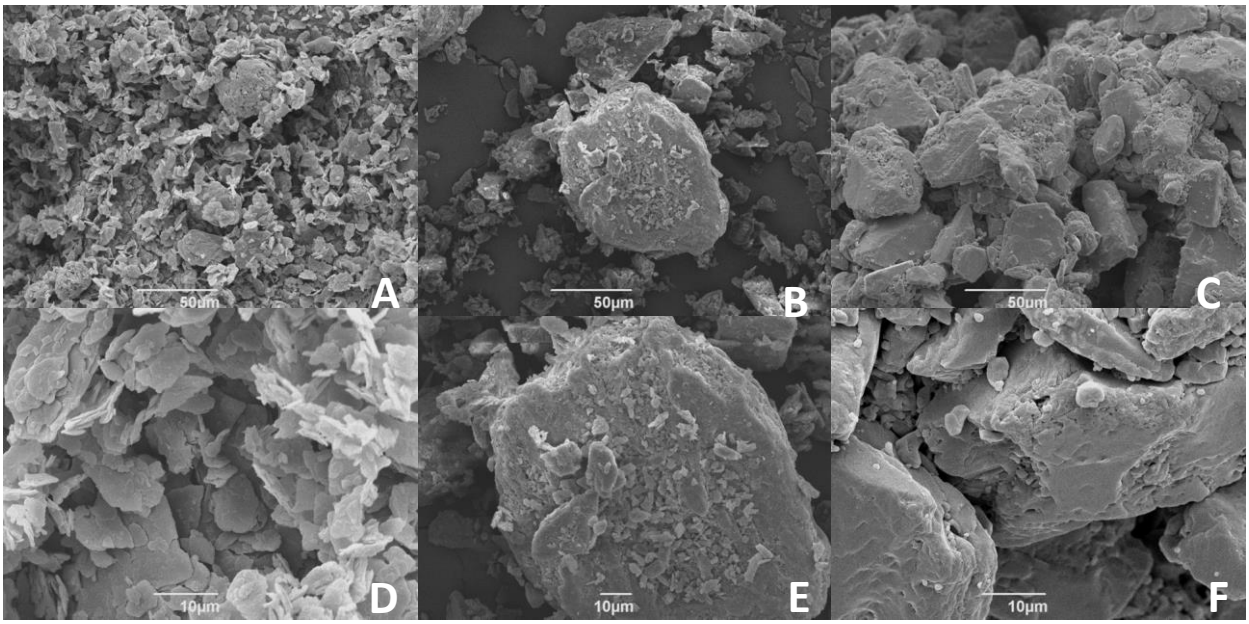

Figure 3.2. SEM images. MgSt at 500X (A), naproxen at 500X (B), lactose at 500X (C), MgSt at 20000X (D), naproxen at 1000X (E), and lactose at 1000X (F).

Using two different magnifications for the three components differences between each one are observed and these results are in agreement with the PSD results that show a low particle size for magnesium stearate and a higher particle size for lactose. These differences are a factor to consider because they influence the differences between physical properties (particle size, shape, and roughness) of the particles that affect the mixing performance of a blend[10] requiring a major effort to reach an optimal mixing and increasing the segregation problems.[11,12]

3.2. Flow behavior inside the mixer

The first step to characterize the continuous mixer was to study the material behavior inside the tumble mixer as a function of the operating parameters (mixer RPM and powder flow rate) and the powder properties (powder flowability and cohesion). This function can provide an understanding of the parameters necessary to reach the optimal flow regime that will produce higher particle-particle interactions and provide optimal mixing. The design of experiments (DOE)

included the following: three different RPM values (30, 50, and 70), three flow rates, and three materials with different properties (glass beads (Figure 3.3A), lactose 70 (Figure 3.3B), and a blend of 70% lactose 70 and 30% lactose 140 (Figure 3.3C)).

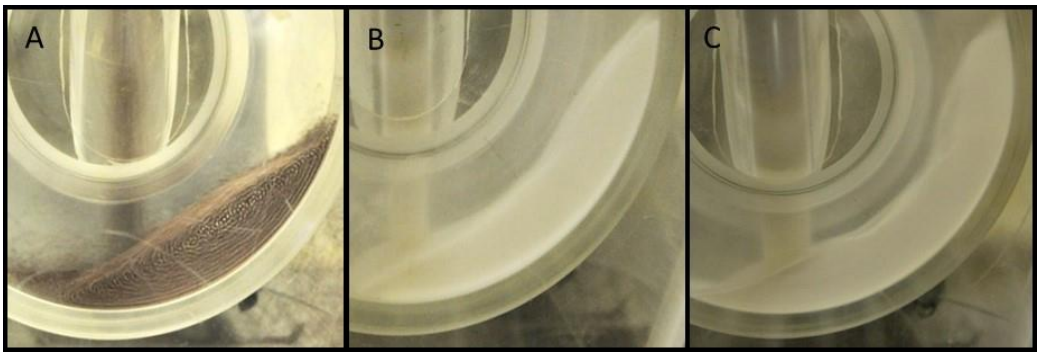

Figure 3.3. Photographs of flow regime characterization for glass beads (A), lactose 70 (B), and lactose blend (70% lactose 70 and 30% lactose 140) (C).

Figure 3.3 illustrates the powder behavior inside the mixer at 50 RPM. The glass beads showed a rolling behavior (Figure 3.3A), and the lactose and lactose blend (Figures 3.3B and C, respectively) showed a cascading behavior based on the avalanche shape and the Froude Number value (0.0767).[13–15] As previously explained, obtaining a rolling or cascading regime is a good indication of the mixing degree based on the behavior of batch mixers.[15] Rolling is the flow regime most widely studied.[14,16–18]

Figure 3.3 also demonstrates the effect of particle size and cohesion on powder phenomena. The use of different flow rates (60, 60, and 55 kg/h for Figures 3.3A, B, and C, respectively) was necessary to maintain a constant mass hold-up. Figure 3.3C shows that the blend had a smaller PSD and a higher cohesion value than the materials in 3.3A and B. Although the blend in 3.3C had a smaller particle size distribution, which could more easily fit in the exit holes of the mixer (4 mm), its cohesion or likeliness to flow together reduced the facility to enter the exit holes and finally exit. This effect reduced the exit flow and thus the inlet flow to maintain a constant mass hold-up.

The same preferences to flow as a pack bed (higher cohesion) caused the difference in avalanche patterns, as mentioned above. This flow regime was similar in both the batch and continuous modes and corresponded to the flow regimes found by Aissa et al.[17] In addition, Figure 3.3A shows a recirculation zone in which the active layer and the stagnant zone can be identified.

The flow rate effect on the powder phenomena was also studied, and the results are shown in Figure 3.4. A change from the cascading to the cataracting regime was obtained as the flow increased (45, 75 and 82 kg/h for Figures 3.4A, B, and C, respectively) for a blend (lactose with 1% MgSt) at 10.5% API and 70 RPM in the mixer. At a constant mixer speed, a change in flow rate produces an increment in the mass hold-up, which corresponds to the accumulation.

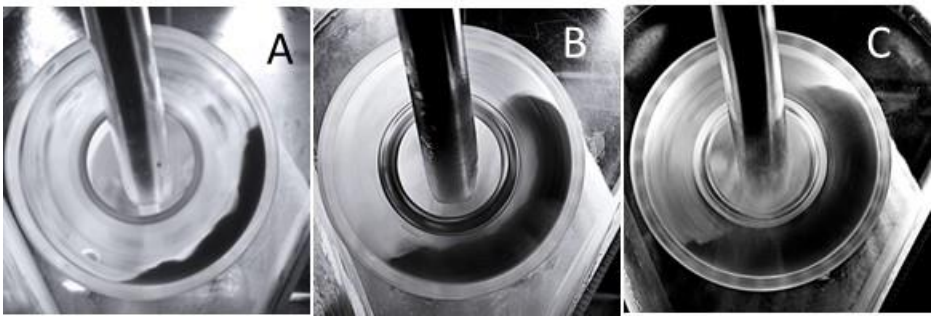

Figure 3.4. Flow rate effect on powder phenomena at 70 RPM and 10.5% naproxen, at 45 (A), 75 (B), and 82 kg/h (C).

A larger flow rate produces a larger mass hold-up to impart a larger normal force on the powders at the bottom of the powder bed. This larger force will push more powder to exit the mixer so that the exit flow matches the inlet flow. When these flows are matched, the mass hold-up reaches steady state. Because more powder is inside the mixer, a higher force is exerted on the bottom powders, and the avalanche pattern changes to the obtained behavior.

In summary, powder properties (PSD and cohesion) and operating conditions, such as the RPMs and inlet flow rate, must be considered to obtain the required mixing.

3.3. Mixing performance

The next objective was to demonstrate the capability of the mixer to achieve the desired levels of mixing. The following conditions were used in the experiment: three flow rates, five RPM values (10, 30, 50, 70, and 90) and three naproxen concentrations (2.5, 10.5, and 20%). As demonstrated in the section 3.1, naproxen is a cohesive material compared to lactose and changes in its concentration produce changes in the flow properties of the mixture. The feeders were adjusted to obtain both the required API concentration and total flow rate. The samples (500 mg) to determine the mixing uniformity were collected every 5 sec at the end of a conveyor belt placed at the outlet of the system.

The mixing performance of these experiments was further quantified using the RSD of the outlet concentration after the system reached steady state. For the experiments at 2.5% and 10.5% the steady state was selected after two minutes and for 20% after four minutes. The RSD parameter is included in the FDA guidancel[19] for batch mixing processes and has been used to measure the mixing uniformity in different studies of continuous mixing processes.[2,3,20] Values higher than 6% RSD are considered undesirable, those below 6% are considered to marginally pass, and those below 4% are considered to readily pass.[19] Because continuous processes are not regulated, this batch parameter was used to monitor the continuous mixing variability and served as an indicator of the process feasibility.

Figure 3.5 displays the results obtained for the experiments at the lowest (10 RPM) and highest (90 RPM) mixer speeds. Only two flow rates could be tested for each speed to avoid low accumulation inside the mixer or overflows on the side of the mixer

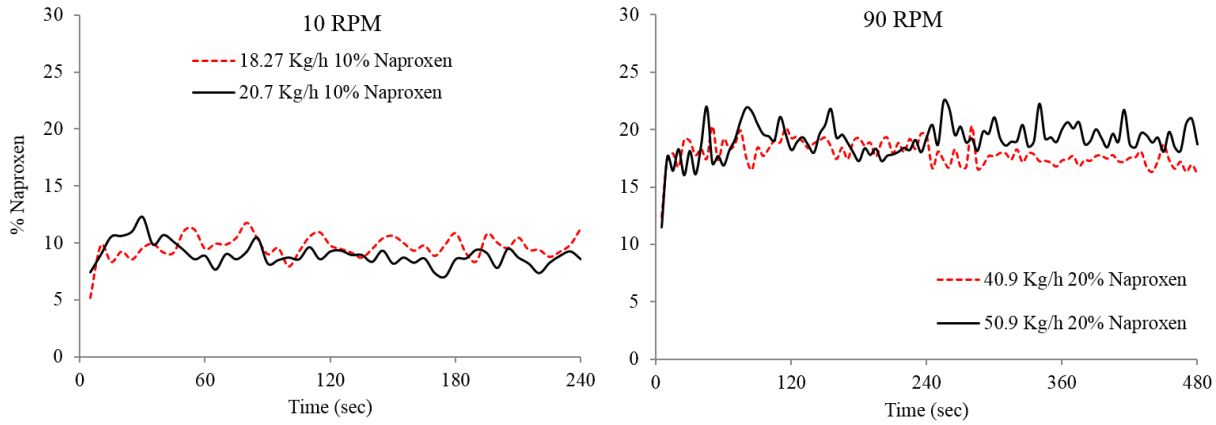

Figure 3.5. Mixing performance for 10 (A) and 90 RPM (B).

Figure 3.5 shows the mixing performance at 10 (A) and 90 (B) RPM for two different flow rates. At 10 RPM, the results showed an oscillatory trend near 10.5% API with a similar RSD of 8% (from Figure 3.7B). The major problem at this speed was the difficulty to operate the system between 18 to 21 kg/h. Flows below 18 kg/h resulted in a very low mass hold-up inside the mixer, while flow rates higher than 21 kg/h caused overflows off the side of the mixer. At 90 RPM, the results for 20% API showed good mixing with RSD values below 6% (from Figure 3.7C). However, the feasible flow rates ranged from 40 to 50 kg/h, which indicate a limited range of operability compared to 30, 50 and, 70 RPM. In summary, the mixer can achieve good mixing at both speeds, but its operability is limited, especially when the flow rate requires adjustments to comply with new operating conditions.

Figures 3.6A, B, and C depict the mixing performance at 30, 50, and 70 RPM, respectively. The RSD at 30 RPM was higher than those at 50 and 70 RPM, as confirmed in Figure 3.7.

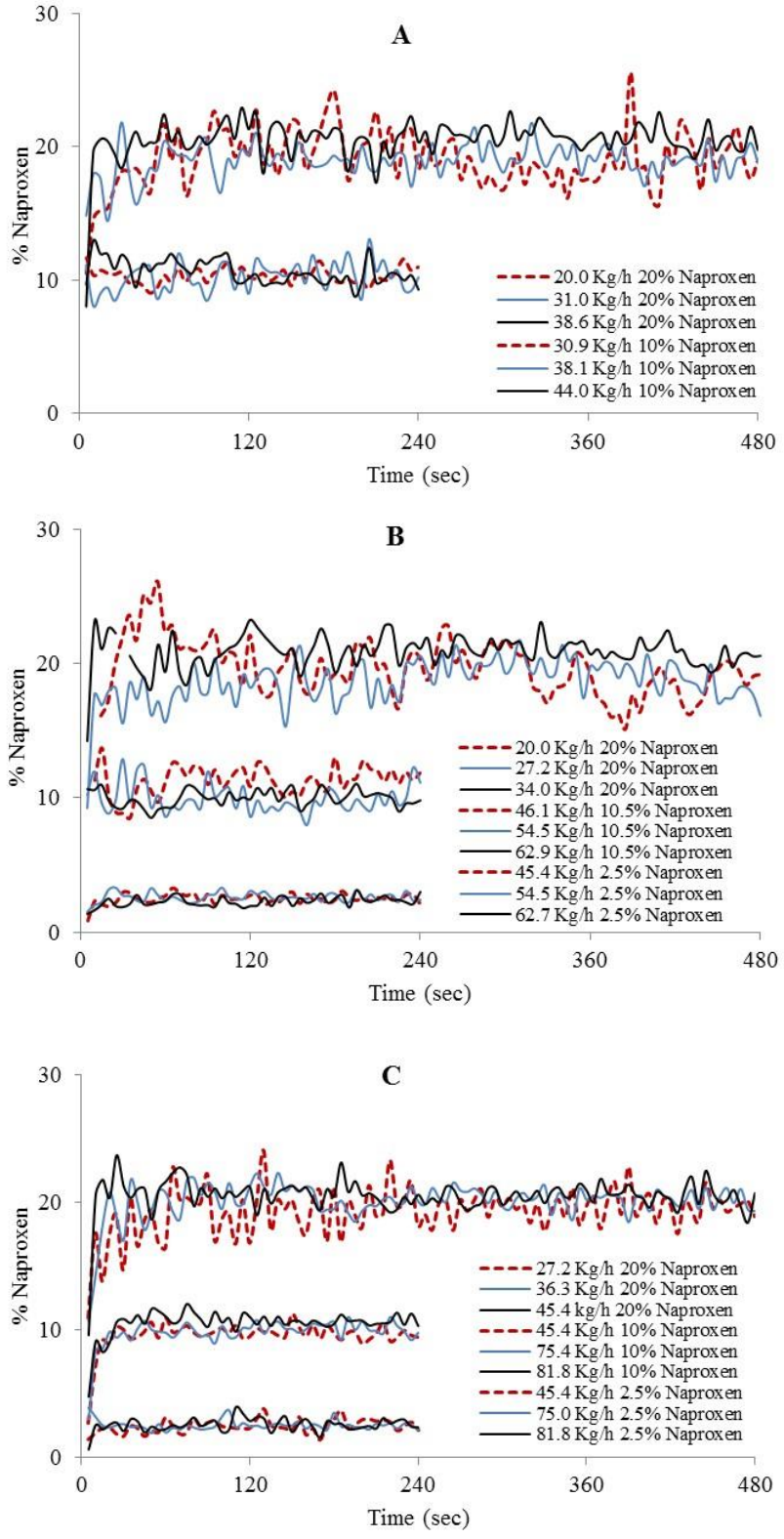

Figure 3.6. Mixing performance for 30 (A), 50 (B), and 90 RPM (C).

Based on these results, the 10, 30, and 90 RPM conditions were discarded, and the remaining experiments focused on 50 and 70 RPM, which resulted in lower RSD values.

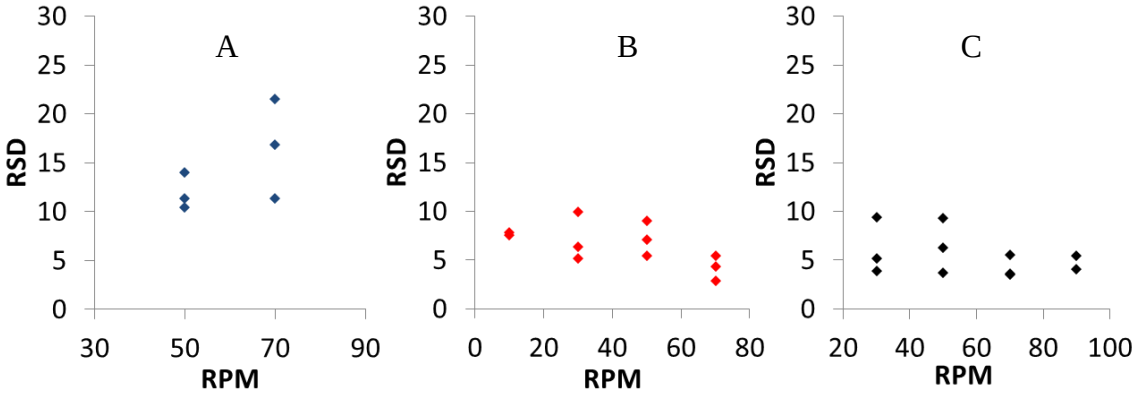

Figure 3.7. RSD values at 2.5 (A), 10.5 (B) and 20% (C) API concentration.

The mixing performances at 50 and 70 RPM are depicted in Figures 3.6B and C for three levels of API concentration (2.5, 10.5, and 20%) and three different flow rates for each concentration. First, the results established that an increment in the API concentration (more cohesion) increased the time required to stabilize mixing and it is necessary to increase the mixer speed to reduce the variability. Second, the flow rate range used at each condition represents the feasible range to avoid the complete emptying of the mixer (lower flow rate) or overflow off the side (largest flow rate). Each flow rate range depended on the mixer speed and the cohesion of the material, which confirmed the results obtained in the experiments shown in Figure 3.4.

Figure 3.7 shows that the medium and higher concentration levels (10.5 and 20% API) showed lower relative standard deviations in comparison to the 2.5% API concentration. A review of the uniformity results is shown in Table 3.2 including average concentration, standard deviation, and relative standard deviation where it is possible to observe that the lower standard deviations were obtained using the lowest concentration. Even, when this concentration produces the highest relative standard deviation.

Table 3.2. Effect of RPM, flow rate, and target concentration on average, standard deviation, and RSD

RPM	50			70		
Concentration	**2.5% of naproxen**					
Flow rate	**Low**	**Medium**	**High**	**Low**	**Medium**	**High**
Average	2.5	2.6	2.4	2.6	2.5	2.5
Standard deviation	0.3	0.3	0.3	0.5	0.3	0.4
RSD	11.4	10.5	14.1	21.1	11.4	16.8
Concentration	**10.5% of naproxen**					
Average	11.4	9.7	10.1	9.7	10.1	10.6
Standard deviation	0.8	0.9	0.6	0.5	0.4	0.3
RSD	7.1	9.0	5.5	5.4	4.4	2.8
Concentration	**20% of naproxen**					
Average	19.1	19.3	20.9	19.6	20.3	20.5
Standard deviation	1.8	1.2	0.8	1.1	0.7	0.7
RSD	9.3	6.3	3.7	5.5	3.5	3.7

The three concentration levels primarily differed in their cohesion and powder flowability. To measure the reproducibility of our system the three experiments at 10.5% and three different flow rates were replicated and the results are shown in Figure 3.8.

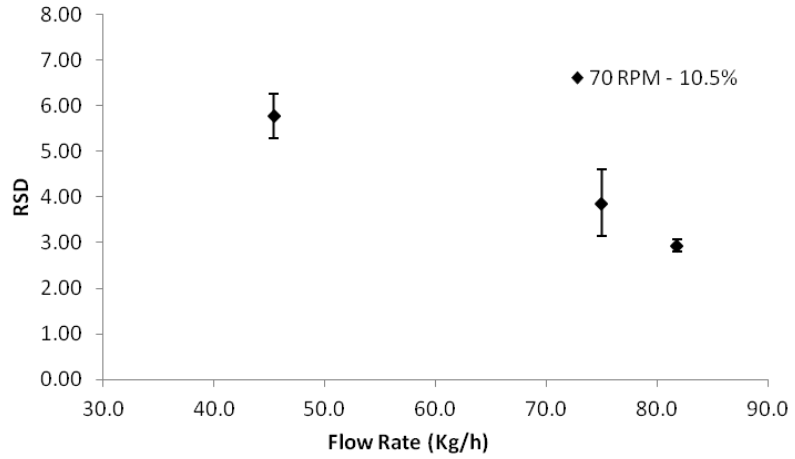

Figure 3.8. Mixing reproducibility at 70 RPM.

These values demonstrated that the system has reproducibility and that the variability is low. At low API concentrations, the flow of powder through the orifices was higher, which reduced the mass hold-up and the time available for mixing (Figure 3.9). As supported by Figure 3.7, the continuous tumble mixer has been demonstrated capable of achieving adequate mixing when using the adequate flow rate and mixer velocity for low to moderate cohesive material.

The behavior depicted in Figure 3.4 was related to the filling ratio, a parameter that has been related to the mixing performance[17] and to some of the changes obtained in flow regimes[21,22] at constant mixer speed. The filling ratio refers to the mass of material inside the mixer (mass hold-up) when the process reached steady state. Figure 3.9 depicts the values obtained for the experiments at 50 and 70 RPM and API concentrations of 2.5, 10.5, and 20%.

In the continuous tumble mixer, the powder principally exits through the orifices at the bottom of the tumble as well as through the orifices in the wall. Because the orifice characteristics are constant, a larger force must be exerted to the powders at the entrance of the orifices to increase the total flow rate and consequently increase the flow through the confined space. Therefore, a larger mass hold-up is necessary to increase the force exerted over the powders and ensure that the powder flow rate equals the inlet flow rate if the material enters the tumble at a higher flow rate. This behavior is confirmed in Figure 3.9.

In addition, if the cohesion of the entering material is increased at constant tumble speeds, a larger mass hold-up is necessary to apply a larger force on the powders at the entrance of the orifices to compensate for the increased tendency of the powders to flow as a pack (larger cohesion) and generate an exit powder flow rate equal to the inlet flow. Figure 3.9 shows that both tumble speeds needed larger mass hold-up values to reach the steady state as the cohesion increased.

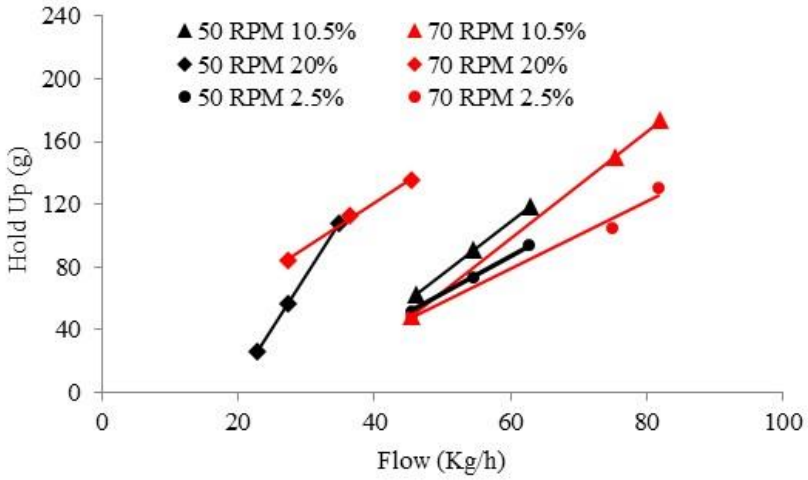

Figure 3.9. Mass hold-up as a function of flow and API concentration.

The combination of Figures 3.7 and 3.9 shows that the RSD decreased as the mass hold-up increased due to higher speeds, flow rates, or cohesion. Therefore, moderately cohesive blends can be well mixed in the continuous tumble mixer. Smaller orifices can be used for low cohesive materials (easier to flow), so that a larger force will be required to obtain the required exit flow. This larger force will be obtained with larger mass hold-up values.

3.4. Residence Time Distribution and Mean Residence Time (MRT)

The residence time distribution and the mean residence time quantify the time that the particles remain inside the mixer interacting among each other. *E*(t) is sometimes referred to as the exit age distribution function and characterizes the time various particles spend in the mixer.[23] This distribution and the mean residence time are related to mixing uniformity.[24] In this research, 1 gram of tracer (blue powder) was used and tracked to determine the RTD. This is a small quantity compared to the mass hold-up inside the system (45-180 grams) and due to the physical characteristics of the tracer; the flow regime inside the system was not affected by it.

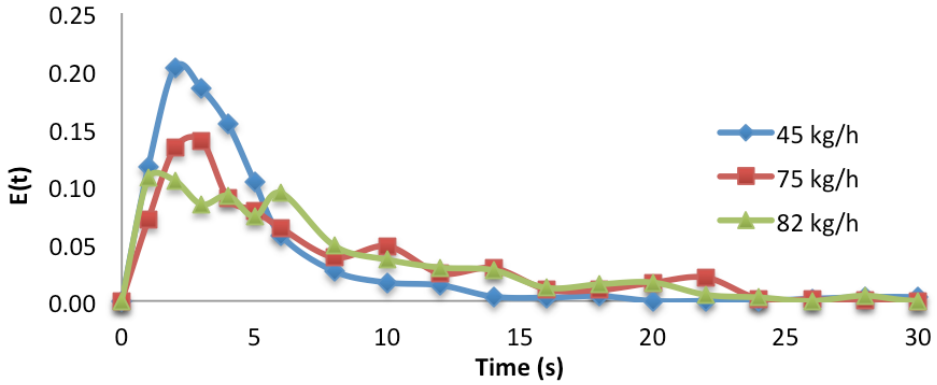

Figure 3.10. Flow rate effect at 70 RPM on RTD.

Figure 3.10 depicts the effect of the total feed rate on the RTD at 10.5% API and 70 RPM. The trend of the RTD of the continuous mixer was compared to an ideal continuous stirrer tank reactor (CSTR) with the same space-time using Eq. 3.1 where τ is the space-time.

$$E(t) = \frac{1}{\tau} e^{-\frac{t}{\tau}} \tag{3.1}$$

Figure 3.11 shows the comparison of the RTD curves of the experiment using 45 kg/h and the corresponding curve computed with Eq. 3.1. The RTD behavior showed a good agreement with an ideal CSTR model following the behavior of a linear first order process.

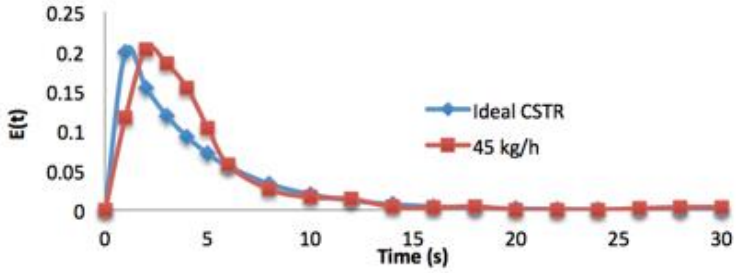

Figure 3.11. Comparison between the ideal RTD of a CSTR and the experimental RTD.

The calculated values of MRT are shown in Table 3.3 and these are relatively small; between 3.17 and 10.54 seconds. This finding indicates that MRT values increase when concentration increases and decrease when RPM increases.

Table 3.3. Effect of mixer speed, flow rate, and concentration on mean residence time

Concentration	RPM	50			70		
2.50%	Flow(kg/h)	45.4	54.50	62.70	45.40	75.00	81.8
	MRT	3.99	4.36	7.14	3.17	4.80	7.7
10.50%	Flow(kg/h)	46.1	54.50	62.90	45.40	75.00	81.80
	MRT	5.46	8.46	8.84	8.42	9.35	10.54

Therefore, the high degree of mixing obtained was the result of the combination of the MRT, the high dilation caused by the speed of the tumbler, and the convective movement in the active zone.

3.5. RPM, flow rate, and material properties effect on powder behavior

Section 3.2 was further expanded with 5 additional blends that had different material properties. Table 3.4 describes the additional 5 blends that were passed through the continuous tumble mixer operating at five different RPM values (10, 30, 50, 70, and 90) and three different mass hold-ups (80, 100, and 120 g). The five velocities (10, 30, 50, 70, and 90) corresponded to Froude numbers of 0.019, 0.17, 0.48, 0.94, and 1.5, respectively. The images of the powder dynamics were collected during operation and analyzed to establish the type of avalanche. This information was then used to develop a map that relates the powder compressibility, type of avalanche, and RPM values. A previous investigation about flow regime used the filling ratio, Froude number, and drum wall friction coefficient to predict flow regime.[25] Our results permit using an optimal combination of operational parameters, and by knowing the material properties predict the flow regime using the proposed maps.

Table 3.4. Sample composition and compressibility values

Composition		Sample	% Compressibility
Tablettose 70	**GranuLac 140**		
100	0	Mix 1	2.54
97.5	2.5	Mix 2	2.65
89.5	10.5	Mix 3	2.98
80	20	Mix 4	4.83
70	30	Mix 5	8.12
Control samples		10.5 % API	2.99
		20.0 % API	5.19

The powder compressibility of each of the five blends was obtained using the FT4 unit. Figures 3.12A and B depict the map of the powder behavior and compressibility values as a function of the RPMs for mass hold-up values of 80 and 120 g, respectively. Both maps include the 3 more common flow regimes found in a batch drum mixer: (1) rolling, (2) cascading, and (3) cataracting. Rolling was only observed for RPM values of 30 or lower, a mass hold-up of 80 g (Figure 3.12A), and compressibility values below 4.83. At a mass hold-up of 120 g, only the cascading and cataracting flow regimes are shown. The large mass hold-up results in a higher pressure over the bottom particles, which changes the avalanche pattern.

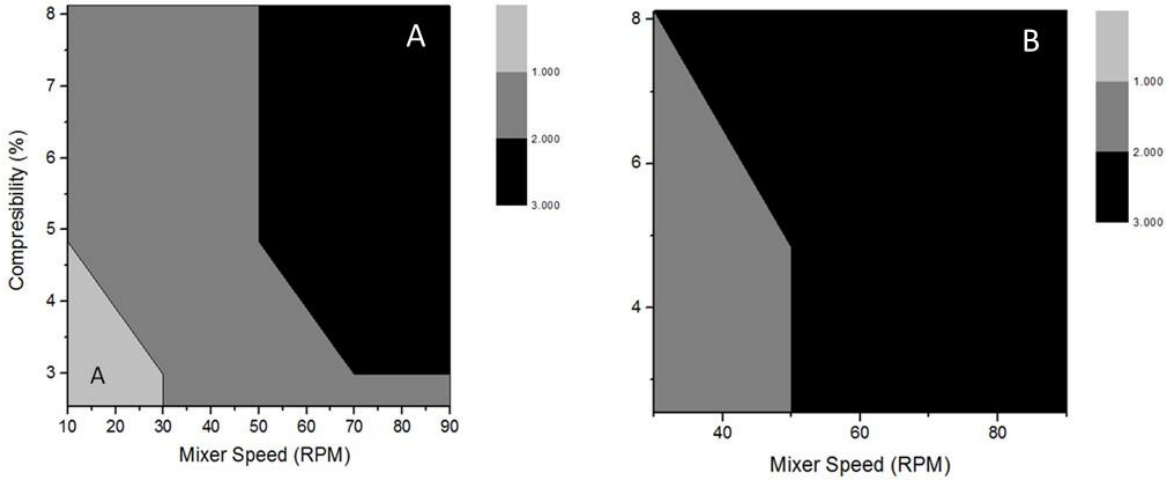

Figure 3.12. Compressibility map at 80 g (A) and 120 g (B) Mass Hold-up.

The 10.5% naproxen blend powder showed a cascading behavior for mass hold-up values below 80 g. This behavior changed to a cataracting behavior at higher mass hold-up values. Only the cataracting regime was observed for the 20% blend. Based on the blend uniformity results, better mixing was obtained at 70 RPM and mass hold-up values above 120 g, which resulted in a cataracting pattern. Therefore, the operating conditions must be set at the continuous tumble mixer following the powder behavior map of Figures 3.12 to ensure a cataracting avalanche pattern.

3.6. Conclusions

The continuous tumble mixer was demonstrated to provide highly uniform blends. The powder phenomena inside the mixer were similar to the batch counterpart and depended on the total flow rate, the material properties, and the operational parameters. The best mixing level was reached using a high powder flow rate and 70 RPM. The powder behavior map permits the selection of operating conditions that would establish a cataracting avalanche, which was the flow regime that produced the highest blend uniformity. Based on the lower MRT, a higher particle-particle interaction was required to improve the mixing.

3.7. References

1. Sarkar A, Wassgren C. Continuous blending of cohesive granular material. *Chem. Eng. Sci.* 2010;65(21):5687-5698. doi:10.1016/j.ces.2010.04.011.
2. Portillo PM, Ierapetritou MG, Muzzio FJ. Effects of rotation rate ,mixing angle, and cohesion in two continuous powder mixers: A statistical approach. *Powder Technol.* 2009;194(3):217-227. doi:10.1016/j.powtec.2009.04.010.
3. Vanarase AU, Muzzio FJ. Effect of operating conditions and design parameters in a continuous powder mixer. *Powder Technol.* 2011;208(1):26-36. doi:10.1016/j.powtec.2010.11.038.
4. Sarkar A, Wassgren CR. Simulation of a continuous granular mixer: Effect of operating conditions on flow and mixing. *Chem. Eng. Sci.* 2009;64(11):2672-2682. doi:10.1016/j.ces.2009.02.011.
5. Leturia M, Benali M, Lagarde S, Ronga I, Saleh K. Characterization of flow properties of cohesive powders: A comparative study of traditional and new testing methods. *Powder Technol.* 2014;253(2014):406-423. doi:10.1016/j.powtec.2013.11.045.
6. Kumar V, Reus-Medina M de la L, Yang D. Preparation, characterization, and tabletting properties of a new cellulose-based pharmaceutical aid. *Int. J. Pharm.* 2002;235:129-40. Available at: http://www.ncbi.nlm.nih.gov/pubmed/11879748.
7. Villanova JCO, Ayres E, Oréfice RL. Design of prolonged release tablets using new solid acrylic excipients for direct compression. *Eur. J. Pharm. Biopharm.* 2011;79(3):664-673. doi:10.1016/j.ejpb.2011.07.011.
8. Fu X, Huck D, Makein L, Armstrong B, Willen U, Freeman T. Effect of particle shape and size on flow properties of lactose powders. *Particuology* 2012;10:203-208. doi:10.1016/j.partic.2011.11.003.
9. Chaudhuri B, Mehrotra A, Muzzio FJ, Tomassone MS. Cohesive effects in powder mixing in a tumbling blender. *Powder Technol.* 2006;165:105-114. doi:10.1016/j.powtec.2006.04.001.
10. Bellamy LJ, Nordon A, Littlejohn D. Effects of particle size and cohesive properties on mixing studied by non-contact NIR. *Int. J. Pharm.* 2008;361:87-91. doi:10.1016/j.ijpharm.2008.05.030.
11. Felix G, Falk V, Ortona UD. Segregation of dry granular material in rotating drum: experimental study of the flowing zone thickness. *Powder Technol.* 2002;128:314-319.
12. Aissa A, Duchesne C, Rodrigue D. Longitudinal segregation of polymer powder in a rotating cylinder. *Powder Technol.* 2011;207:324-334. doi:10.1016/j.powtec.2010.11.014.
13. Yang RY, Yu AB, McElroy L, Bao J. Numerical simulation of particle dynamics in different flow regimes in a rotating drum. *Powder Technol.* 2008;188(2):170-177. doi:10.1016/j.powtec.2008.04.081.
14. Cheng N-S, Zhou Q, Keat Tan S, Zhao K. Application of incomplete similarity theory for estimating maximum shear layer thickness of granular flows in rotating drums. *Chem. Eng. Sci.* 2011;66:2872-2878. doi:10.1016/j.ces.2011.03.050.

15. Aissa AA, Duchesne C, Rodrigue D. Transverse mixing of polymer powders in a rotary cylinder part I: Active layer characterization. *Powder Technol.* 2012;219:193-201. doi:10.1016/j.powtec.2011.12.040.

16. Wightman C, Muzzio FJ. Mixing of granular material in a drum mixer undergoing rotational and rocking motions I. Uniform particles. *Powder Technol.* 1998;98:113-124.

17. Aissa AA, Duchesne C, Rodrigue D. Effect of friction coefficient and density on mixing particles in the rolling regime. *Powder Technol.* 2011;212:340-347. doi:10.1016/j.powtec.2011.06.009.

18. Ding Y, Seville J, Forster R, Parker D. Solids motion in rolling mode rotating drums operated at low to medium rotational speeds. *Chem. Eng. Sci.* 2001;56:1769-1780. Available at: http://www.sciencedirect.com/science/article/pii/S0009250900004681. Accessed October 14, 2014.

19. FDA. *Guidance for Industry. Powder Blends and Finished Dosage Units — Stratified In-Process Dosage Unit Sampling and Assessment*.; 2003.

20. Arratia PE, Duong N, Muzzio FJ, Godbole P, Reynolds S. A study of the mixing and segregation mechanisms in the Bohle Tote blender via DEM simulations. *Powder Technol.* 2006;164:50-57. doi:10.1016/j.powtec.2006.01.018.

21. Aissa A, Duchesne C, Rodrigue D. Polymer powders mixing part II: Multi-component mixing dynamics using RGB color analysis. *Chem. Eng. Sci.* 2010;65:3729-3738. doi:10.1016/j.ces.2010.03.007.

22. Aissa A, Duchesne C, Rodrigue D. Polymer powders mixing part I: Mixing characterization in rotating cylinders. *Chem. Eng. Sci.* 2010;65:786-795. doi:10.1016/j.ces.2009.09.031.

23. Fogler HS. *Element of Chemical Reaction Engineering*. 3rd ed. Prentice Hall; 1999:812-822.

24. Gao Y, Vanarase A, Muzzio F, Ierapetritou M. Characterizing continuous powder mixing using residence time distribution. *Chem. Eng. Sci.* 2011;66:417-425. doi:10.1016/j.ces.2010.10.045.

25. Mellmann J. The transverse motion of solids in rotating cylinders—forms of motion and transition behavior. *Powder Technol.* 2001;118(3):251-270. doi:10.1016/S0032-5910(00)00402-2.

Chapter 4

Published in *AIChE Journal*, 2014, DOI 10.1000/aic.14694

4. Blend Uniformity and Powder Phenomena inside the Continuous Tumble Mixer using DEM Simulations

The goals of this chapter were to understand the effect of operating parameters and materials properties on powder phenomena inside the continuous tumble mixer and mixing uniformity inside and at the exit of the system using DEM simulations. In addition, the velocity profiles and the flow regimes were validated experimentally. The mean residence time was measured to determine the system response and measure the time available for particle interaction and mixing.

Figure 4.1 shows a schematic model based on the real system that was used to simulate the mixing process. The system includes the mixer and two factories where particles 1 and 2 are produced. These factories play the role of the feeders in the experimental part.

In this mixing process the incoming material interacts with the powder that is already in the system. Points A and B in Figure 4.1 represent particles generation using a flow of 0.009 Kg/h of particles 1 and 2 which are identified with colors red and blue, respectively. Particle generations are placed on top of the system and these positions agree with the manner in which particles are fed on the experimental system.

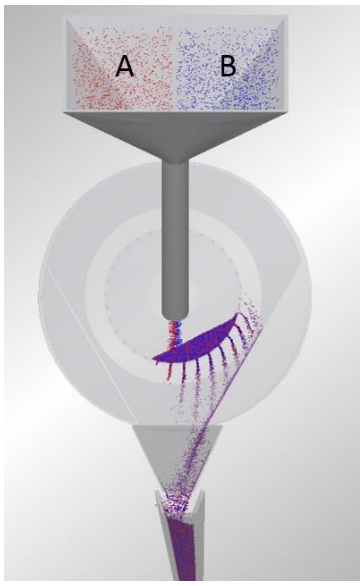

Figure 4.1. Simulated continuous tumble mixer.

The DOE includes mixer speed (50 and 70 RPM), and four different values were selected for the cohesion energy density. Other simulation parameters and the particle characteristics used in these simulations are shown in Tables 4.1 and 4.2, respectively.

Table 4.1. Simulation parameters and reference values

Simulation Parameters	Used values	Reference values
Poison Radius	0.5	0.25-0.3 [1–4]
Shear Modulus (Pa)	2.00E+06	2.00E06-3.00E08 [1,2]
Coefficient of restitution	0.05	0.5-0.9 [1–6]
Coefficient of static friction	0.5	0.3-0.5 [2,3,6]
Coefficient of rolling friction	0.005	0.001-0.005 [2–6]
Generation rate (Kg/s)	0.018	-

Materials properties of particulate material are affected by different characteristics, such as particle size distribution, particle shape, surface of the particles, density, and others. These characteristics produce changes in the flow properties of the powder, and these flow properties are reflected in the materials cohesion. Using DEM simulations it is possible to add a cohesion effect to the material. Several studies demonstrated the cohesion effect on the flow properties and in the final mixing uniformity, using simulations.[7–10]

Table 4.2. Particle characteristics

Mass (g)	0.00073
Density (g/cm^3)	1.4
Standard Deviation	0.0
Diameter (mm)	1.0

The cohesion equation included in DEM software® used to add this property to the particles was obtained using the linear cohesion model (Eq. 4.1). Where A is the contact area (m^2) and *k* represents the cohesion energy density (J/m^3). This model is a modification of the default Hertz-Mindling contact model for particle interactions and for particle geometry adding a normal cohesion force.

$$F=kA \tag{4.1}$$

To select the values of the cohesion energy density, a batch tumble mixer was simulated using different values until a change on powder behavior was observed. Figure 4.2 shows the results for simulations without cohesion and cohesion 2 at 50 RPM. An increment in the angle formed by the powder bed before sliding or avalanching was observed. This change affects the powder flow behavior and is caused by particle-particle and particle-wall cohesion. Based on this result a higher cohesion value was added to the simulations' DOE to obtain a better understanding of the cohesion effect on powder flow phenomena and mixing performance.

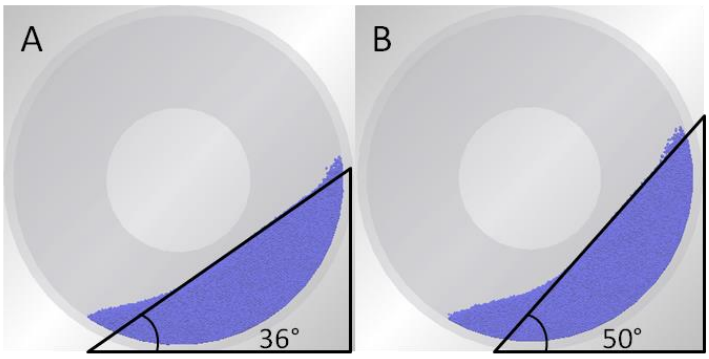

Figure 4.2. Batch mixer using cohesion 0 (A) and 2 (B) at 70 RPM.

The complete DOE includes four different cohesion values; at 70 RPM, 0, 10000, 20000, and 30000 J/m^3 that were used as the cohesion energy density. At 50 RPM the highest cohesion value caused an overflow. The material drops through the feeding side of the mixer to the powder-collecting zone inside the system, affecting blend uniformity and reducing the range of system operability at 0.018 kg/s. A similar behavior was found in the experimental part where the use of highly cohesive materials produced overflow inside the system at a certain flow rate. To avoid this effect and keep the flow rate constant the value of 30000 J/m^3 was changed for 25000 J/m^3 (50 RPM simulation). For the cohesions mentioned above, the results do not demonstrated the presence of agglomerates or clumps.

From now on, to identify the simulations (Table 4.3), these will be referenced with the mixer RPM (50 or 70) and the cohesion value (0, 1, 2, or 3). For all the simulations the particle-particle interaction is two times the particle-wall interaction.

Table 4.3. Particle characteristics

Cohesion Energy Density	0	1	2	3
Cohesion particle-wall at 50 RPM (J/m^3)	0	5000	10000	12500
Cohesion particle-wall at 70 RPM (J/m^3)	0	5000	10000	15000
Cohesion particle-particle at 50 RPM (J/m^3)	0	10000	20000	25000
Cohesion particle-particle at 70 RPM (J/m^3)	0	10000	20000	30000

The following variables were analyzed for the complete simulation set: concentration at the end of the system, mass hold-up inside the mixer, RTD, mixing uniformity inside the system, exits effect on final concentration, flow regimes, and velocity profiles.

To measure the quantity and concentration of particles, volume selections were created in different places of the system. The mass hold-up and mixing uniformity at the exit, tumble exits, and inside the mixer were calculated using these volumes. DEM software® calculates the quantity of particles 1 and 2 in each selection. Using these values the concentration was calculated. Particles shared or overlapping two or more cells or volume selections are only counted one time, based on the position of its center of mass. Other methods such as Point Approximated Method (PAM) and Discrete Particle Method (DPM) use different forms to approach the effect of particles divided in different cells. PAM omits the particle shape replacing it by a point, which as in our case neglects the split of particles between cells. On the other hand, an analytical method based on DPM was developed in order to take into account the fraction of a particle that belongs to each cell in the accurate calculation of void fraction.[11]

4.1. Mass hold-up

Mass hold-up is an important variable in continuous processes related to mixer speed and flow rate.[12,13] Mass hold-up was obtained from the total particle mass of a volume selection inside the tumble. Figure 4.3 depicts changes in mass hold-up as a function of time until the mixer reaches mass steady state. At 50 RPM, for the simulations with cohesion 0 and 1, the time needed to achieve the steady state was similar and close to 30 s, for a cohesion slightly higher (cohesion 2) the steady state time increases by more than 2 times, and for the highest cohesion time it increases by 6 times relative to cohesion 0. At the highest RPM (70) the effect of cohesion energy density on the steady state time was smaller and the results showed practically the same time for cohesion 0, 1, and 2, and only showed a significant effect on steady state time for cohesion 3 that was comparable to the value at 50 RPM for cohesion 2.

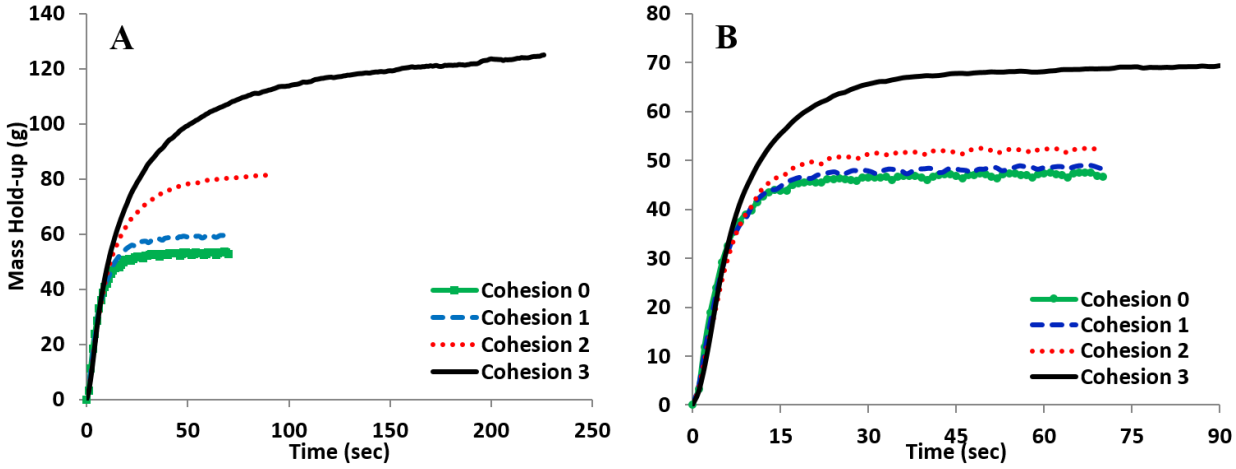

Figure 4.3. Mass hold-up at 50 RPM (A) and 70 RPM (B).

These results indicated a higher effect of normal and centrifugal forces due to the increment in rotational velocity, which reduces the effect of the cohesion energy density. A higher cohesion value was required to promote a change in powder flow regime.

Summarizing the results in Table 4.4, it is possible to observe that for a given mixer speed, larger cohesion values require larger accumulation of material to achieve steady state. The results showed an increment in the accumulation at constant feed rate when the mixer speed decreases and the cohesion values increase. This is an effect of the reduction in material flowability through the mixer exits due to particle-particle interaction caused by the cohesion.

Table 4.4. Cohesion effect on mass hold-up and MRT

Cohesion	Mass hold-up (g)		MRT	
	50 RPM	70 RPM	50 RPM	70 RPM
0	52.64	46.66	4.10	4.03
1	58.91	48.27	4.30	4.26
2	81.27	52.18	7.83	5.13
3	123.66	69.34	9.94	7.95

4.2. Mean Residence Time and Residence Time Distribution

The residence time distribution (Eq. 4.2) and the mean residence time (Eq. 4.3) are responses from the system that can be affected by the mass hold-up and the flow regime[14–16] and were used to quantify the time that the particles remained inside the mixer. The concentration of a tracer was tracked along time at the exit of the system using the age distribution function *E(t)*. This function characterizes how much time the particles spend in the mixer.[17]

$$E(t) = \frac{C(t)}{\int_0^\infty C(t)\,dt} \tag{4.2}$$

$$MRT = \int_0^\infty tE(t)\,dt \tag{4.3}$$

The residence time was measured using approximately 300 particles as a tracer during the mixing process. The tracer concentration was measured in 1 s intervals since the mixer reached the mass steady state. Results in Figure 4.4 illustrate the effect of the material cohesion on the age distribution function at 50 RPM. The results show a similar residence time distribution for cohesions 0 and 1. For the simulation with cohesion 3 the age distribution depicts a wider and symmetrical distribution related to better dispersion of the tracer in the powder bed inside the mixer. Figure 4B shows a more narrow distribution at cohesion 0 compared to the distribution at 50 RPM that is consistent with a lower RTD. For the highest cohesion at 70 RPM and cohesion 2 at 50 RPM the RTD values are similar, indicating that the mixer speed reduced the cohesion effect on the RTD which caused the tracer to take less time to leave the mixer.

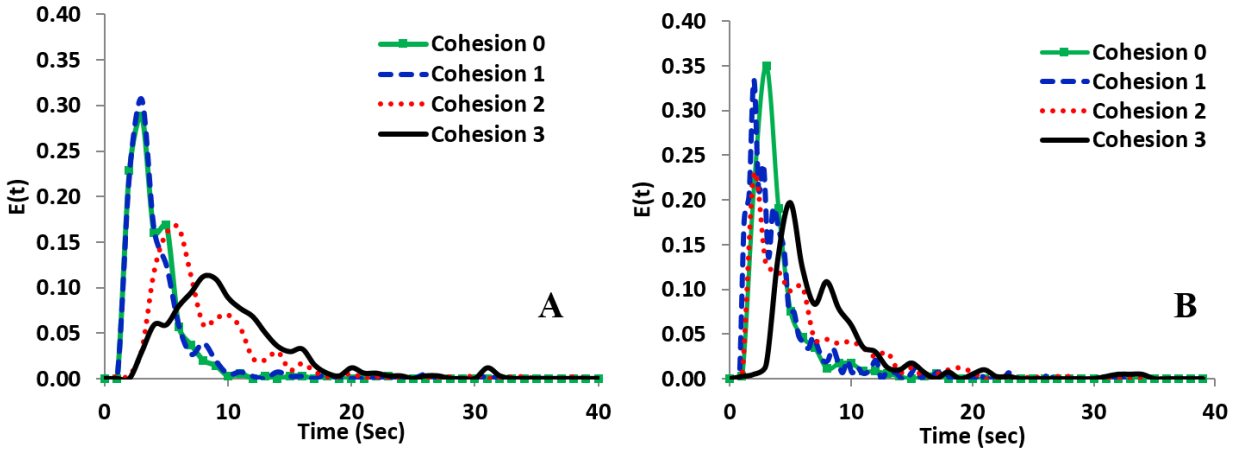

Figure 4.4. Residence time distribution at 50 RPM (A) and 70 RPM (B).

The MRT was calculated using Equation 4.2 and the highest values were found for the simulations with the highest cohesion and these results were close to 10 and 8 s for 50 and 70 RPM, respectively. The MRT values were affected principally by the mixer speed and the particles cohesion.

4.3. Velocity profile and powder phenomena

Powder phenomena inside the mixer were initially characterized using the velocity profile after the mixer reached the mass steady state (feed rate equals exit flow rate). Results for the velocity profile at 50 RPM and 70 RPM are shown in Figure 4.5 where we can observe the effect of the rotational velocity and the cohesion on the mass hold-up, powder phenomena inside the mixer, particles movement, and the size of the active layer and the stagnant zone. Cohesion energy density affects the material flow behavior inside the tumbling mixer[10] and represents, in certain manner, the addition of a cohesive API to the experiments. This effect was more noticeable for the simulations at 50 RPM.

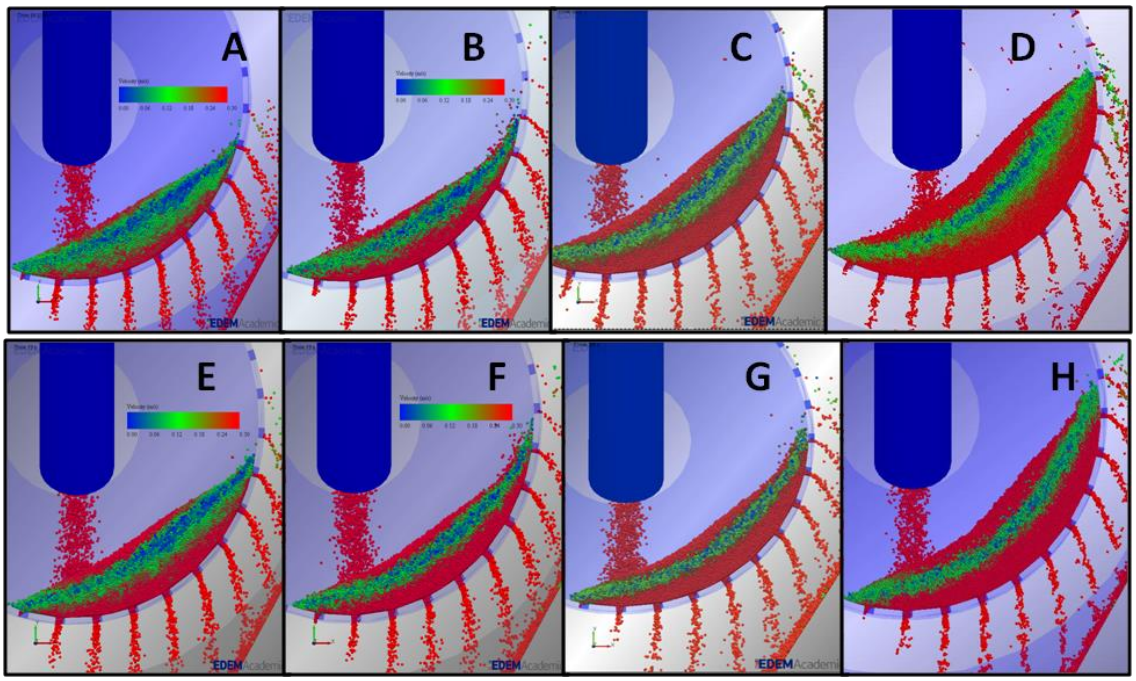

Figure 4.5. Velocity profile at 50 RPM, with cohesion 0 (A), cohesion 1 (B) cohesion 2 (C), and cohesion 3 (D), and at 70 RPM with cohesion 0 (E), cohesion 1 (F), cohesion 2 (G), and cohesion 3 (H).

The colors in Figure 4.5 represent the velocity of the particles; red particles have the highest velocity (0.20 to 0.30 m/s), followed by the green particles (0.04 to 0.20 m/s), and the blue ones that are the slowest particles inside the system (0 to 0.04 m/s). The materials moving inside the mixer were divided in three regions, the top of the powder bed was the active layer, particles in the center correspond to the stagnant zone, and particles near the mixer wall were the recirculation zone. Focusing on Figure 4.5A, the active layer included a combination of green particles when the particle starts falling down in the active zone, followed by a small amount of red particles relative to the other velocity profile at larger cohesion. The behavior changed as the cohesion energy density increased in Figures 4.5C and D, in which practically all the particles in the active layer are red (highest velocity). In addition, the size of the active layer increased due to the cohesion effect on mass hold-up and flow behavior. The bottom of Figure 4.5 corresponds to 70 RPM and it is possible to observe a similar trend, with less variability in flow behavior compared

to 50 RPM, indicating that changes in flow behavior were more susceptible to changes in mass hold-up. These results show less slow particles and a higher number of faster particles for the simulations with cohesion obtaining an increment on the thickness of the active layer, which is the layer where particles move faster and where most of the mixing takes place.[18–20] The highest velocity particles close to the exits represent the recirculation zone and the amount of particles in this area is directly proportional to the mass hold-up and causes a higher frequency of particle-particle interactions and higher mean residence time values.

To validate the velocity profile of the simulations a set of experiments with the same operational parameters and similar particle characteristics, except the restitution coefficient, were developed. Glass beads of 1 mm diameter were used to validate the simulation without cohesion (Figure 4.6).

Figure 4.6. Simulation and validation using lactose and glass beads at 70 RPM.

Figure 4.6 shows the results for 70 RPM show similar velocity profiles in the simulation without cohesion and the experiment with the glass beads. It is possible to identify the stagnant and the active layer based on the velocity profile and the resolution of the glass beads in the picture. The main difference occurs at the start and end of the sliding zone due to the higher restitution value of the glass beads compared to the simulation particles. The powder regime was characterized using the avalanche shape and the velocity profile. For the simulations, the flow

regimes corresponded principally to rolling and cascading, these results were different compared to the experimental part in which the cascading and cataracting regimes dominated the flow behavior. Possible explanations are related to the particle size and the cohesion model used in the simulation, which only includes the contact effect between the particles and the particles and the wall. Based on the results in Figure 4.6 the values of the cohesion energy density used in the simulations do not completely represent the real cohesive material.

Using the velocity profiles, images, and simulation videos it was possible to conclude that the particle trajectory and the powder phenomena inside the continuous mixer are similar to the behavior observed in batch tumble mixers. The flow regimes were classified as rolling (50 and 70 RPM, cohesion 0 and 1) and cascading for the other simulations. Simulation at 50 RPM with cohesion 3, shows a well-defined cascading regime.[20] This regime provides a higher mixing uniformity and is characterized by the presence of a flat surface, where it is possible to identify two regions: the active and the inactive layer. The particles movement in the active layer produces a powder dilation improving mixing performance. Also, the mechanisms occurring inside the mixer are similar to the mechanisms of the batch tumbling mixers previously reported in the literature. For these mixers, the mixing is generally based on convection in the particle flow direction. Diffusive mixing is considered relatively small compared to convective mixing mechanisms,[20,21] because this only occurs when there are displacements between particles in the two principal layers (active and inactive). The analysis of the simulations validated the existence of the two well-defined layers where particles remained before leaving the mixer.

4.4. Mixing Uniformity

Mixing uniformity is the principal response of the system and depends on all the parameters and variables discussed above. Based on Figure 4.1 it is possible to quantify the blend uniformity at the exit of the system, after the chute used to collect the powder of each exit point in one stream. In this section the blend uniformity was analyzed in each mixer exit point, and inside the mixer to understand the effect of powder phenomena on powder uniformity at the exits of the mixer and to elucidate if the design of the chute affects the final blend uniformity.

4.4.1. Mixing Uniformity at the Exit of the System

For the simulations, a volume selection (Figure 4.7) was created after the chute to measure the quantity of particles 1 and 2 at the exit of the simulation system. The sample size was equal to 1 gram of particles, and the concentration was calculated every second. The total mass analyzed was equal to 40 grams for each simulation.

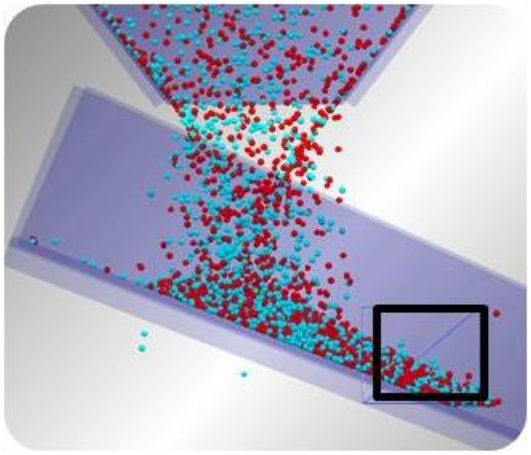

Figure 4.7. Sampling volume at system exit.

With these values the mixing uniformity was calculated (Table 4.5) and plotted in Figure 4.8, the results for the simulations are shown in Figures 9 and 10. These two plots depict the concentration variability as a function of time after the system reached mass steady state. This

variability and the deviation between the target concentration value and the calculated value are higher as cohesion increases, except for the simulation at 50 RPM with cohesion 3, in which the deviation decreases relative to the target concentration value. The RSD is the parameter used to measure the mixing uniformity and according to the FDA guidances for batch mixing processes, 6% values are considered to marginally pass and those below 4% are considered to really pass.[22] RSD has been used previously, to measure mixing uniformity in continuous mixers.[14,15,23]

Table 4.5. Relative standard deviation

Cohesion	50 RPM	70 RPM
0	2.50	2.46
1	3.10	2.51
2	3.55	2.79
3	2.63	3.28

The results were summarized in Table 4.5 and Figure 4.8 demonstrating good mixing with RSD values below 4%. These results demonstrated an increment in the RSD values as the cohesion energy density increases and the velocity decreases, except for the simulation at 50 RPM with cohesion 3. The lowest RSD was obtained for the simulation using 70 RPM without cohesion; at this rotational velocity the RSD values are similar to the results for slightly cohesive particles (cohesion 2 or lower) found at 50 RPM.

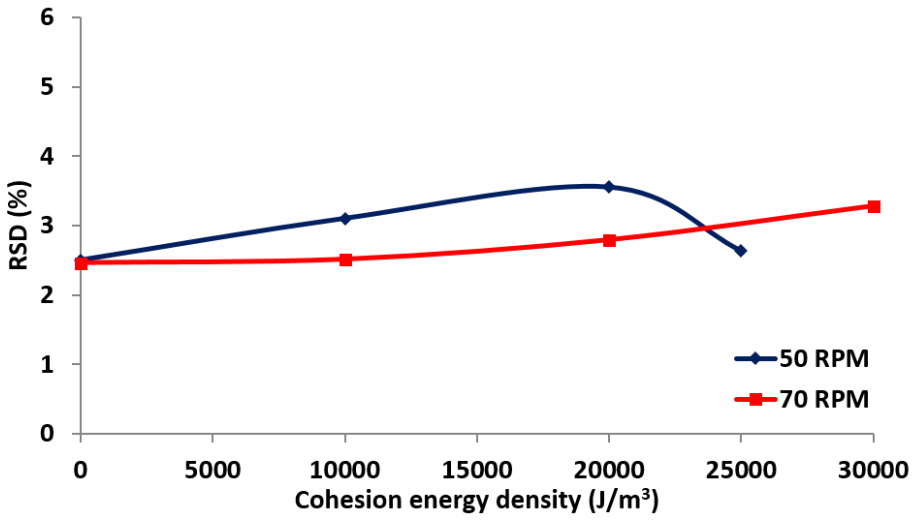

Figure 4.8. Effect of cohesion on final blend uniformity.

These results indicate a better mixing capability of the system for slightly cohesive material at higher velocity and are in agreement with the velocity profile analysis at 70 RPM in which a larger active zone and faster moving particles improve mixing performance. This trend validates the experimental results in which a high mixing degree for the blends with 10 and 20% of API were found as the rotational velocity increases.

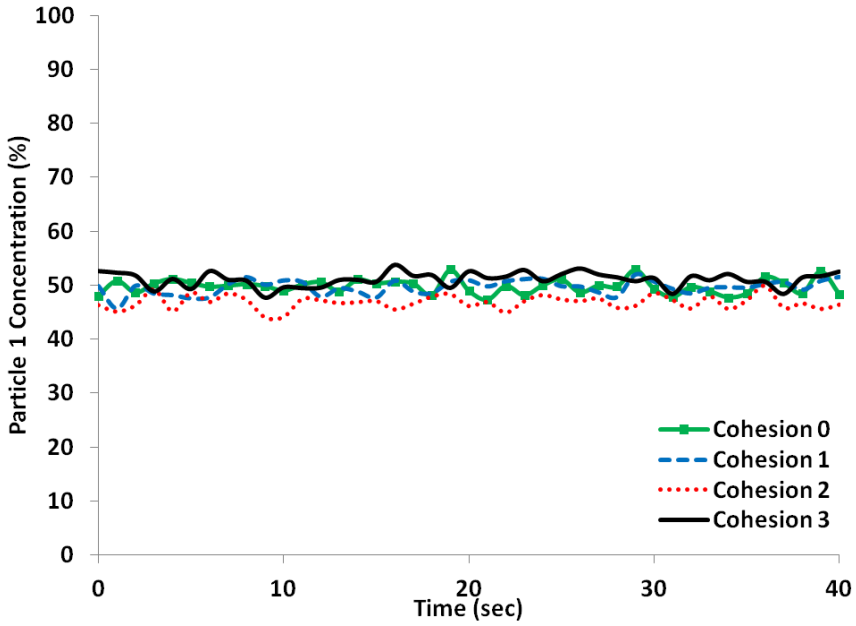

Figure 4.9. Mixing uniformity after the mixer reached the steady state at 50 RPM.

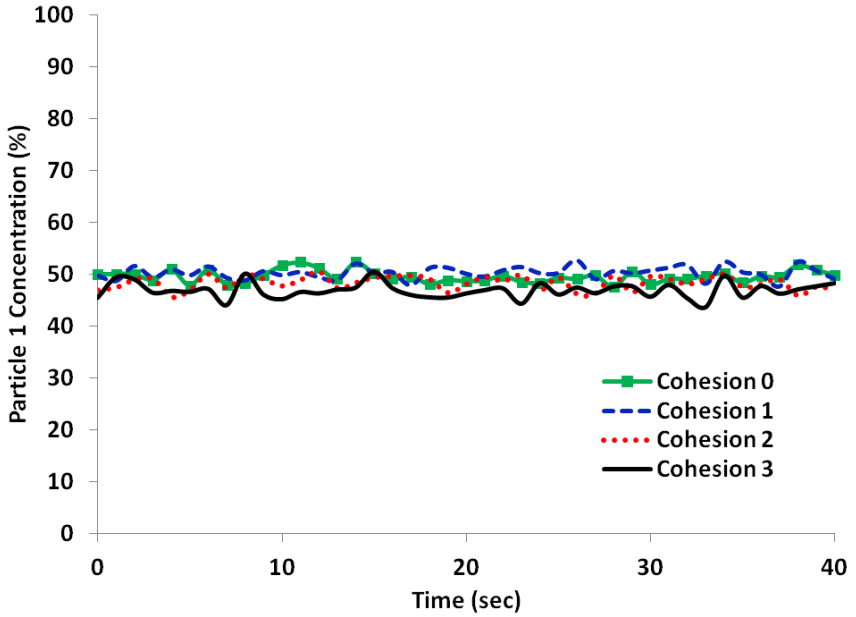

Figure 4.10. Mixing uniformity after the mixer reached the steady state at 70 RPM.

4.4.2. Collision Frequency Effect on the Final Uniformity

The previous mixing uniformity results showed that concentration variability decreases when the mixer speed increases. Results also show that the RSD increases with the cohesion, except for the simulation at 50 RPM and cohesion 3 for which the RSD value was lower than the RSD for cohesions 1 and 2. To explain this behavior the collision frequency inside the mixer for each simulation was calculated (Figure 4.11). A collision is defined as a complete impact between two particles and the frequency of collisions has previously been related to the mixing uniformity.[24] An increment of approximately 20%, in the collision frequency relative to cohesion 0 was obtained for the simulation at 50 RPM and cohesion 3 using the DEM software©. The increase in the collision frequency is explained for the change in powder phenomena inside the mixer showed in Figure 4.5D, using this figure it is possible to observe that the number of particles moving faster increases in comparison to the other simulations.

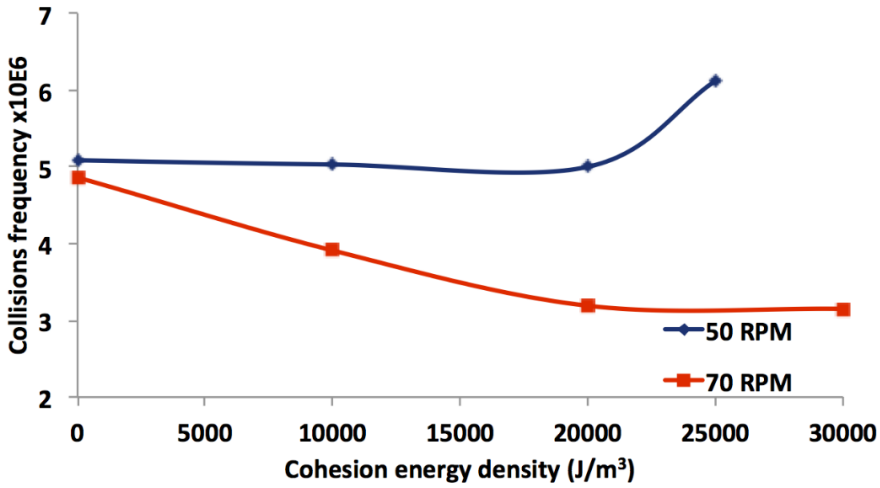

Figure 4.11. Effect of cohesion parameter on collision frequency.

4.4.3. Mixing Uniformity at the Exit of the Mixer

By using simulation videos it was observed that the uniformity is the contribution of the material flowing by each exit and its interaction in the chute. To demonstrate the effects of the exit position on the final uniformity, the concentration was measured in each exit to compare it with the global concentration. To quantify the blend uniformity at the mixer exits, eight different selections with a volume of 12.6 cm^3 (Figure 4.12) were created at the tumble exits to measure differences in concentration between each one and its contribution on the final blend uniformity.

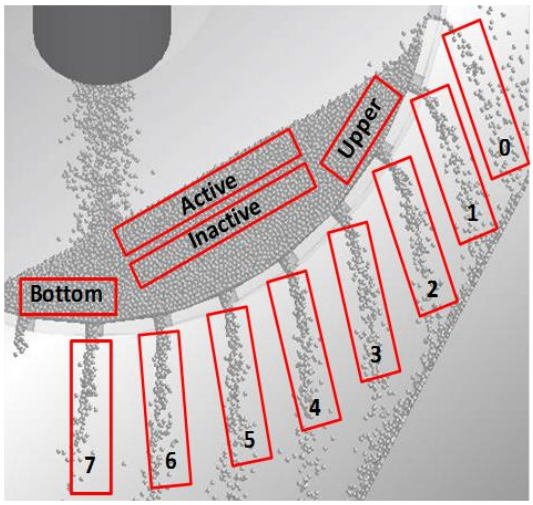

Figure 4.12. Sampling volumes inside and at the tumble exits.

Measuring the concentration at each exit helps to understand the mixing dynamics inside the continuous tumble mixer. The results in Figure 4.13 show a concentration profile that indicates that the highest concentrations occur at the exits closer to the feed inlet. The values obtained in exits 7 and 6 indicate the possibility of a shortcut in which particles are exiting the system without interacting with the material that is already inside, due to the recirculation zone. The higher deviations in the positions closer to the feeding position at 50 RPM were lower at 70 RPM, and indicated that the higher velocity in the recirculation zone reduces the particle shortcut.

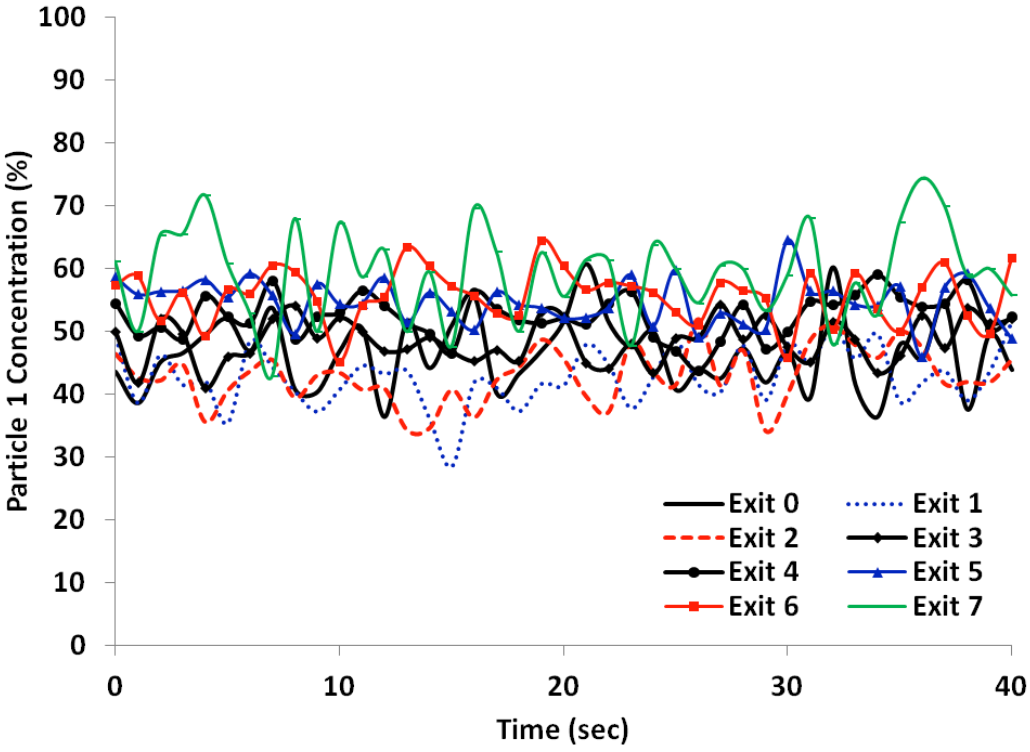

Figure 4.13. Effect of position of exits on final concentration at 70 RPM cohesion 0.

When the cohesion was added (Figure 4.14), an inverse relationship was found between the cohesion and particle deviation in positions 7 and 6. For cohesions 2 and 3 the concentration oscillates around the target concentration indicating a reduction on particle shortcut.

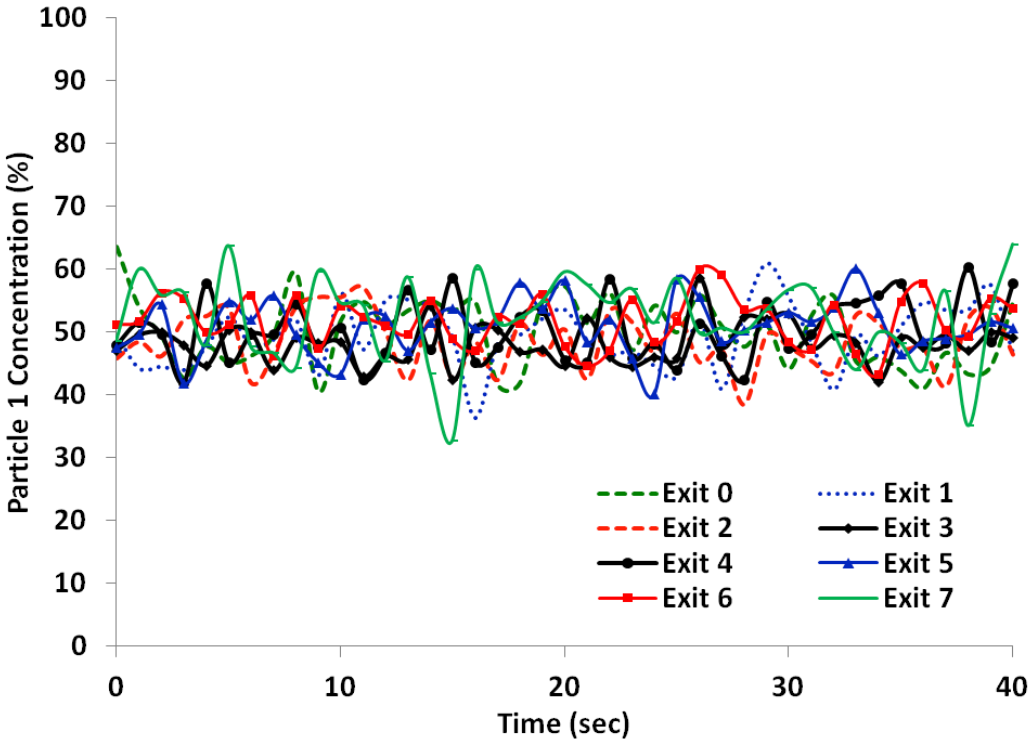

Figure 4.14. Effect of position of exits on final concentration at 70 RPM and cohesion 3.

In general, the concentration at each exit depicts a concentration profile in which the highest values occur at the bottom and the lowest correspond to the exit on the top of the powder bed. A reduction in the concentration deviation was observed as the material cohesion increased, producing a more uniform material leaving the mixer.

4.4.4. Mixing inside the system

Previous studies using batch tumble mixers showed that the mixing occurs principally in the active layer.[20] Four different selections with a volume of 8.8 cm^3 were developed inside the avalanche to study the mixing uniformity inside the system (Figure 4.12). Two volumes were selected in the active and inactive layer (stagnant layer) based on the particle velocity profile (Figure 4.5). Other two selections were created with the name of upper and bottom layer

corresponding to the base and top of the slide or avalanche zone, these two zones were closer to the exits with the higher concentration deviation.

The first volume was the active layer and the results show that the concentration values were oscillating around a concentration of 40% for non-cohesive powder. For simulations at 50 RPM the average concentration in the active zone is equal to 40.3 and 49.5% for cohesion 0 and 3, respectively. The increment in concentration shows a trend to achieve the target value (50%) as cohesion increases. The second was the inactive layer (stagnant zone) with concentration values around 27.0 and 53.3% for cohesion 0 and 3, respectively. The upper concentrations were 41.0 and 51.0 and the bottom ones were 43.5 and 51.8, respectively for cohesions 0 and 3. The variability inside the system was plotted and is shown on Figure 4.15 (cohesion 0) and Figure 4.16 (cohesion 3) for the simulations at 50 RPM. These results show that the particle uniformity changes with the position inside the mixer and this behavior was similar for all simulations.

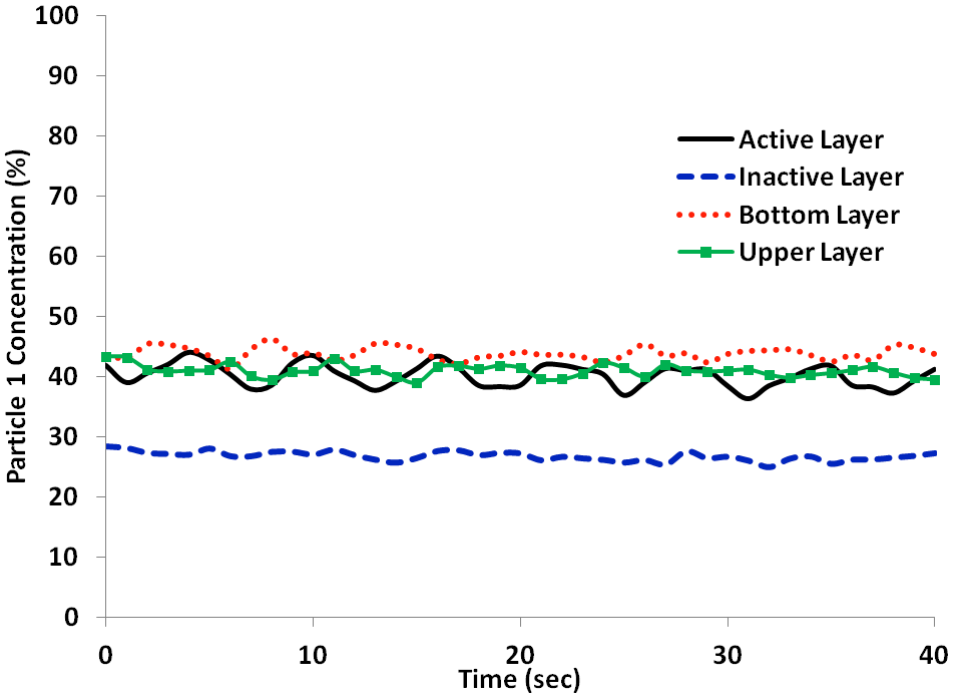

Figure 4.15. Mixing uniformity inside the system at 50 RPM and cohesion 0.

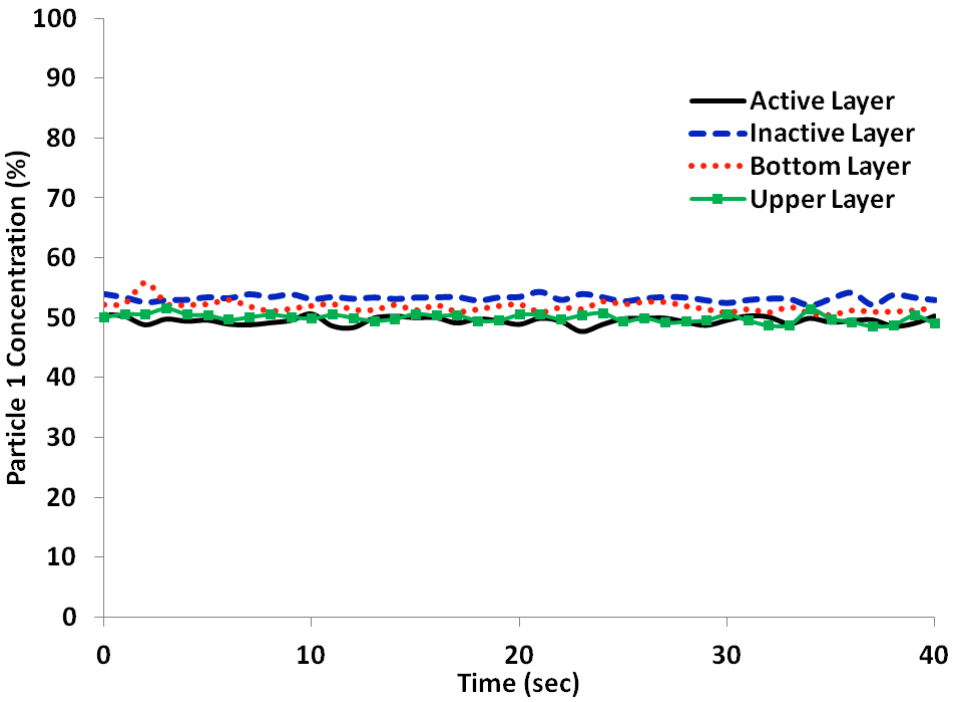

Figure 4.16. Mixing uniformity inside the system at 50 RPM and cohesion 3.

Summarizing, it was found that particle-particle and particle-wall interactions significantly reduce the shortcut, and the concentration inside the mixer was closer to 50% for cohesions 2 and 3. Combining the results at the mixer exit points and inside the mixer, the addition of certain cohesion to the material promotes a better particle interaction and improves mixing uniformity.

4.4.5. Mixing uniformity comparison at the mixer exit points and after the chute

The use of DEM simulations demonstrated that this mixer is capable of achieving high mixing uniformity, and how the operation parameters and the material properties are related with the final blend uniformity. The addition of cohesion to the simulations has a direct impact to the mass hold-up increasing particles interactions due to the higher particle velocity and the size of the recirculation zone. The combination of effects, the mass hold-up, and the velocity profile promoted a higher mean residence time. These results were consistent with the experimental part in which the increase in material cohesion reduced the operation capability of the system at

constant flow rate and constant mixer speed. In this case it was required to increase the mixer speed or reduce the inlet flow rate.

The blend uniformity at the exit of the system was characterized based on the parameters mentioned above and an increment in RSD with cohesion was found, except for the highest cohesion at 50 RPM in which a reduction in RSD was observed. This demonstrated that cohesion negatively affects blend uniformity when the flow regime is rolling, and small changes in flow regime (to cascading) provide a significant increment in the collisions frequency improving blend uniformity. This behavior was similar to the results obtained in the experimental part, in which a regime with higher particle-particle interactions (cascading or cataracting) was required to obtain good blend uniformity. The concentration was analyzed for each mixer exit point and inside the mixer to have a better understanding of the effect of powder phenomena on blend uniformity. The results in each exit point and inside the mixer demonstrated that cohesion reduces the concentration variability due to higher mass hold-up, particle interactions, and MRT. In addition, a closer concentration to the target value was found for both mixer speeds. Summarizing, these results are not consistent with the reduction in blend uniformity found at the exit of the system; except for cohesion 3 at 50 RPM. This disagreement could be related to the particle-particle interaction between material moving in the chute with the material leaving the mixer in each exit point (Figure 4.12) causing an additional mixing effect. For example, at cohesion 0 the outgoing material in exits 6 and 7 with concentrations higher than the target value (due to the shortcut) interacted with the material leaving the other exits, including the material with concentration below the target value.

4.5. Conclusions

Based on the previous results, we show that the continuous tumble mixer has the capacity to reach an optimal production with low concentration variability. The velocity profiles and the flow regime results demonstrated that powder behavior inside the mixer is similar to those observed for batch systems. These were validated using glass beads, showing a similar behavior based on the avalanche shape, powder phenomena, and the velocity profile inside the mixer.

The focus of this chapter was to understand the powder phenomena and determine the material uniformity at the exits of the system, to find a better blend uniformity for simulations at 70 RPM at low cohesion. For the case with the highest cohesion, the uniformity was a function of the mixer speed and the flow regime. The regime was the predominant effect increasing the cohesion frequency. The change in flow regime from rolling to cascading was a combination of the cohesion and the mass hold-up inside the mixer at constant mixer speed. The results demonstrated that the change of flow regime improved blend uniformity.

We also observed a concentration profile at the exits of the tumble mixer, with highest and lowest values at the exits closer to the bottom and top of the powder bed, respectively. In addition, a variability reduction inside the mixer and at the system exits was found when the cohesion values increased.

To improve the mixing performance, the shortcut effect (mentioned above) will be studied in the next chapter, using a new feeding position to force the feeding material to fall on top of the active layer, reducing the possibility of it leaving the system without interacting with the material that is already inside the mixer.

4.6. References

1. Yu Y, Saxén H. Discrete element method simulation of properties of a 3D conical hopper with mono-sized spheres. *Adv. Powder Technol.* 2011;22(3):324-331. doi:10.1016/j.apt.2010.04.003.
2. Marigo M, Cairns DL, Davies M, Ingram A, Stitt EH. A numerical comparison of mixing efficiencies of solids in a cylindrical vessel subject to a range of motions. *Powder Technol.* 2012;217:540-547. doi:10.1016/j.powtec.2011.11.016.
3. Gao Y, Muzzio FJ, Ierapetritou MG. Optimizing continuous powder mixing processes using periodic section modeling. *Chem. Eng. Sci.* 2012;80:70-80. doi:10.1016/j.ces.2012.05.037.
4. Jain A, Metzger MJ, Glasser BJ. Effect of particle size distribution on segregation in vibrated systems. *Powder Technol.* 2013;237:543-553. doi:10.1016/j.powtec.2012.12.044.
5. Jiang M, Zhao Y, Liu G, Zheng J. Enhancing mixing of particles by baffles in a rotating drum mixer. *Particuology* 2011;9(3):270-278. doi:10.1016/j.partic.2010.06.008.
6. Sarkar A, Wassgren CR. Simulation of a continuous granular mixer: Effect of operating conditions on flow and mixing. *Chem. Eng. Sci.* 2009;64(11):2672-2682. doi:10.1016/j.ces.2009.02.011.
7. Faqih AN, Chaudhuri B, Mehrotra A, Tomassone MS, Muzzio F. Constitutive model to predict flow of cohesive powders in bench scale hoppers. *Chem. Eng. Sci.* 2010;65(10):3341-3351. doi:10.1016/j.ces.2010.02.028.
8. Alexander AW, Chaudhuri B, Faqih A, Muzzio FJ, Davies C, Tomassone MS. Avalanching flow of cohesive powders. *Powder Technol.* 2006;164:13-21. doi:10.1016/j.powtec.2006.01.017.
9. Sarkar A, Wassgren C. Continuous blending of cohesive granular material. *Chem. Eng. Sci.* 2010;65(21):5687-5698. doi:10.1016/j.ces.2010.04.011.
10. Chaudhuri B, Mehrotra A, Muzzio FJ, Tomassone MS. Cohesive effects in powder mixing in a tumbling blender. *Powder Technol.* 2006;165:105-114. doi:10.1016/j.powtec.2006.04.001.
11. Wu CL, Zhan JM, Li YS, Lam KS, Berrouk a. S. Accurate void fraction calculation for three-dimensional discrete particle model on unstructured mesh. *Chem. Eng. Sci.* 2009;64(6):1260-1266. doi:10.1016/j.ces.2008.11.014.
12. Marikh K, Berthiaux H, Mizonov V, Barantseva E. Experimental study of the stirring conditions taking place in a pilot plant continuous mixer of particulate solids. *Powder Technol.* 2005;157:138-143. doi:10.1016/j.powtec.2005.05.020.
13. Marikh K, Berthiaux H, Gatumel C, Mizonov V, Barantseva E. Influence of stirrer type on mixture homogeneity in continuous powder mixing: A model case and a pharmaceutical case. *Chem. Eng. Res. Des.* 2008;6:1027-1037. doi:10.1016/j.cherd.2008.04.001.
14. Vanarase AU, Muzzio FJ. Effect of operating conditions and design parameters in a continuous powder mixer. *Powder Technol.* 2011;208(1):26-36. doi:10.1016/j.powtec.2010.11.038.

15. Gao Y, Vanarase A, Muzzio F, Ierapetritou M. Characterizing continuous powder mixing using residence time distribution. *Chem. Eng. Sci.* 2011;66:417-425. doi:10.1016/j.ces.2010.10.045.

16. Portillo PM, Vanarase AU, Ingram A, Seville JK, Ierapetritou MG, Muzzio FJ. Investigation of the effect of impeller rotation rate, powder flow rate, and cohesion on powder flow behavior in a continuous blender using PEPT. *Chem. Eng. Sci.* 2010;65:5658-5668. doi:10.1016/j.ces.2010.06.036.

17. Fogler HS. *Element of Chemical Reaction Engineering*. 3rd ed. Prentice Hall; 1999:812-822.

18. Aissa AA, Duchesne C, Rodrigue D. Effect of friction coefficient and density on mixing particles in the rolling regime. *Powder Technol.* 2011;212:340-347. doi:10.1016/j.powtec.2011.06.009.

19. Santomaso A, Olivi M, Canu P. Mechanisms of mixing of granular materials in drum mixers under rolling regime. *Chem. Eng. Sci.* 2004;59(16):3269-3280. doi:10.1016/j.ces.2004.04.026.

20. Aissa AA, Duchesne C, Rodrigue D. Transverse mixing of polymer powders in a rotary cylinder part I: Active layer characterization. *Powder Technol.* 2012;219:193-201. doi:10.1016/j.powtec.2011.12.040.

21. Abouzeid A-ZM. On the Contribution of Convective Dispersion and Diffusion Mechanisms to the Dispersion of Particulates in Rotating Drums. *Ind. Eng. Chem.* 1976;15(1):3-4.

22. FDA. *Guidance for Industry. Powder Blends and Finished Dosage Units — Stratified In-Process Dosage Unit Sampling and Assessment*.; 2003.

23. Portillo PM, Muzzio FJ, Ierapetritou MG. Using Compartment Modeling to Investigate Mixing Behavior of a Continuous Mixer. *J. Pharm. Innov.* 2008;3:161-174. doi:10.1007/s12247-008-9036-0.

24. Yang RY, Yu AB, McElroy L, Bao J. Numerical simulation of particle dynamics in different flow regimes in a rotating drum. *Powder Technol.* 2008;188(2):170-177. doi:10.1016/j.powtec.2008.04.081.

Chapter 5

5. Effect of the Materials Properties and Design Parameters on the Final Blend Uniformity using Experimental and Simulation Results

The main goals of this chapter were to understand the effect of cohesion, API concentration, and a new feed position on the final blend uniformity using experiments and simulations by DEM. Previous studies demonstrated that material properties[1–3] and design parameters affect the final mixing uniformity.[1,3–5] Based on the experimental design performed and analyzed in chapter 3, two experiments at 2.5% with the highest RSD were selected and replicated using a new feed position. To study the angle effect, the simulations at 50 and 70 RPM without cohesion (Chapter 4) were replicated using the same particle characteristics, operational parameters (Table 4.1 and 4.2), and using the new feed position. The complete set includes ten different simulations (Table 5.1), and these were developed to study the effect of the material properties (two different cohesion values), particle concentration (2.5, 10, and 50%), and the feed angle on the final blend uniformity.

Table 5.1. Experimental design

Simulation	RPM	Cohesion	Angle	Particle Concentration
1	50			50.0%
2	50		x	50.0%
3	70			50.0%
4	70		x	50.0%
5	70			10.0%
6	70		x	10.0%
7	70	x		10.0%
8	70	x	x	10.0%
9	70	x		2.5%
10	70	x	x	2.5%

For each simulation, concentration at the end of the system, mass hold-up inside the mixer, RTD, mixing uniformity inside the system, effect of the exit position on final concentration, flow regime, and velocity profiles were analyzed.

5.1. Experimental Section

Figure 5.1 is a summary of the principal results for the mixing uniformity obtained in Chapter 3. The results show a different trend for the experiments done at concentration of 10 and 20% compared with 2.5 %. For concentrations of 10 and 20 % the increment in the mixer speed improves the blend uniformity, but not for 2.5%.

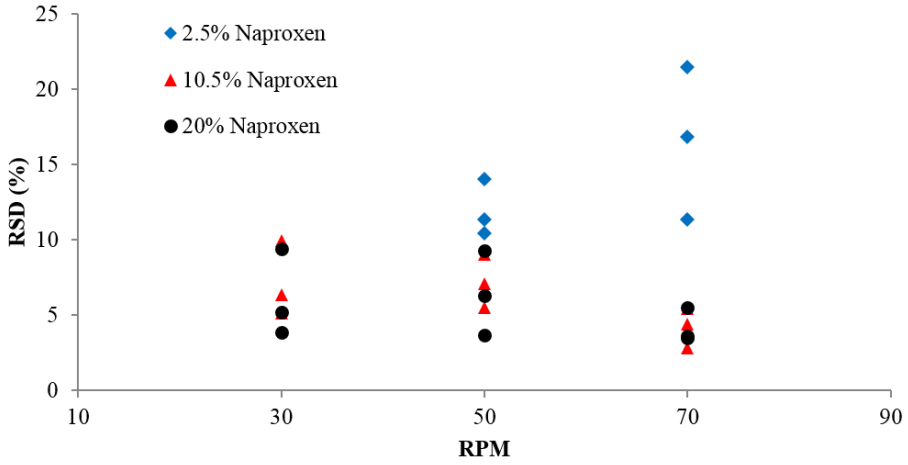

Figure 5.1. Review of experimental results.

The RSD values at 2.5% suggested that other parameters are affecting the mixing performance. Studying in detail images and videos of some experiments, it was found that the feed angle impacts the position at which the incoming material interacts with the material inside the system. In the initial setup the material falls with an angle of 0˚ (Figures 5.2A and C) and interacts just with the final part of the avalanche, losing the opportunity to interact with the material in the active layer, which is the zone where the mixing principally occurs.[6,7] Based on these results the feed angle was modified to study the effect of this design parameter on the final uniformity.

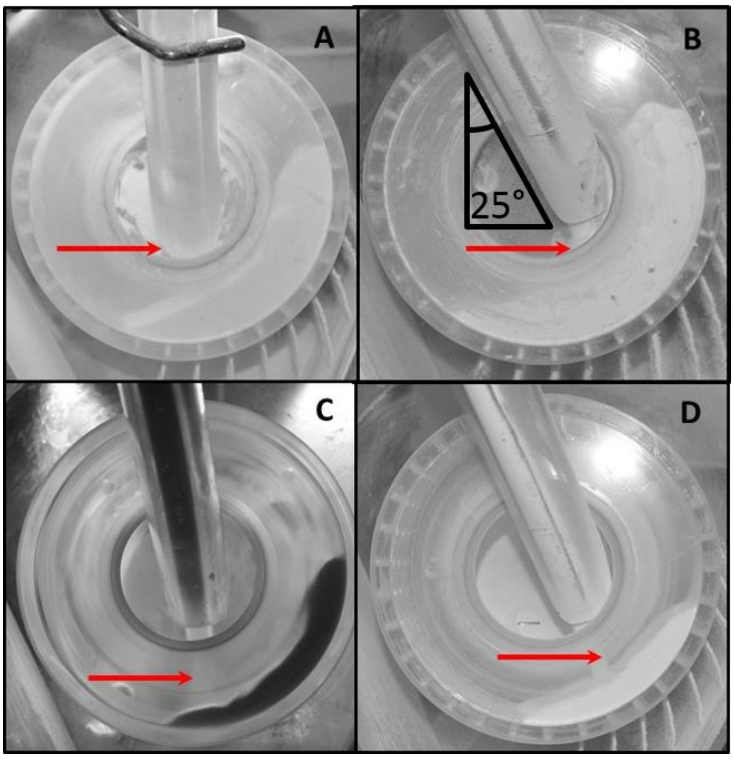

Figure 5.2. Feed angle position: 50 RPM (A, B) and 70 RPM (C, D).

Figures 5.2B and D show the change of the system design for 50 and 70 RPM at 62.0 and 45.5 Kg/h, respectively. Effects of the feed angle on the mixing variability are shown in Figure 5.3 for 50 RPM (A) and 70 RPM (B).

The results show a lower variability for naproxen concentration using the feed angle of 25° compared to the feed angle of 0°, for both experiments at 50 and 70 RPM (Figure 5.3). In terms of the mixer speed, 50 RPM showed a lower variability. To measure the mixing performance the RSD value was calculated after the system reached steady state.[8]

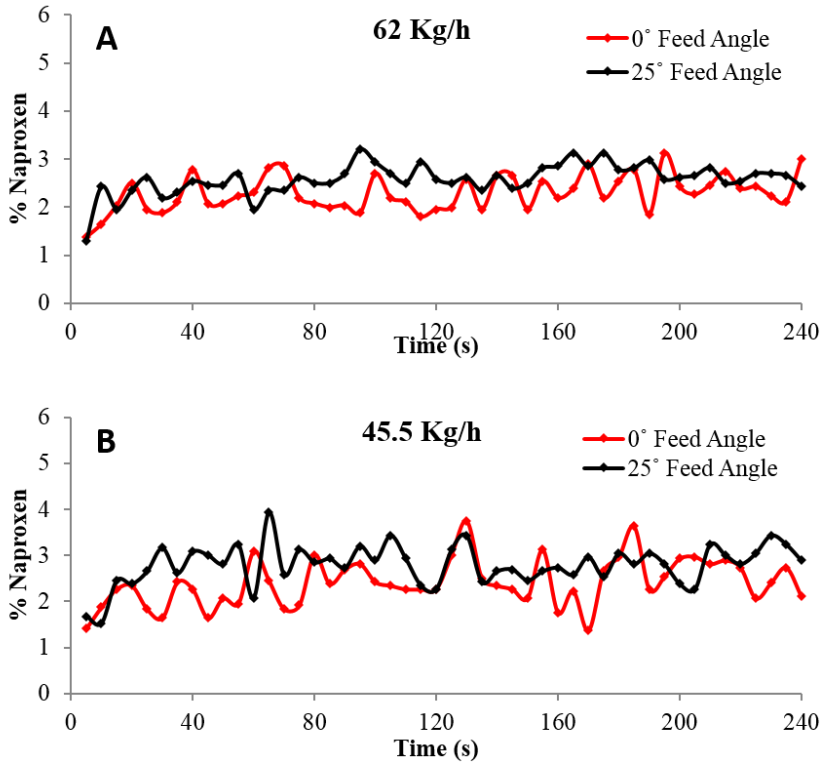

Figure 5.3. Feed angle effect on variability at 50 (A) and 70 RPM (B).

The results were plotted in Figure 5.4 and the results show an RSD reduction for both RPM's. The highest RSD reduction was found for the experiments at 70 RPM, with 46%. These results demonstrated that the position at which the inlet material interacts with the active layer is crucial to improve the uniformity of the blend.

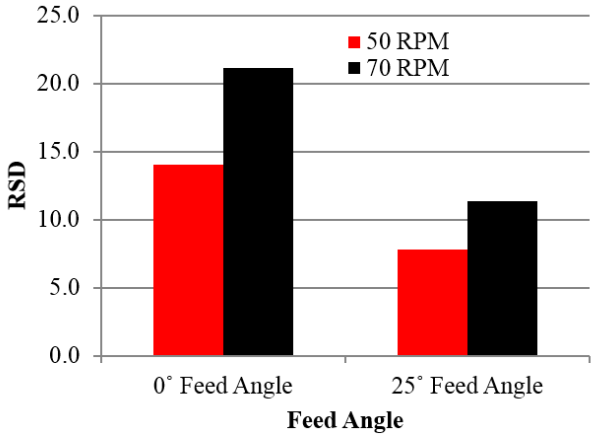

Figure 5.4. RSD reduction by feed angle position effect.

5.2. Simulation Results

To obtain a better understanding of the cohesion effect and the new feeding position on the final blend uniformity, a set of simulations was performed (Table 5.1). The complete set was analyzed to determine the mass hold-up, mean residence time, velocity profile, powder phenomena, and the mixing uniformity (inside the mixer, at the mixer exit points, and at the final exit). A review of the principal results is shown in Table 5.2.

Table 5.2. Flow, Cohesion and feed angle effect on Hold-up, MRT, and RSD

Simulation	RSD (%)	Hold-Up (g)	MRT (s)	Flow (Kg/h)
1	2.50	52.64	4.10	64.8
2	3.14	51.09	4.20	64.8
3	2.46	46.66	4.03	64.8
4	3.43	45.40	4.46	64.8
5	6.60	67.35	2.99	72.8
6	7.78	56.56	3.23	72.8
7	8.24	67.33	3.57	72.8
8	7.53	56.58	3.50	72.8
9	16.60	67.12	4.54	72.8
10	13.35	56.61	5.24	72.8

From now on, to identify the simulations these will be referenced with numbers from 1 to 10 based on Table 5.1.

5.2.1. Mass Hold-up

The mass hold-up inside the mixer at steady state is an important variable that is related to the mixer design, material properties, and operation parameters such as the mixer speed and flow rate.[9–11] The mass hold-up was calculated using the same procedure explained in Chapter 4, section 4.1. An example of the change of the accumulation as a function of time is shown in Figure 5.5.

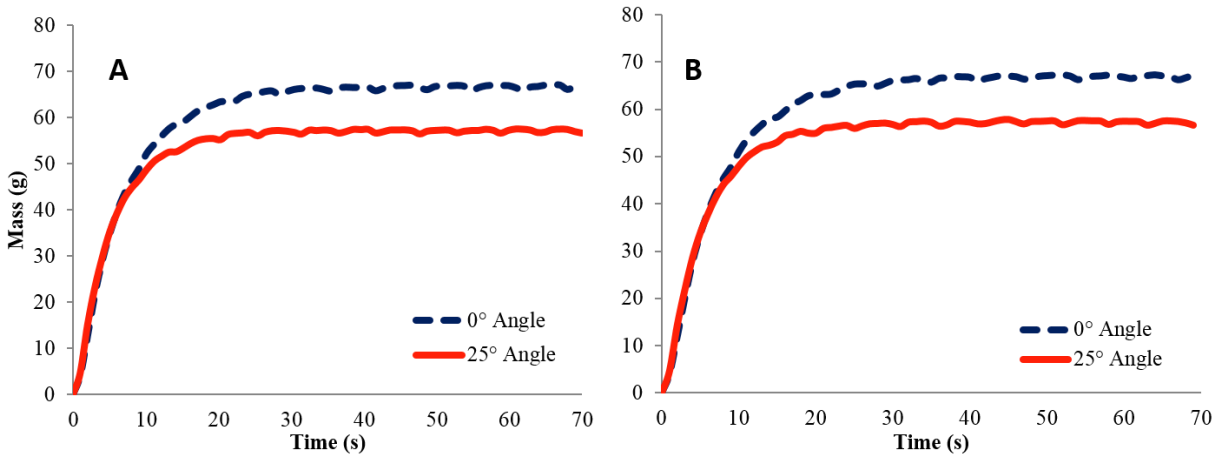

Figure 5.5. Mass hold-up as a function of time at 70 RPM and 2.5 (A) and 10% (B) concentration.

At 50 RPM the mass hold-up inside the mixer was higher compared to 70 RPM (Simulations 1-4). This effect is a result of the increment in the centrifugal force, which increases the flow of the material through the exits of the mixer. The use of the new feeding position produces a higher normal force over a larger particle area compared to the normal feeding position, reducing the material accumulation. This effect was more noticeable for the case of 2.5 and 10.0% of API. The addition of cohesion for particle 1 at 2.5 and 10% concentration did not produce significant changes on the mass hold-up.

5.2.2. Residence Time Distribution and Mean Residence Time

The residence time distribution and the mean residence time were calculated using the same procedure explained in section 4.2. These times are a response from the system to the changes in material properties and operation parameters, and are useful to quantify the time that the particles remain inside the mixer.[12] This time is related to mixing uniformity.[13]

Figure 5.6 depicts the effect of the feeding angle on the residence time distribution at 70 RPM for concentrations of 2.5 (Figure 5.6A) and 10% of API with and without cohesion (Figures 5.6B and C). All three figures are similar and show a slightly broad distribution and a lower dead

time for the feeding angle case relative to the normal feeding position. This change in *E*(t) produces an increment in the time available for interaction before the particles leave the system. This result was more relevant for the simulation at 10%, in which the addition of the feeding angle increases the mean residence time by approximately 10% even when the mass hold-up decreases by 16%. These results were similar for the simulations at 2.5% (Table 5.2). Both effects, mass hold-up and MRT are directly related to the blend uniformity and will be discussed in the following sections.

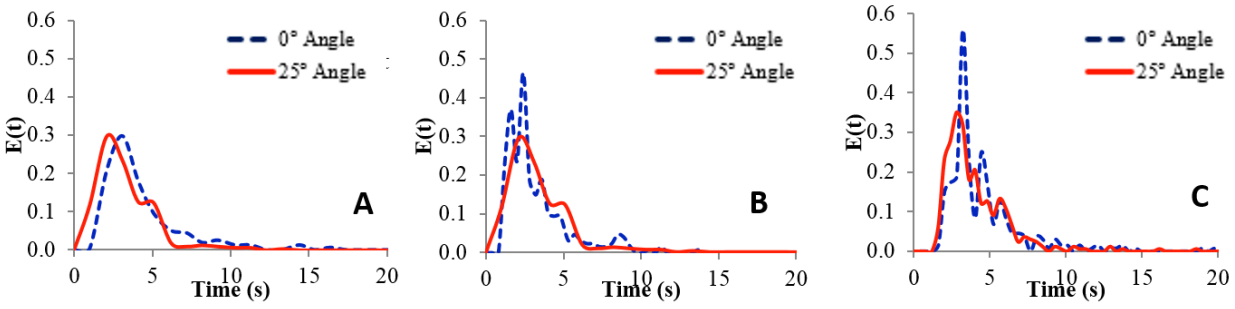

Figure 5.6. Residence time distribution at 70 RPM and 2.5 (A), 10% (B), 10% of API without cohesion (C).

The results demonstrated that the new position affects the position where the feeding material interacts with the avalanche inside the system, causing a mass hold-up reduction. This result is similar to the one found in the literature where the operational parameters are related to the residence time distribution.[14] With an angle of 0°, the material falls at the end of the avalanche and close to the exits, while with the angle of 25° the material falls in the middle of the avalanche increasing the possibility to interact with the material inside the avalanche. This effect was noticeable for all the simulations except for the simulations at 10% with cohesion, however values where similar with a difference of 0.07 seconds. For this simulation it is important to analyze the synergy of mean residence time and the mass hold-up to understand the impact on blend uniformity.

Based on these results the effect of cohesion, RPM, flow rate, mass hold-up, and feed angle on the MRT were analyzed. These changes are an effect of the combination of all these factors. To establish a direct relationship that can be used in all the simulations a new value was calculated. This value was named Interaction Time, which is the ratio between MRT and mass hold-up. The results for these values are shown in Table 5.3 where it is possible to observe an increment on this ratio when the feed angle of 25° was used.

Table 5.3. Interaction time values

Simulation	MRT (sec)	Mass Hold-Up (g)	Interaction Time (sec/g)
1	4.10	52.64	0.078
2	4.20	51.09	0.082
3	4.03	46.66	0.086
4	4.46	45.40	0.098
5	2.99	67.35	0.044
6	3.23	56.56	0.057
7	3.57	67.33	0.053
8	3.5	56.58	0.062
9	4.54	67.12	0.068
10	5.24	56.61	0.093

Mass hold-up is a response of the system to the material properties and mixer operational parameters, and is related to the mean residence time of the particles used as a tracer. This residence time is also affected by material properties, operational and design parameters, which helps to conclude that the changes on these values are the results of different components. The uses of the interaction time demonstrated that there exists a proportional relationship between all the factors affecting the mass hold-up and the MRT.

5.2.3. Velocity profile and powder phenomena inside the mixer

After the system reached the steady state an image of each simulation was obtained with the particles colored based on their velocity. Figure 5.7 illustrates a picture of the last eight simulations in accordance with Table 5.1.

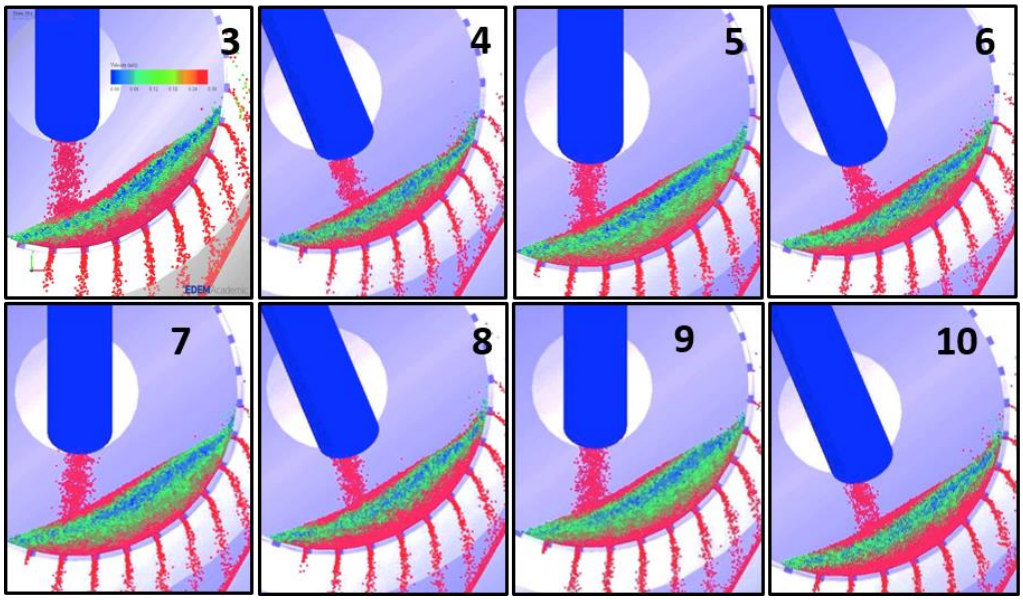

Figure 5.7. Velocity profiles numbered according to Table 5.1.

In these figures the red particles are the faster ones (0.20 to 0.30 m/s) and the blue ones represent the particles with the lowest velocity (0 to 0.06 m/s), while the particles with the intermediate velocity are colored in green (0.06 to 0.20 m/s). These pictures also show the effect of the RPM and the feed position on the active and inactive layer, and the distribution of the faster and slower particles inside the avalanche. As previously mentioned the mass hold-up inside the mixer and the proportion of slow particles decrease with the addition of the new feed position. Table 5.4 summarizes the percentage of slow particles and the average velocity of the particles inside the mixer for the whole simulation set. The results demonstrate that the feed position reduces by 5% the amount of slow particles (from 35 to 30%) for the simulation at 10% without cohesion

and 7% for simulations with cohesion at 2.5 and 10%. This reduction in the quantity of slow particles was consistent with the increment in the average particle velocity in more than 10% for simulations of concentrations of 2.5 and 10%. The behavior was different for the simulations corresponding to concentration of 50% at 50 and 70 RPM, showing a minimal reduction in the slow particles (1%) and in the average particle velocity.

Table 5.4. Proportion of faster particles

Simulation	RPM	Concentration (%)	Cohesion	Angle	Slow Particles (%)	Velocity (m/s)
1	50	50			48.58	0.131
2	50	50		x	47.49	0.125
3	70	50			36.43	0.164
4	70	50		x	34.67	0.166
5	70	10			34.97	0.152
6	70	10		x	29.98	0.176
7	70	10	x		36.78	0.153
8	70	10	x	x	29.01	0.178
9	70	2.5	x		35.94	0.152
10	70	2.5	x	x	29.17	0.177

The cohesion and the feed angle did not cause an effect on the flow regime, under the conditions used in this chapter, since all the avalanches inside the system were classified as rolling.[6]

5.3. Mixing Uniformity using DEM simulations

The principal response of the system is the mixing uniformity at the end of the system (chute). Based on the mixer design and in the pictures of the simulations, this final uniformity is affected by the material properties, design, and operational parameters. The material properties affect the behavior of the material inside the mixer and the material flowing through the tumble orifices. Based on this information the mixing uniformity was measured in four different positions

inside the mixer (active, inactive, upper, and bottom layer), at each exit (exits 0 to 7) of the tumble, and at the final exit of the system (Figure 4.12). Mixing uniformity was measured using RSD, which is a parameter used for continuous processes.[4,14,15]

5.3.1. Mixing inside the system

The degree of mixing inside the continuous tumble mixer is crucial to obtain the highest blend uniformity at the exit of the system. This final uniformity is a contribution of the material behavior inside the tumble, the exit points, and the combination of these exit points in a chute located before the final exit of the system. The goal of this section is to understand the effect of the material properties, design, and operational parameters on the powder phenomena and blend uniformity inside the mixer. As mentioned before, four different volumes were analyzed. The first one, was the active layer, which is the region where most of the mixing occurs.[6,7] The second one was selected in the inactive layer, which is the place bellow the active zone where the particles have the lowest velocity. The last two selections (third and fourth zones) correspond to the upper and the bottom of the powder bed. Figures 5.8 and 5.9 show the simulation results for the different layers mentioned before, for concentrations of 2.5 and 10% of API with cohesion.

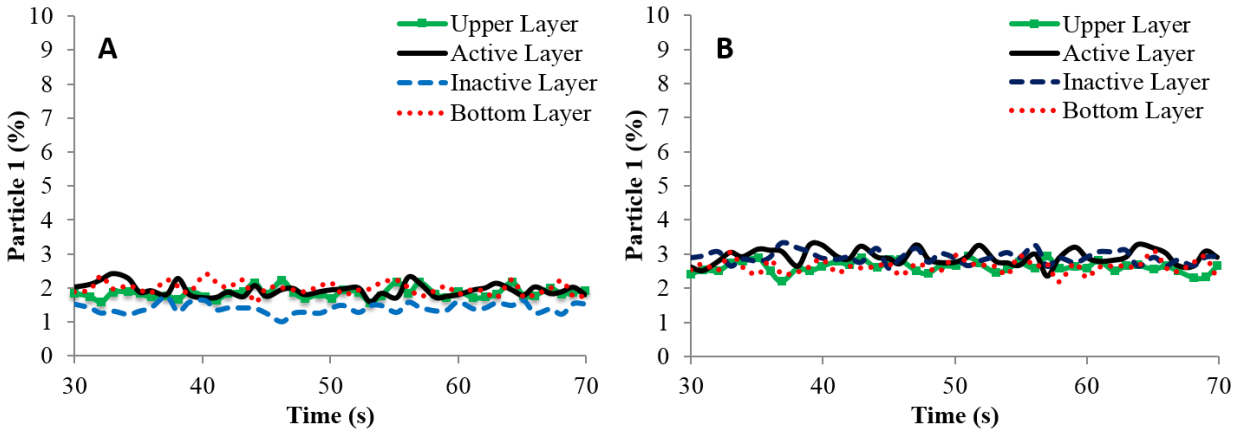

Figure 5.8. Mixing uniformity inside at 70 RPM and 2.5% API with an angle of 0° (A) and with an angle of 25° (B).

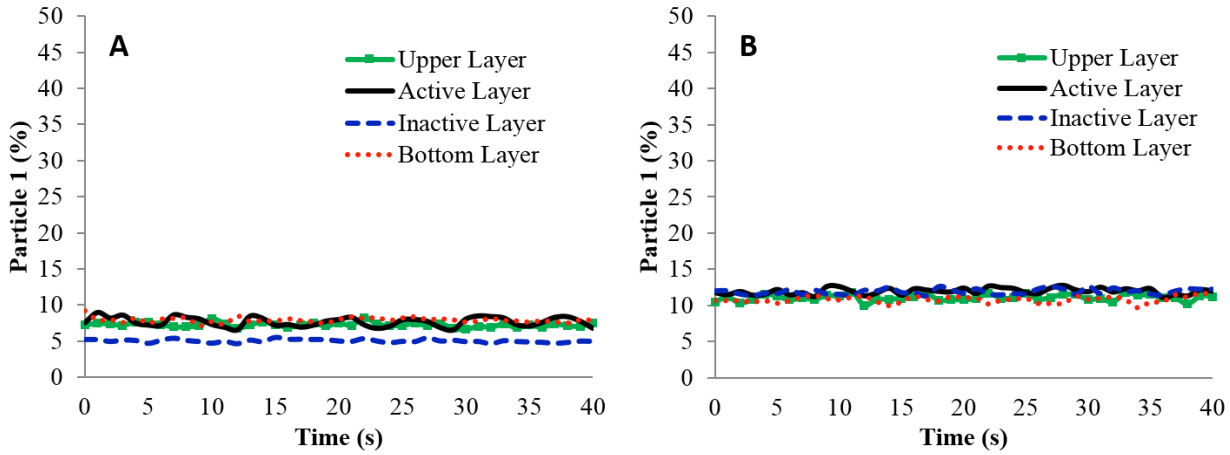

Figure 5.9. Mixing uniformity inside the mixer at 70 RPM and 10% API with an angle of 0° (A) and with an angle of 25° (B).

For the simulations corresponding to concentrations of 2.5 and 10% of concentration with cohesion it is possible to observe the effect of the feed position on the uniformity inside the mixer. For the simulation at 2.5%, with an angle of 0° the results oscillate between 1.0% and 2.4%. On the other hand, the simulation using the new feed position shows concentrations oscillating between 2.20 and 3.0%, which is closer to the desired value. While at 10% (Figure 5.9) with an angle of 0°, the concentration fluctuates between 5.0 and 8.2%, and using a feed angle of 25° the values oscillate between 10.0 and 11.5% of concentration. This trend was also found in the simulations without cohesion at 50% concentration. Based on these results it was possible to conclude that the feed position improves the particle uniformity inside the mixer, and this position was related to the changes in the velocity profile due to the reduction in the slow particles proportion and in the higher average velocity.

5.3.2. Mixing Uniformity at the Exits of the Mixer

The second factor that impacts the final uniformity is the contribution of the particles flowing through the tumble exits and the interaction of the material in the chute. This effect was studied measuring the concentration of particle 1 as a function of time at each exit of the tumble

mixer and calculating the average concentration. These measurements help us to understand the mixing dynamics. The results shown in Figure 5.10A for the simulation at 70 RPM, 50% of concentration, with angles of 0° and 25°, show a concentration profile where the higher concentrations are at the exits closer to the feed inlet (Exits 5 to 7).

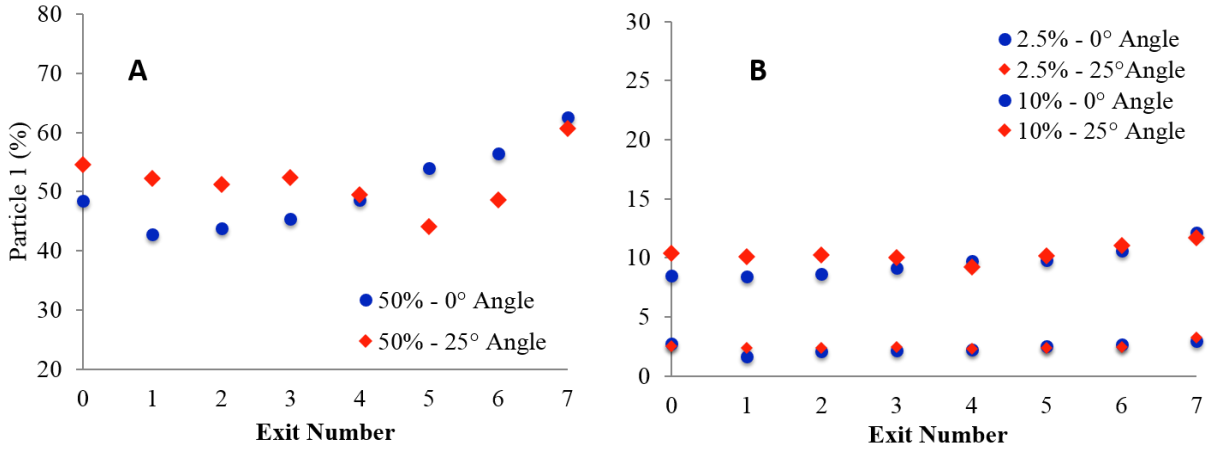

Figure 5.10. Mixing uniformity at the tumble exits at 70 RPM and 50% without cohesion (A), and 2.5 and 10% API (B).

These trends confirm the results presented in section 4.4.3 about the possibility of a shortcut, where the feed material leaves the system without interacting with the material that is already inside the tumble, and demonstrated that the feed angle reduces the powder shortcut. In general the deviation of the exits concentration was lower for simulations with the feed angle and were consistent with a better uniformity inside the mixer. This behavior was similar to the results at 2.5 and 10% of concentration (Figure 5.10B). For the highest concentration the changes in the feed position produce a more significant effect. Summarizing, it was found that the feed position impacts the concentration in each exit point except for the lower exit (exit 7).

5.3.3. Mixing Uniformity at the Exit of the System

Finally, the uniformity outside the system is the contribution of the mixing phenomena inside the continuous mixer, the concentration profile in each exit point, and the particle interaction between each exit point in the chute and the flow in the chute. Blend uniformity was measured following the methodology presented in section 4.4.1. The concentration values show a small reduction in variability when feed angle of 25° was used (Figure 5.11). The effect of the angle was less noticeable at the exit of the system compared to the reduction in variability inside the mixer and in the exit points. These results suggest the possibility that the particle uniformity was affected by the flow through the chute causing additional mixing for low cohesive blend.

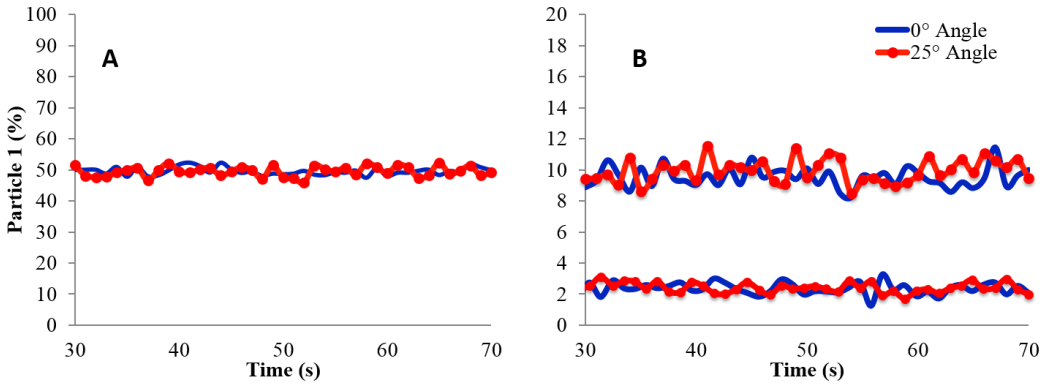

Figure 5.11. Final mixing uniformity at 70 RPM and 50% without cohesion (A), and 2.5 and 10% API (B) with cohesion.

Similar to chapter 4, RSD was used to report uniformity degree of the simulations, because this is the parameter used according to the FDA guidance.[8] The obtained results are shown in Table 5.2. Figure 5.11 depicts the concentration variability as a function of time after the system reached the steady state, for the simulations at 70 RPM, concentrations of 2.5, 10, and 50% of API, and cohesion. The RSD values oscillate between 2.59 and 16.6%. The highest mixing uniformity was obtained for the simulation at 70 RPM, with the angle of 0°, and using a concentration of 2.5%. When this result is compared to 50 RPM it is possible to conclude that the mixer speed produces

a positive effect on the final uniformity. For these four simulations (1-4) the effect of the angle of 25° does not have a significant effect on the final blend uniformity.

Based on these results, it is possible to observe that the uniformity decreases when the particle concentration decreases (Table 5.2). When comparing these results to the experimental part, the behavior was similar. In the experimental part, the lower mixing uniformities were found using the lower concentrations (Figure 5.1). The major differences between the experimental and the simulation results were related to the changes in the flow regimes. For all the simulations the flow regime was rolling and for the experiments the most predominant flow regime was cascade or cataracting. Previous results demonstrated a higher particle-particle interaction and better blend uniformity for the cataracting regime. The angle of 25° only caused a positive effect on the simulation with the highest RSD and the lowest concentration suggesting that the feed position is effective to improve the uniformity of the mixing process using low concentration.

5.4. Conclusions

A summary of the experimental results demonstrated that the blend uniformity was higher for the lowest concentration and that the effect of the mixer speed was different, relative to the higher concentrations (10.5 and 20%). The implementation of a higher feed angle in the system design demonstrated that the position at which the inlet material interacts with the active layer was crucial to reduce in approximately 46% the RSD values for the experiments and 20% for simulations with cohesion, improving the blend uniformity. This result was more significant for the blends with lower concentrations. Simulations demonstrated that the feed position promotes better particle interaction and enhances the uniformity inside the mixer, obtaining less variability in the mixer exits.

5.5. References

1. Portillo PM, Vanarase AU, Ingram A, Seville JK, Ierapetritou MG, Muzzio FJ. Investigation of the effect of impeller rotation rate, powder flow rate, and cohesion on powder flow behavior in a continuous blender using PEPT. *Chem. Eng. Sci.* 2010;65:5658-5668. doi:10.1016/j.ces.2010.06.036.
2. Chaudhuri B, Mehrotra A, Muzzio FJ, Tomassone MS. Cohesive effects in powder mixing in a tumbling blender. *Powder Technol.* 2006;165:105-114. doi:10.1016/j.powtec.2006.04.001.
3. Portillo PM, Ierapetritou MG, Muzzio FJ. Effects of rotation rate ,mixing angle, and cohesion in two continuous powder mixers: A statistical approach. *Powder Technol.* 2009;194(3):217-227. doi:10.1016/j.powtec.2009.04.010.
4. Vanarase AU, Muzzio FJ. Effect of operating conditions and design parameters in a continuous powder mixer. *Powder Technol.* 2011;208(1):26-36. doi:10.1016/j.powtec.2010.11.038.
5. Marikh K, Berthiaux H, Gatumel C, Mizonov V, Barantseva E. Influence of stirrer type on mixture homogeneity in continuous powder mixing: A model case and a pharmaceutical case. *Chem. Eng. Res. Des.* 2008;6:1027-1037. doi:10.1016/j.cherd.2008.04.001.
6. Aissa AA, Duchesne C, Rodrigue D. Transverse mixing of polymer powders in a rotary cylinder part I: Active layer characterization. *Powder Technol.* 2012;219:193-201. doi:10.1016/j.powtec.2011.12.040.
7. Ding Y., Forster R, Seville JP., Parker D. Granular motion in rotating drums: bed turnover time and slumping–rolling transition. *Powder Technol.* 2002;124:18-27. doi:10.1016/S0032-5910(01)00486-7.
8. FDA. *Guidance for Industry. Powder Blends and Finished Dosage Units — Stratified In-Process Dosage Unit Sampling and Assessment*.; 2003.
9. Aissa AA, Duchesne C, Rodrigue D. Effect of friction coefficient and density on mixing particles in the rolling regime. *Powder Technol.* 2011;212:340-347. doi:10.1016/j.powtec.2011.06.009.
10. Aissa A, Duchesne C, Rodrigue D. Polymer powders mixing part II: Multi-component mixing dynamics using RGB color analysis. *Chem. Eng. Sci.* 2010;65:3729-3738. doi:10.1016/j.ces.2010.03.007.
11. Aissa A, Duchesne C, Rodrigue D. Polymer powders mixing part I: Mixing characterization in rotating cylinders. *Chem. Eng. Sci.* 2010;65:786-795. doi:10.1016/j.ces.2009.09.031.
12. Fogler HS. *Element of Chemical Reaction Engineering*. 3rd ed. Prentice Hall; 1999:812-822.
13. Marikh K, Berthiaux H, Mizonov V, Barantseva E. Experimental study of the stirring conditions taking place in a pilot plant continuous mixer of particulate solids. *Powder Technol.* 2005;157:138-143. doi:10.1016/j.powtec.2005.05.020.

14. Gao Y, Vanarase A, Muzzio F, Ierapetritou M. Characterizing continuous powder mixing using residence time distribution. *Chem. Eng. Sci.* 2011;66:417-425. doi:10.1016/j.ces.2010.10.045.

15. Portillo PM, Muzzio FJ, Ierapetritou MG. Using Compartment Modeling to Investigate Mixing Behavior of a Continuous Mixer. *J. Pharm. Innov.* 2008;3:161-174. doi:10.1007/s12247-008-9036-0.

Chapter 6

6. Correlations for Material Properties and Mixing Uniformity

The principal studies related to continuous mixing processes have been focused on two areas: the first one includes the application and validation of theoretical developments and the second one the characterization and understanding of the performance of continuous mixers to find useful patterns.[1] Simulations are useful tools that help reduce experimental work and optimize operating conditions, and reduce laboratory time. They have proven to be a useful tool to study powder behavior providing a better understanding of these complex systems. The principal disadvantage in this area is that currently there are no equations to completely explain the powder behavior.[2] For instance, when compared to fluid mixing, powder phenomena are not well understood due to the complex behavior of these systems.[3]

Powder mixing uniformity is principally affected by material properties, operational parameters, and equipment design.[4–7] Without a model to predict the mixture uniformity the only solution is to try different conditions until an optimal combination that produces good mixing is found. Material properties are affected by particle size, particle shape, density, particle surface, API concentration, and others.[8,9] Operational parameters include mixer speed and flow rate, and the equipment design variation for this research was the feeding position.

For the experimental characterization of the continuous tumble mixer the following factors that affect final mixing uniformity were identified: mixer speed, flow rate, and material properties. Its characterization included five mixer speeds (10, 30, 50, 70, and 90), three API concentrations (2.5, 10.5, and 20%), and three different flow rates for each API concentration. Using these

experimental data an optimal operational range was found, where the mixer reached good mixing uniformity based on the FDA guidance[10] (Chapter 3). Using simulations, this number of experiments can be reduced. For the continuous tumble mixer a set of simulations was performed using 50 and 70 RPM as mixer speeds and four different material properties. A review of the principal results is shown in Table 6.1.

Table 6.1. Review of the simulation results

Cohesion Energy Density (J/m^3)		MRT (Sec)		Hold-Up (g)		RSD (%)	
50	**70**	**50**	**70**	**50**	**70**	**50**	**70**
0	0	4.1	4.03	52.64	46.66	2.5	2.46
10,000	10,000	4.3	4.26	58.91	48.27	3.1	2.51
20,000	20,000	7.83	5.13	81.27	52.18	3.55	2.79
25,000	30,000	9.94	7.95	123.66	69.34	2.63	3.28

6.1. Relation between final uniformity and collision number

As mentioned in chapter 4, the results for the simulations of the continuous mixer show a proportional relationship between the material property (cohesion energy density) and the final uniformity; except for the last point at 50 RPM where the RSD value was lower compared to the second and third simulations (Figure 6.1).

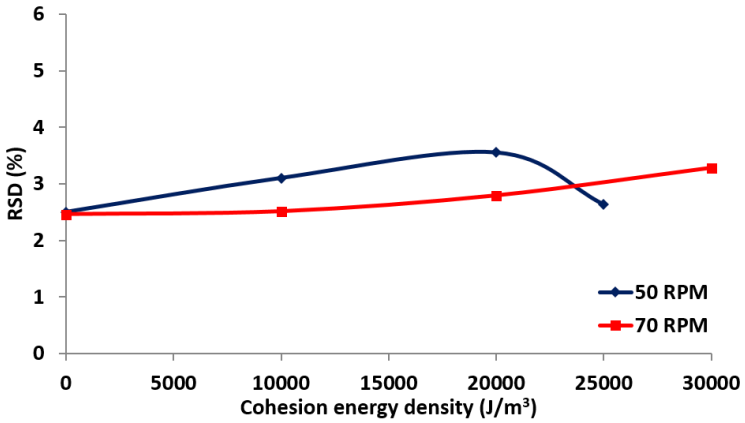

Figure 6.1. Effect of cohesion on final blend uniformity.

The number of collisions is related to the mixing uniformity.[11] Using DEM Software this number was calculated and the values were plotted against the cohesion energy density (Figure 6.2). Similar to the previous figure the simulation at 50 RPM and the highest cohesion energy density does not follow the same trend. Analysis of the images of each simulation was used to explain this behavior, the change in the powder phenomena inside the mixer for this last simulation showed a well-defined cascading regime, instead of rolling regime, which was the behavior obtained for the simulations at 50 RPM and lower cohesion energy densities (0 and 1). The principal difference between these two regimes is that rolling shows a flat and stable surface, while in the cascading regime the surface is curved and shows an expansion, forming a dilated layer.[12–14] Additionally, using these images it was possible to observe an increment in the proportion of particles moving faster compared to the other simulations, therefore the number of collisions increases.[15]

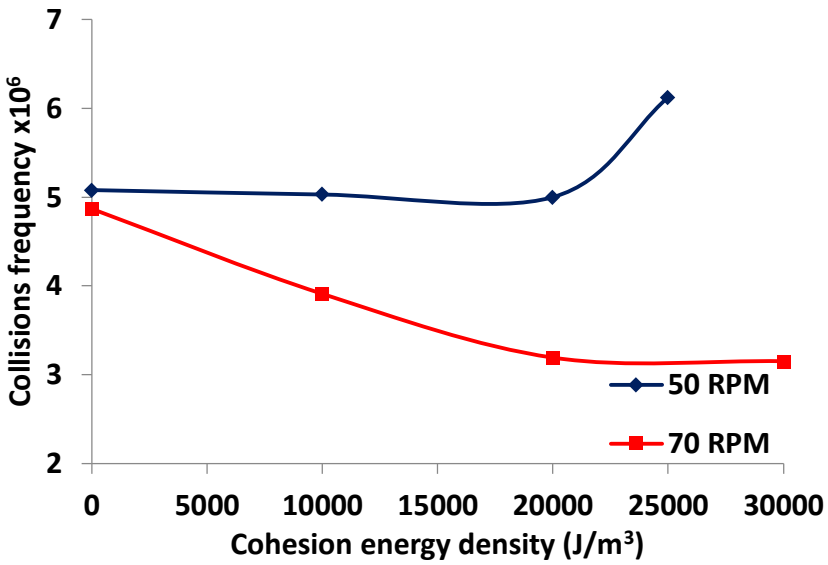

Figure 6.2. Material properties vs RSD.

6.2. Correlations between cohesion, mass hold-up, and MRT at constant flow

Using the values from Table 6.1 two principal correlations were found. Figure 6.3 shows a nonlinear relationship between the material property (cohesion) and the mass hold-up inside the mixer. Figure 6.4 shows a linear relation between mean residence time and the mass hold-up. Both correlations were made without using the last point at 50 RPM due to the difference in flow regime inside the system. Previous studies have shown a relationship between material properties, mass hold-up, and MRT.[5,7,16]

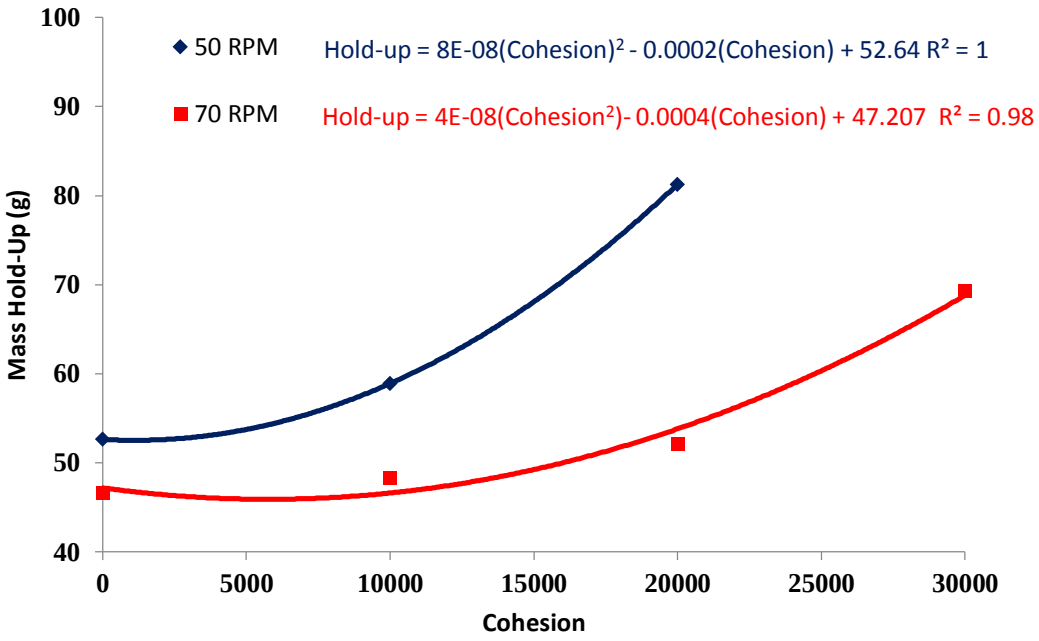

Figure 6.3. Effect of cohesion on mass hold-up.

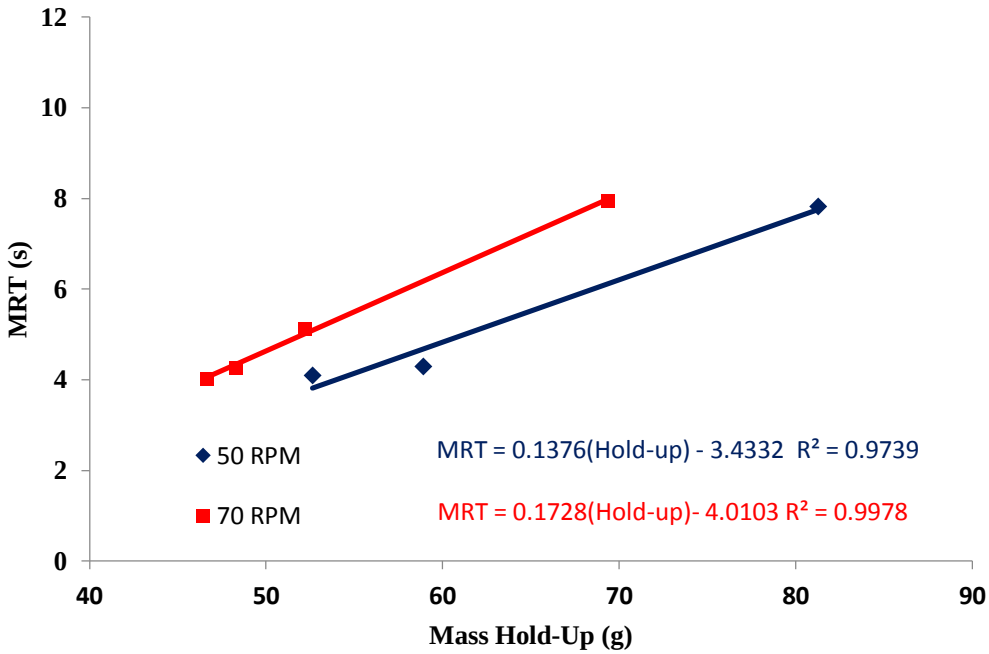

Figure 6.4. Effect of cohesion on MRT.

6.3. Correlation between mass hold-up and collision frequency

After the system reached the steady state, the mass hold-up was quantified and at the same time the collision number was calculated. The collision frequency was divided by the mass hold-up and this value was plotted as shown in Figure 6.5.

The results show two linear correlations for 50 and 70 RPM with R-squared values of 0.9999 and 0.9002, respectively. Using the previous correlations it is possible to predict the mass hold-up based on the material property (cohesion energy density) and with this value and the new correlations the collision number can be obtained. As previously mentioned the collision number is a parameter related to the mixing uniformity.

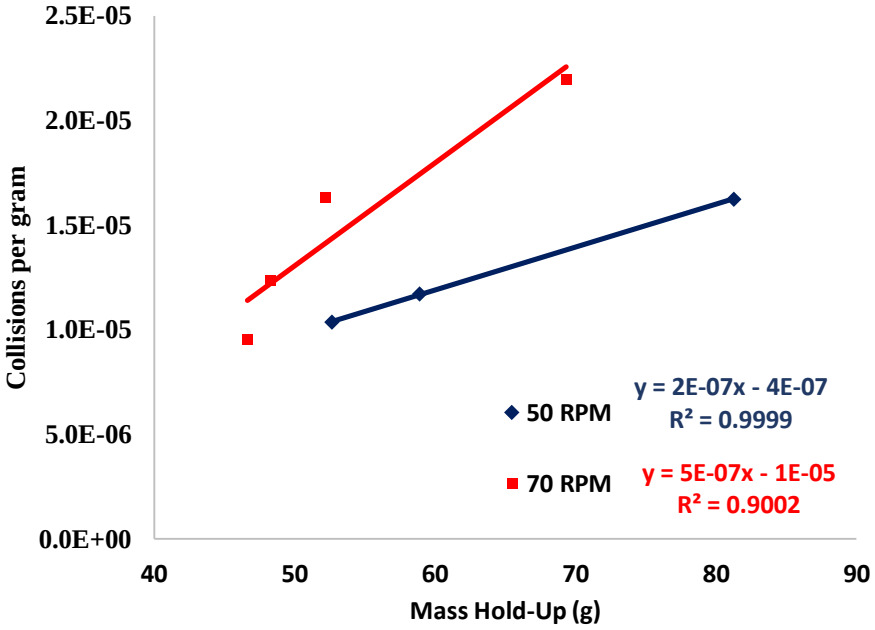

Figure 6.5. Effect of cohesion on mass hold-up.

6.4. RSD Predictions

The relative standard deviation is the measurement of uniformity used in this study to report the mixing degree of a particulate mixture. The first step was to determine a relation between the material properties, collision frequency, and MRT to plot them versus relative standard deviation (Figure 6.6). MRT quantifies the time that a group of particles remains inside the mixer at steady state and its related to the final mixing homogeneity.[17,18]

Material properties are represented by the cohesion, while collisions frequency, and MRT were calculated after the system reached the steady state. After evaluating different options a linear relationship was found with coefficients of determination (R^2) of 0.9183 and 0.9916 for 50 and 70 RPM, respectively.

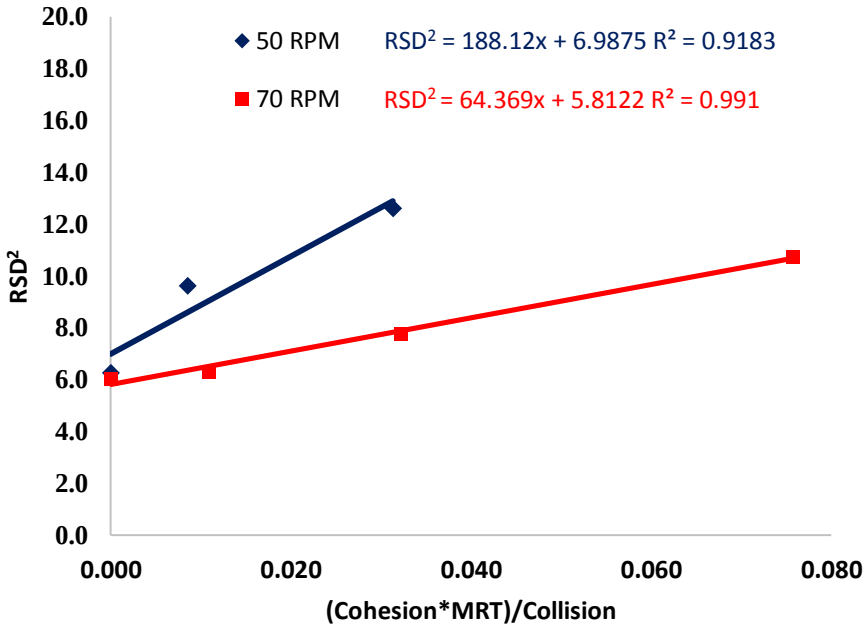

Figure 6.6. RSD^2 predictions.

6.5. Validation of the proposed correlations

A new simulation was performed and the mass hold-up, MRT, and RSD were predicted using the previous correlations and the error percents were calculated using the predicted and the obtained values. The flow rate was maintained constant, the cohesion energy density was equal to 25,000 and the mixer speed was equal to 70 RPM. The results show that the simulation using a cohesion value equal to 25,000 maintains the same behavior with a 6.17% of error (Table 6.2).

Table 6.2. Validation results of simulation at 70 RPM with cohesion 2.5

70 RPM-Cohesion 2.5-Validation			
Responses	**Real**	**Predicted**	**Error**
Mass Hold-Up	57.70	62.21	7.81
MRT	7.78	6.73	13.50
RSD	3.08	2.89	6.17

These correlations provide an *a priori* understanding useful to establish initial conditions that can be related to a final mixing degree and establish a methodology that can be implemented in mixing continuous processes reducing the number of experiments needed. A review of the procedure for the continuous tumble mixer is show in Figure 6.7.

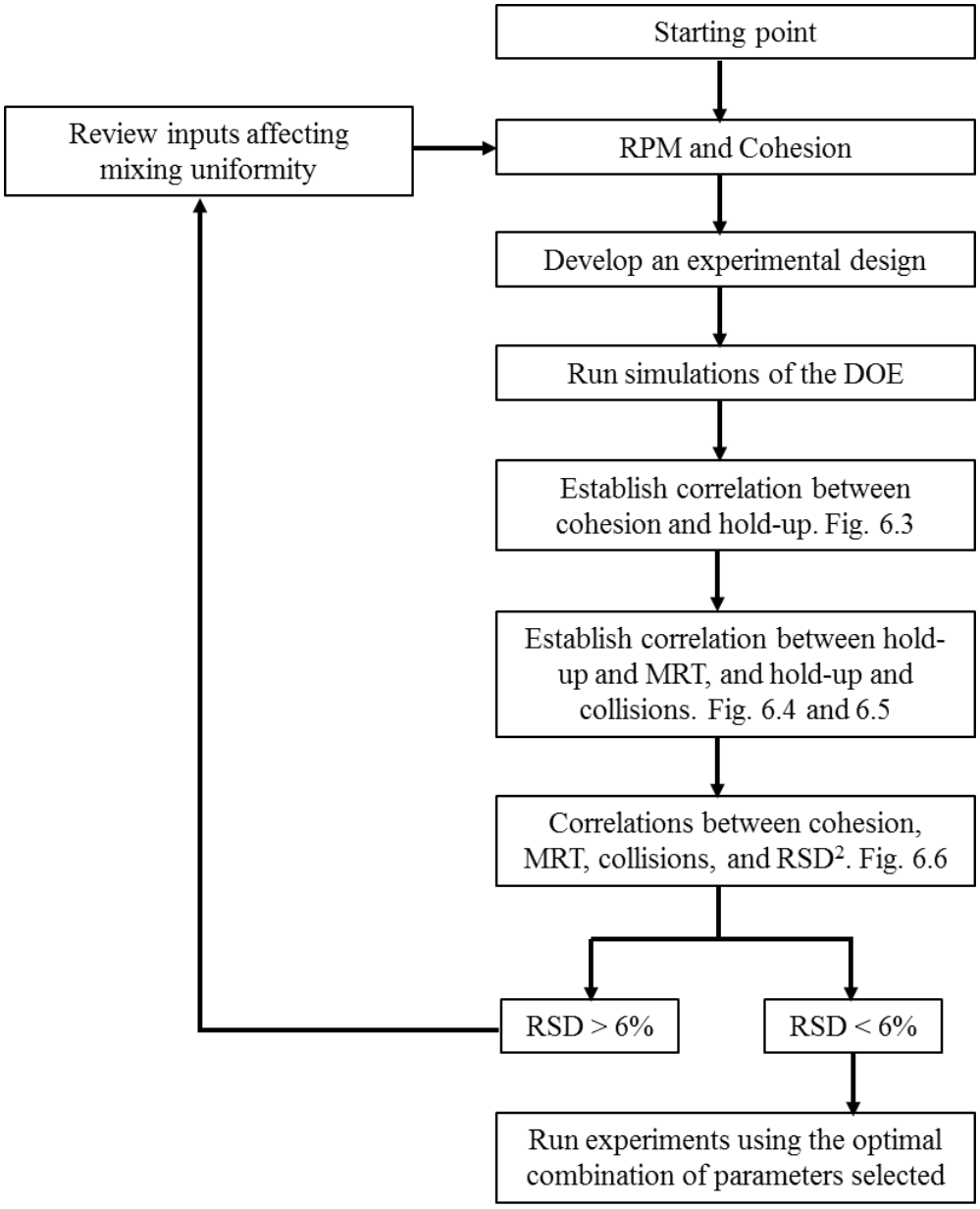

Figure 6.7. Review of the procedure used to estimate an optimal operational range.

This methodology will be useful to define the Design Space of a mixing process, which is defined according to FDA as the relationship between the process inputs (such as: material properties and process parameters) and the critical quality attributes.[19] For this research case, the final mixing uniformity is the critical quality attribute, because inadequate mixing in the pharmaceutical industry may result in rejection of the final product. Following FDA guidelines

about space design, the correct strategy based on an empirical approach includes: selection of experimental design, conducting experiments, analysis of the data, and definition of the design space.

6.6. Methodology to estimate an optimal operation range for continuous mixing

Using DEM simulations it was possible to develop an experimental design to evaluate the effect of material property (cohesion energy density) and operational parameters (mixer speed) in the mixing uniformity. Results demonstrate that both affect the final blend uniformity, and a relationship between uniformity and collision number was demonstrated. These simulations provide useful information to reduce the experimental part and minimize the process of trial and error necessary to find the optimal operating conditions.

Experimental and simulation results demonstrate that the cohesion energy density produces an increment in the mass hold-up and MRT of the material inside the mixer, at constant mixer speed. Also, a relationship between cohesion energy density, MRT, and collision frequency was established with the squared RSD.

Using the information obtained from the simulations, a general procedure to understand the behavior of a mixer and the effect of the material properties in the final uniformity was developed (Figure 6.8). This procedure can be extrapolated to experimental systems given that the behavior and correlations presented above are similar to the simulations.

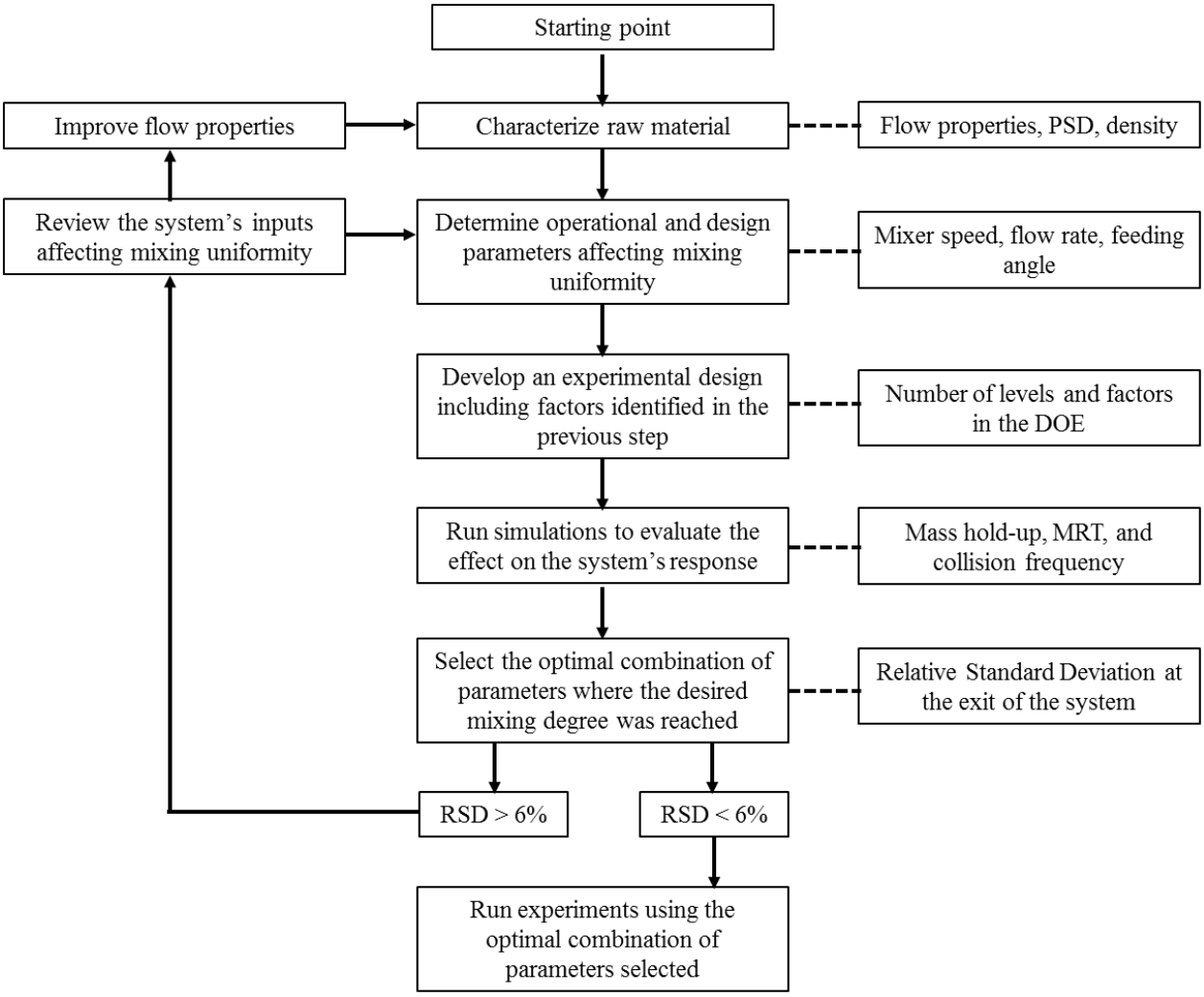

Figure 6.8. Flowchart of the methodology proposed to reduce experimental part.

6.7. Conclusions

The main goal of this chapter was to establish correlations between material properties, operational parameters, and mixing uniformity based on the relative standard deviation. Using DEM simulations a quadratic relationship between cohesion energy density and mass hold-up was found, this accumulation was related to MRT with a linear correlation, and using a relationship between cohesion energy density, collision frequency, and MRT vs RSD^2 another linear

relationship was found. Proposed correlations were validated using a new simulation at 70 RPM and a cohesion energy density of 25,000 J/m^3 obtaining a percent of error close to 6%.

Following the procedure used for the simulations a methodology was proposed to minimize trial and error during the experimental study. This methodology consists on the identification of material properties, operational, and equipment parameters that affect the final uniformity. For the continuous tumble mixer, mixer speeds, and material properties were the main factors affecting the final mixing uniformity.[20] After running the DOE the effect of cohesion energy density on final uniformity was depicted and the behavior of the system in an operational range was established.

6.8. References

1. Pernenkil L, Cooney CL. A review on the continuous blending of powders. *Chem. Eng. Sci.* 2006;61:720-742. doi:10.1016/j.ces.2005.06.016.
2. Bridgwater J. Mixing of particles and powders: Where next? *Particuology* 2010;8(6):563-567. doi:10.1016/j.partic.2010.07.001.
3. Zhu HP, Zhou ZY, Yang RY, Yu AB. Discrete particle simulation of particulate systems: A review of major applications and findings. *Chem. Eng. Sci.* 2008;63(23):5728-5770. doi:10.1016/j.ces.2008.08.006.
4. Weinekötter R. Compact and efficient continuous mixing processes for production of food and pharmaceutical powders. *Trends Food Sci. Technol.* 2009;20:S48-S50. doi:10.1016/j.tifs.2009.01.037.
5. Vanarase AU, Muzzio FJ. Effect of operating conditions and design parameters in a continuous powder mixer. *Powder Technol.* 2011;208(1):26-36. doi:10.1016/j.powtec.2010.11.038.
6. Marikh K, Berthiaux H, Mizonov V, Barantseva E, Ponomarev D. Flow analysis and Markov Chain modelling to quantify the agitation effect in a continuous powder mixer. *Chem. Eng. Res. Des.* 2006;84:1059-1074. doi:10.1205/cherd05032.
7. Gao Y, Vanarase A, Muzzio F, Ierapetritou M. Characterizing continuous powder mixing using residence time distribution. *Chem. Eng. Sci.* 2011;66:417-425. doi:10.1016/j.ces.2010.10.045.
8. Freeman R. Measuring the flow properties of consolidated , conditioned and aerated powders – a comparative study using a powder rheometer and a rotational shear cell. *Powder Technol.* 2007;174:25-33.
9. Fu X, Huck D, Makein L, Armstrong B, Willen U, Freeman T. Effect of particle shape and size on flow properties of lactose powders. *Particuology* 2012;10:203-208. doi:10.1016/j.partic.2011.11.003.
10. FDA. *Guidance for Industry. Powder Blends and Finished Dosage Units — Stratified In-Process Dosage Unit Sampling and Assessment*.; 2003.
11. Yang RY, Yu AB, McElroy L, Bao J. Numerical simulation of particle dynamics in different flow regimes in a rotating drum. *Powder Technol.* 2008;188(2):170-177. doi:10.1016/j.powtec.2008.04.081.
12. Santomaso A, Olivi M, Canu P. Mixing kinetics of granular materials in drums operated in rolling and cataracting regime. *Powder Technol.* 2005;152(1-3):41-51. doi:10.1016/j.powtec.2005.01.011.
13. Wightman C, Muzzio FJ. Mixing of granular material in a drum mixer undergoing rotational and rocking motions I. Uniform particles. *Powder Technol.* 1998;98:113-124.
14. Santomaso A, Olivi M, Canu P. Mechanisms of mixing of granular materials in drum mixers under rolling regime. *Chem. Eng. Sci.* 2004;59(16):3269-3280. doi:10.1016/j.ces.2004.04.026.

15. Xu Y, Xu C, Zhou Z, Du J, Hu D. 2D DEM simulation of particle mixing in rotating drum: A parametric study. *Particuology* 2010;8(2):141-149. doi:10.1016/j.partic.2009.10.003.

16. Portillo PM, Vanarase AU, Ingram A, Seville JK, Ierapetritou MG, Muzzio FJ. Investigation of the effect of impeller rotation rate, powder flow rate, and cohesion on powder flow behavior in a continuous blender using PEPT. *Chem. Eng. Sci.* 2010;65:5658-5668. doi:10.1016/j.ces.2010.06.036.

17. Fogler HS. *Element of Chemical Reaction Engineering*. 3rd ed. Prentice Hall; 1999:812-822.

18. Marikh K, Berthiaux H, Mizonov V, Barantseva E. Experimental study of the stirring conditions taking place in a pilot plant continuous mixer of particulate solids. *Powder Technol.* 2005;157:138-143. doi:10.1016/j.powtec.2005.05.020.

19. FDA. *Guidance for Industry. Q8(R2) Pharmaceutical Development Guidance for Industry*.; 2009.

20. Florian M, Velázquez C, Méndez R. New continuous tumble mixer characterization. *Powder Technol.* 2014;256:188-195. doi:10.1016/j.powtec.2014.02.023.

Chapter 7

7. Modified Froude Number (Fr_{mf}) based on Simulation Results

The main goal of mixing processes is to obtain a uniform mixture. For particulate materials, the probability to produce mixtures with the desired quality is small. When all the components are uniform in relation to the whole material, a particulate system is called uniform. In a drum mixer the uniformity has been related to the flow regime occurring during the mixing process. To describe the behavior inside a drum mixer, six different flow regimes have been identified.[1–3] The Froude number (Eq. 1.1) has typically been used to describe the flow regimes and the transitions between these behaviors[1,4,5] and represents the relation between gravitational and centrifugal forces. When Fr=1, gravitational and centripetal forces balance each other, at these conditions the critical velocity (w_c) is reached[6] (Eq. 7.1). Froude numbers higher than 1 represent centrifugal behaviors.[1]

$$w_c = \sqrt{\frac{g}{R}} \tag{7.1}$$

The rolling regime has been used for mixing in the industry.[7] Rolling provides a higher mixing degree and this flow regime is divided in two different layers, stagnant, or inactive, and active which is the layer where the mixing principally occurs.[7,8] In this layer, the particles move rapidly causing material expansion, which enhances the possibility of the particles to exchange positions producing a uniform mixing. Segregation can occur in a similar way. In the stagnant layer, expansion is not occurring and the particles are in a compacted mode. Cascading tumbling (slumping, rolling, and cascading) depends on RPM and particle size of the material inside the mixer. Mellman et al. demonstrated that rolling occurs with loadings greater than 10%.[1] Aissa et

al. demonstrated that the Froude number alone cannot describe powder behavior and that an optimal filling ratio is necessary to achieve rolling regime.[4] Mellman et al. also demonstrated that the Froude number depends on filling ratio, with optimal values between 17 and 43%. However, this range depends on the material properties.[1,9] To avoid this disadvantage of the *Fr* number, a modification was proposed on the basis of the Mohr-Coulumb failure criterion and using the angle of repose and the fill fraction[6] (Eq. 7.2).

$$w_c = \sqrt{\frac{g}{Rsin\beta_s\sqrt{1-\theta}}} \tag{7.2}$$

Where g, R, β_s, and Θ represent gravitational force, mixer radius, angle of repose, and fill level, respectively. Angle of repose measures the inclination of the free surface to the horizontal of a bulk solid pile.[10] It is a measurement of the material flow properties, and is affected by density, shape, humidity, coefficient of friction, and other variables.[11–13] Using DEM simulations the angle of repose can be calculated, but it is limited by the circular shape of particles which causes them to roll and prevents the formation of the pile.[14] However, the dynamic angle of repose can be measured easily from simulations. This dynamic angle is defined as the angle formed by the inclined surface of powder material with the horizontal when it rotates in a drum.[15] For this analysis, the dynamic angle is used in the continuous tumble mixer. Based on this information a modified *Fr* number was proposed using the dynamic angle of repose (α), to include the material properties in this value. Including α in equation 7.2, making equation 7.2 equal to equation 7.1 and solving for g/R and substituting on equation 1.1 the proposed $\boldsymbol{Fr_{mf}}$ number is as follows:

$$Fr_{mf} = \frac{Rw^2}{g}\left(sin\alpha\left(\sqrt{1-\theta}\right)\right) \tag{7.3}$$

Where R, w, g, α, and Θ represent the radius of the tumble mixer, angular velocity, gravity, dynamic angle of repose, and fill fraction. To evaluate the proposed Froude number, an

experimental design using a batch tumble mixer was developed and included mass hold-up (40, 80, 120, and 160g), cohesion energy density (0, 20000, and 30000 J/m^3), and mixer speeds (30, 50, 70, and 90 RPM). Figure 7.1 shows the effects of these inputs on the shape of the avalanche at 90 RPM. Figures for mixers speed 30, 50, and 70 RPM are presented on Appendix A.

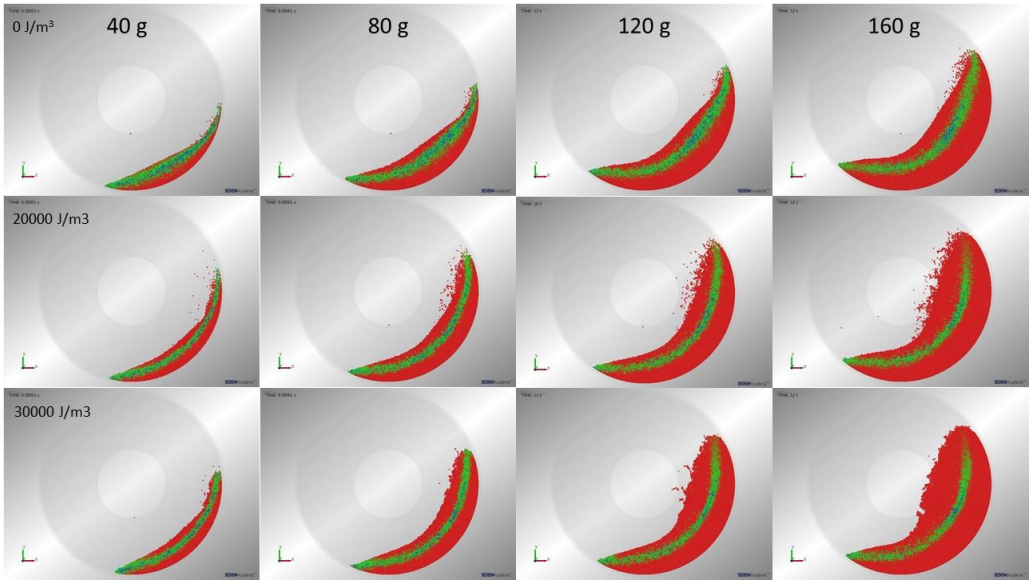

Figure 7.1. Effect of cohesion and mass hold-up on the shape of the avalanche at 90 RPM.

Flow regime was classified inside the mixer based on the avalanche shape (Table 7.1) and the Froude number was calculated using the conventional form (Eq. 7.1), which corresponds to 0.173, 0.482, 0.944, and 1.56 for 30, 50, 70, and 90 RPM, respectively. Rolling regime was selected when the surface of the avalanche was flat, cascading when the surface changed to a curved form, and cataracting was distinguished because particles are separated of the avalanche during a short period of time.

Table 7.1. Visual classification of the flow regime inside the tumble mixer

Cohesion	Hold-up	Visual behavior			
		30 RPM	50 RPM	70 RPM	90 RPM
Cohesion 0	40	Rolling	Rolling	Cascading	Cascading
	80	Rolling	Rolling	Cascading	Cascading
	120	Rolling	Cascading	Cascading	Cataracting
	160	Rolling	Cascading	Cascading	Cataracting
Cohesion 2	40	Rolling	Rolling	Cascading	Cataracting
	80	Rolling	Cascading	Cascading	Cataracting
	120	Rolling	Cascading	Cascading	Cataracting
	160	Rolling	Cascading	Cascading	Cataracting
Cohesion 3	40	Rolling	Rolling	Cascading	Cataracting
	80	Rolling	Cascading	Cascading	Cataracting
	120	Rolling	Cascading	Cascading	Cataracting
	160	Rolling	Cascading	Cascading	Cataracting

The dynamic angle of repose was measured in the surface of the avalanche, where the highest material angle was formed (Figure 7.2) and the fill fraction was calculated measuring the area occupied by the particles inside the mixer. Results are shown in Table 7.2.

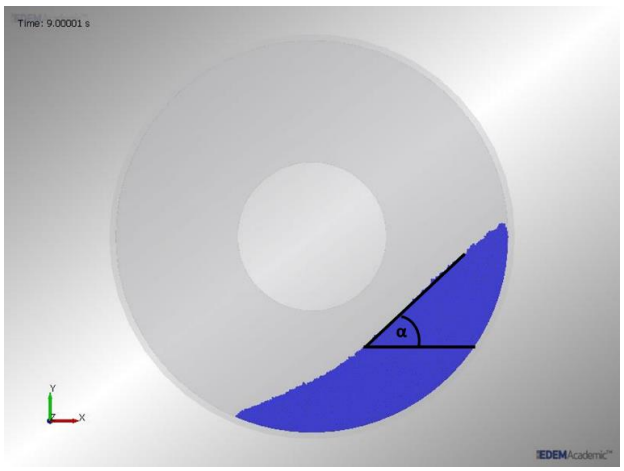

Figure 7.2. Measurement of dynamic angle of repose.

Results demonstrated that the material properties, mass hold-up, and mixer speed affect this angle, producing changes in its value. Increases in cohesion, mass hold-up, and mixer speed produce an increment in the dynamic angle of repose.

Table 7.2. Modified Fr number values

Cohesion	Hold-up	Modified Froude Number			
		30 RPM	50 RPM	70 RPM	90 RPM
Cohesion 0	40	0.071	0.235	0.457	0.670
	80	0.076	0.229	0.455	0.801
	120	0.083	0.271	0.549	0.971
	160	0.082	0.280	0.616	1.076
Cohesion 2	40	0.085	0.280	0.585	1.031
	80	0.089	0.312	0.653	1.155
	120	0.086	0.298	0.687	1.237
	160	0.090	0.303	0.669	1.183
Cohesion 3	40	0.089	0.292	0.649	1.067
	80	0.097	0.310	0.693	1.233
	120	0.093	0.306	0.711	1.257
	160	0.090	0.304	0.688	1.194

Using the obtained results a new flow regime classification based on the $\boldsymbol{Fr_{mf}}$ was established as shown in Table 7.3. This new classification is proposed just for rolling, cascading and cataracting.

Table 7.3. New flow regime classification based on Fr_{mf} values.

Classification	Froude Number Mod		Transition
Rolling	0.05	0.25	0.25-0.3
Cascading	0.3	0.95	0.9-1.1
Cataracting	>0.95	-	-

The continuous simulations presented in Chapter 4 (Figure 4.5) were evaluated using $\boldsymbol{Fr_{mf}}$ and the results are presented in Table 7.4. Results for the continuous mixing simulations present a perfect match between the visual behavior and the proposed classification using the $\boldsymbol{Fr_{mf}}$.

Table 7.4. Modified Froude number for the continuous simulations

Mixer Speed	Cohesion	Dynamic Angle	Froude Number	Modified Froude Number	Visual Behavior
50 RPM	0	30.80	0.482	0.234	Rolling
	1	31.72	0.482	0.240	Rolling
	2	39.89	0.482	0.284	Cascading
	3	46.47	0.482	0.305	Cascading
70 RPM	0	34.25	0.944	0.508	Cascading
	1	37.37	0.944	0.545	Cascading
	2	36.22	0.944	0.528	Cascading
	3	48.72	0.944	0.652	Cascading

7.1. Conclusions

The Froude number has been used to characterize and describe changes in the flow regime inside a drum mixer. This dimensionless number was used in the continuous tumble mixer and a modification that includes the effect of material properties was made. The dynamic angle of repose was used to add this effect in the Froude number and the results showed a proportional relationship between this angle and mass hold-up, mixer speed, and cohesion energy density.

Using a set of batch simulations, this modified Fr number was estimated and a new classification was proposed for the following flow regimes: rolling, cascading, and cataracting. Continuous simulations presented in Chapter 4 were evaluated using this modified Fr number. The obtained numerical and visual results showed an agreement in flow regimes (rolling and cascading).

7.2. References

1. Mellmann J. The transverse motion of solids in rotating cylinders—forms of motion and transition behavior. *Powder Technol.* 2001;118(3):251-270. doi:10.1016/S0032-5910(00)00402-2.
2. Yang RY, Zou RP, Yu AB. Microdynamic analysis of particle flow in a horizontal rotating drum. *Powder Technol.* 2003;130(1-3):138-146. doi:10.1016/S0032-5910(02)00257-7.
3. Yang RY, Yu AB, McElroy L, Bao J. Numerical simulation of particle dynamics in different flow regimes in a rotating drum. *Powder Technol.* 2008;188(2):170-177. doi:10.1016/j.powtec.2008.04.081.
4. Aissa AA, Duchesne C, Rodrigue D. Effect of friction coefficient and density on mixing particles in the rolling regime. *Powder Technol.* 2011;212:340-347. doi:10.1016/j.powtec.2011.06.009.
5. Ding Y., Forster R, Seville JP., Parker D. Granular motion in rotating drums: bed turnover time and slumping–rolling transition. *Powder Technol.* 2002;124:18-27. doi:10.1016/S0032-5910(01)00486-7.
6. Juarez G, Chen P, Lueptow RM. Transition to centrifuging granular flow in rotating tumblers: a modified Froude number. *New J. Phys.* 2011;13(5):053055. doi:10.1088/1367-2630/13/5/053055.
7. Ding Y, Seville J, Forster R, Parker D. Solids motion in rolling mode rotating drums operated at low to medium rotational speeds. *Chem. Eng. Sci.* 2001;56:1769-1780. Available at: http://www.sciencedirect.com/science/article/pii/S0009250900004681. Accessed October 14, 2014.
8. Marigo M, Cairns DL, Davies M, Ingram A, Stitt EH. A numerical comparison of mixing efficiencies of solids in a cylindrical vessel subject to a range of motions. *Powder Technol.* 2012;217:540-547. doi:10.1016/j.powtec.2011.11.016.
9. Aissa AA, Duchesne C, Rodrigue D. Transverse mixing of polymer powders in a rotary cylinder part I: Active layer characterization. *Powder Technol.* 2012;219:193-201. doi:10.1016/j.powtec.2011.12.040.
10. Ileleji KE, Zhou B. The angle of repose of bulk corn stover particles. *Powder Technol.* 2008;187(2):110-118. doi:10.1016/j.powtec.2008.01.029.
11. Leturia M, Benali M, Lagarde S, Ronga I, Saleh K. Characterization of flow properties of cohesive powders: A comparative study of traditional and new testing methods. *Powder Technol.* 2014;253(2014):406-423. doi:10.1016/j.powtec.2013.11.045.
12. Santomaso A, Olivi M, Canu P. Mechanisms of mixing of granular materials in drum mixers under rolling regime. *Chem. Eng. Sci.* 2004;59(16):3269-3280. doi:10.1016/j.ces.2004.04.026.
13. Faqih AMN, Mehrotra A, Hammond SV, Muzzio FJ. Effect of moisture and magnesium stearate concentration on flow properties of cohesive granular materials. *Int. J. Pharm.* 2007;336:338-345. doi:10.1016/j.ijpharm.2006.12.024.

14. Zhou YC, Xu BH, Yu AB, Zulli P. An experimental and numerical study of the angle of repose of coarse spheres. *Powder Technol.* 2002;125(1):45-54. doi:10.1016/S0032-5910(01)00520-4.

15. Bodhmage A. Correlation between physical properties and flowability indicators for fine powders. 2006;(July). Available at: http://www.collectionscanada.gc.ca/obj/s4/f2/dsk3/SSU/TC-SSU-07032006115722.pdf. Accessed October 15, 2014.

Chapter 8

8. Concluding Remarks

Based on the experimental results, the low shear continuous tumble mixer is capable of producing powder blends with a high degree of mixing and low variability. Results demonstrate that powder phenomena occurring inside the mixer was similar to the batch tumble mixer and depended on flow rate, material properties, and operational parameters. The highest degree of mixing was reached using higher flow rates and 70 RPM. A behavior map was developed to select the appropriate operating conditions to establish a cataracting avalanche, which was the flow regime that produced the highest blend uniformity.

Simulations of the continuous mixing processes were performed using DEM software and these were validated using glass beads of 1 mm. Results confirmed that simulations show a similar behavior based on the avalanche shape, flow regime, and the velocity profile inside the mixer. The DOE of the simulations included two mixer speeds (50 and 70 RPM) and four different cohesion energy density levels. Similar to the experimental part, the uniformity was a function of the materials properties, mixer speed, and flow regime. The change in flow regime from rolling to cascading was a combination of the cohesion and the mass hold-up at constant mixer speed. Using simulations, a concentration profile at the exits of the tumble was demonstrated, with highest and lowest values at the exits closer to the bottom and top of the powder bed, respectively. A reduction in the variability inside the mixer and at the tumble exits was also found when the cohesion energy density values increased. The concentration profile at the tumble exits was attributed to a shortcut effect, where the particles leave the mixer without interacting with the particles inside the system.

To reduce the shortcut effect, a new feed position was implemented to force the material entering the mixer to fall on top of the active layer. This design parameter reduces the probability

of the incoming material leaving the system without interacting with the material in the avalanche. The feed position was studied using experiments and simulations and the results demonstrate that the position at which the inlet material interacts with the active layer is crucial to reduce the RSD values for both, experiments and simulations with cohesion. This result was more noticeable for the blends with lower concentrations. Also, the new feed position promotes particle interaction and reduces the variability inside the mixer and at the mixer exits.

Using the results of the simulations set, correlations between material properties, operational parameters, and mixing uniformity were established. A quadratic relationship between cohesion energy density and mass hold-up was found and mass hold-up was related to MRT with a linear correlation. A relation between cohesion energy density, collision frequency, and MRT was plotted against RSD^2 and the results show a linear relationship. A new simulation was performed using 70 RPM and a cohesion energy density of 25,000 J/m^3. The systems responses were predicted (mass hold-up, MRT, and RSD) using the proposed correlations and the percent of error was close to 6%. A methodology was proposed to minimize trial and errors in the experimental part using the correlations obtained with DEM simulations.

Additionally, a modified Froude number ($\boldsymbol{Fr_{mf}}$) was proposed to characterize and describe changes in flow regime inside drum mixers. The modification includes the effect of material properties by including the dynamic angle of repose into the traditional equation. The dynamic angle of repose was affected by mass hold-up, mixer speed, and cohesion energy density. A new classification was proposed for rolling, cascading, and cataracting using the results obtained with the $\boldsymbol{Fr_{mf}}$**.** Continuous simulations were evaluated using $\boldsymbol{Fr_{mf}}$ and numerical and visual behavior showed an agreement in flow regime (rolling and cascading).

Finally, to obtain detailed information of the mixer behavior, simulations and experiments under the following conditions are suggested: different particles sizes and densities to study segregation, reduce the number of exits in the mixer to produce an increment in the mass hold-up and MRT, which will improve the final blend uniformity, and study the scale-up effect on the final blend uniformity using the same mixer with different dimensions.

Appendix A

Effect of materials properties, mass hold-up, and mixer speed on flow regime

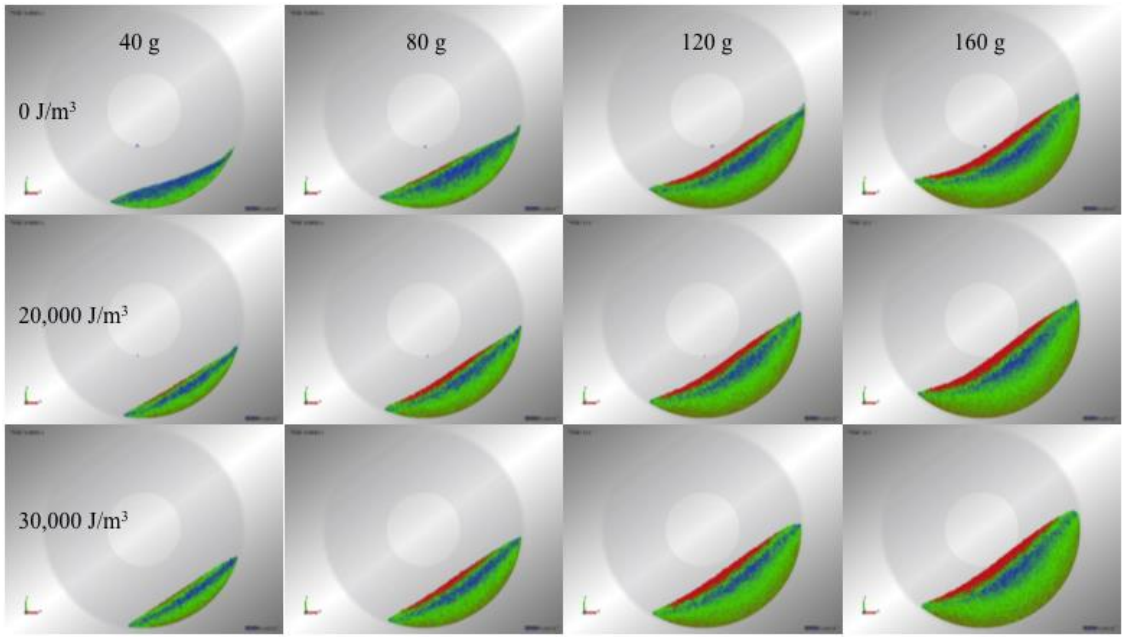

Figure A.1. Effect of cohesion and mass hold-up on the shape of the avalanche at 30 RPM.

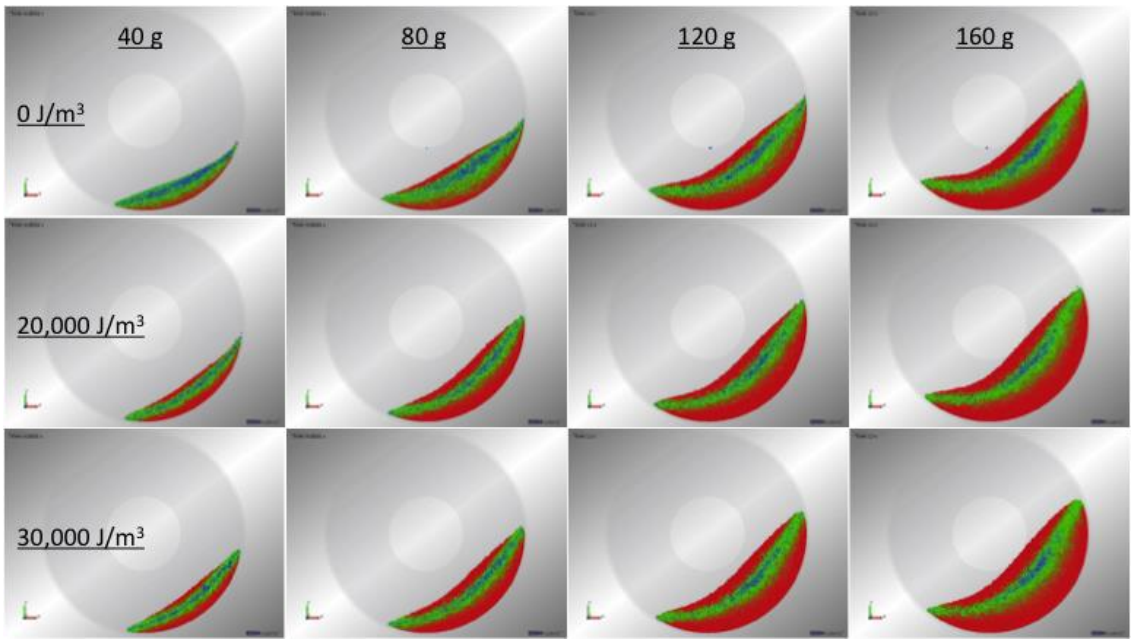

Figure A.2. Effect of cohesion and mass hold-up on the shape of the avalanche at 50 RPM.

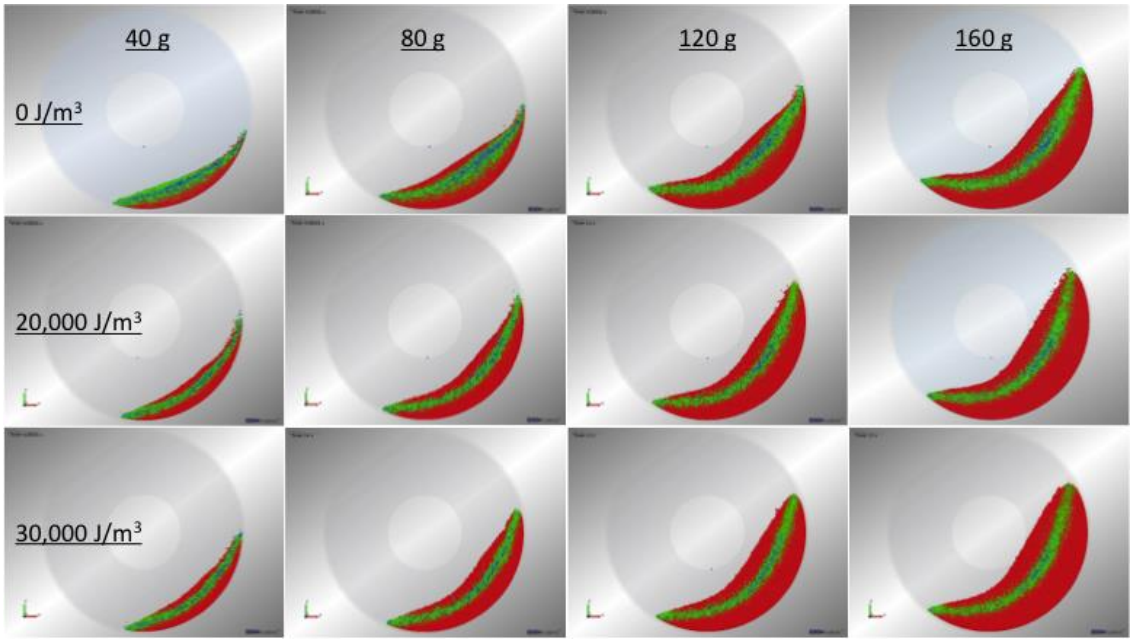

Figure A.3. Effect of cohesion and mass hold-up on the shape of the avalanche at 70 RPM.

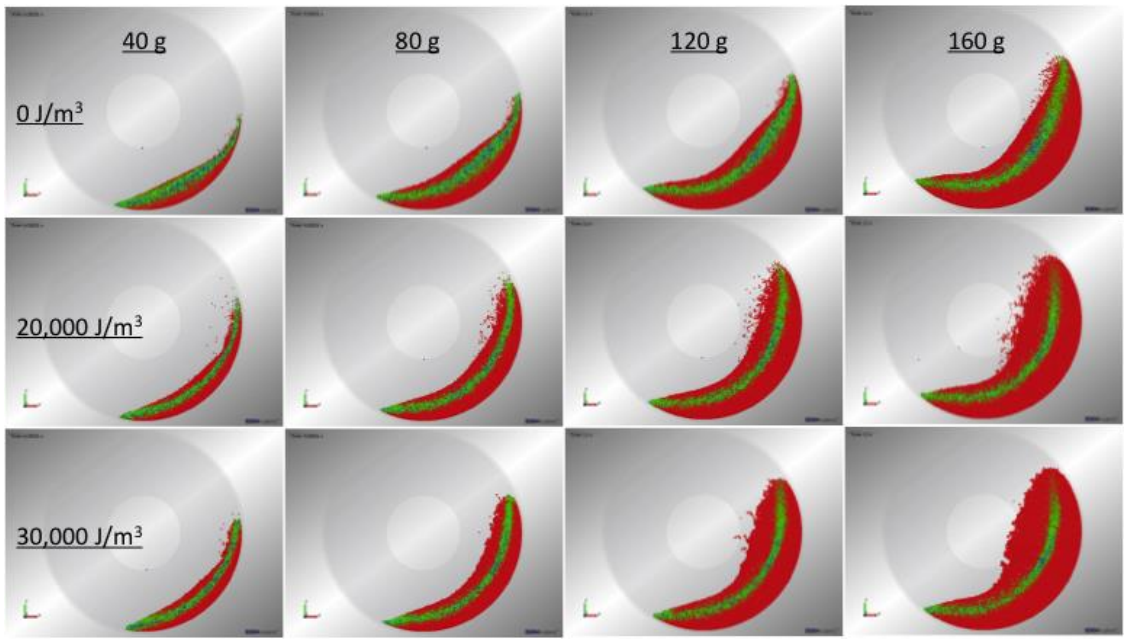

Figure A.4. Effect of cohesion and mass hold-up on the shape of the avalanche at 90 RPM.